

Trabajo Fin de Máster
Máster Universitario en Sistemas de Energía
Térmica

Potential of Solar Photovoltaic and Wind
technologies for industrial water treatment in mining
operations in Ecuador and Chile.

Autor: Blanca Petit Miranda

Tutores: Lourdes García Rodríguez y David Tomás Sánchez Martínez

Dpto. Ingeniería Energética
Escuela Técnica Superior de Ingeniería
Universidad de Sevilla

Sevilla, 2020



Trabajo Fin de Máster
Máster Universitario en Sistemas de Energía Térmica

Potential of Solar Photovoltaic and Wind technologies for industrial water treatment in mining operations

Autor:

Blanca Petit Miranda

Tutores:

Lourdes García Rodríguez
Catedrática de Universidad

David Tomás Sánchez Martínez
Catedrático de Universidad

Dpto. de Ingeniería Energética
Escuela Técnica Superior de Ingeniería
Universidad de Sevilla
Sevilla, 2020

Trabajo Fin de Máster: Potential of Solar Photovoltaic and Wind technologies for industrial water treatment in mining operations

Autor: Blanca Petit Miranda

Tutores: Lourdes García Rodríguez
David Tomás Sánchez Martínez

El tribunal nombrado para juzgar el Proyecto arriba indicado, compuesto por los siguientes miembros:

Presidente:

Vocales:

Secretario:

Acuerdan otorgarle la calificación de:

Sevilla, 2020

El Secretario del Tribunal

A mi familia

A mis amigos

A Ale

Agradecimientos

En este año, tengo mucho que agradecer y a muchas personas:

En primer lugar, a mis padres y mi hermana su paciencia y apoyo, sin estos no habría podido superar este año, ellos han hecho que todo haya sido mucho más fácil.

A Ale, porque siempre tiene las palabras de ánimo adecuadas para que no me rinda y es un apoyo esencial, porque su constancia, esfuerzo y fuerza de voluntad son para mí una fuente de inspiración.

A todos mis amigos, porque siempre están cuando necesito despejarme, por sus ganas de que cumpla todas mis metas y celebrar mis éxitos conmigo como si fuesen suyos.

A David, por haberme acogido en el grupo de Motores y hacerme sentir una más.

A Lourdes, por haberme brindado la oportunidad de enfrascarme en esta aventura, animarme a matricularme en el Máster y a empezar a trabajar para la Universidad, no tengo manera de agradecerle lo mucho que ha hecho por mí. Y por último y no menos importante, por su guía en el desarrollo de este trabajo y por sacar siempre tiempo para ello.

Blanca Petit Miranda

Sevilla, 2020

Resumen

El agua es un bien escaso, puesto que, a pesar de tratarse del elemento más abundante en el planeta, tan sólo un pequeño porcentaje es agua dulce. El aumento de la población, así como el cambio en sus hábitos de consumo junto con el desarrollo de la economía son factores que están provocando que el consumo de agua sea una función creciente, de hecho, con una tasa de un 1% anual. Este hecho hace que la desalación se convierta en la mejor opción para utilizar una fuente de agua, que de otra manera no podría aprovecharse.

Tal y como ocurre con el agua, la energía también es recurso escaso en muchas zonas del planeta. Las fuentes de energía renovable se presentan como una opción a considerar con la creciente concienciación por la preservación del medioambiente, puesto que su utilización permite disminuir la dependencia de la importación de combustibles fósiles, así como la reducción de la emisión de gases de efecto invernadero procedentes de éstos, influyendo directamente de este modo en el calentamiento global y contaminación del aire. A pesar de esto, resulta de vital interés recordar que las fuentes de energía renovables no presentan sólo ventajas, sino que también acarrear desventajas como la intermitencia de su disponibilidad o los mayores costes asociados, inconvenientes que buscarán ser resueltos también en este trabajo.

Son muchos los estudios y plantas piloto que han demostrado la viabilidad de las fuentes de energía renovables acopladas con plantas de ósmosis inversa; Thomson e Infield (2003) simularon e implementaron una planta de ósmosis inversa accionada mediante fotovoltaica diseñada para Eritrea, el Instituto Tecnológico de Canarias ha desarrollado sistemas independientes que funcionan tanto con fotovoltaica (DESSOL) como con energía eólica (AEROGEDESA).

La minería es de por sí, una actividad con alto impacto en el medioambiente, este proyecto pretende evaluar la viabilidad de diferentes diseños de plantas de ósmosis inversa para la producción de agua desalada mediante la utilización de tecnología fotovoltaica y eólica en las cuencas mineras de Ecuador y Chile.

No sólo se ha evaluado la producción energética en cada una de las localizaciones seleccionadas como más favorables en previos estudios, sino que se ha analizado la producción de agua para diferentes diseños; sin sistemas de almacenaje de energía, con sistemas de almacenamiento de energía y operación por escalones. Por último, se analizan los costes derivados de cada uno de los subsistemas y cómo estos influyen en la elección del diseño de planta más favorable.

Abstract

Water is a scarce commodity, while it is true that it is the most abundant element on planet Earth, only a small percentage is freshwater. Population growth, as well as changing consumption habits along with economic development are factors that are causing water consumption to be an increasing function, in fact, with a growth rate of 1% yearly. This causes desalination to be the best option in order to utilise a source of water, that otherwise could not be used.

Energy, likewise water, is a scarce resource in many parts of the world. Renewable Energy Sources portray as an option to consider due to rising awareness of environmental preservation, since its utilisation allows diminishing fossil fuels dependence, as well as greenhouse gas emissions, directly influencing on global warming and air pollution. Yet it is important to have in mind that renewable energy sources do not only imply advantages, but they also entail drawbacks such as their availability intermittence, higher associated costs, inconveniences that will be solved in this work.

Many studies have been carried out about this topic and pilot plants have demonstrated the feasibility of renewable energy resources coupled with reverse osmosis; Thomson and Infield (2003) simulate and implement a PV-driven Reverse Osmosis designed for Eritrea, The Canary Islands Technological Institute (ITC, Spain) developed stand-alone systems for both PV (DESSOL) and wind (AEROGEDESA) technologies.

Mining is on its own an activity with high impact on the environment, this project pretends evaluating the feasibility of different designs of reverse osmosis plants for desalinated water production through the use of photovoltaic and wind technologies in mining operations in Ecuador and Chile.

Not only energy production in each of the locations selected as most favourable on previous studies but also water production have been studied for different designs; without energy storage, with energy storage and gradual capacity. Lastly, costs derived of all the subsystems are analysed and how they influence system selection.

Index

Agradecimientos	vii
Resumen	ix
Abstract	xi
Index	xiii
Index of Tables	xvii
Index of Figures	xix
Notation	xxiii
1 Introduction	1
1.1. <i>Water scarcity</i>	1
1.2. <i>Use of water in mining industry</i>	3
1.3. <i>Context. REMIND</i>	3
1.4. <i>Objectives</i>	4
1.5. <i>Structure</i>	4
2 Preliminary assessment	7
2.1. <i>Selection criteria for localisations</i>	7
2.2. <i>Renewable energy systems</i>	8
2.1.1. METEONORM 7	8
2.1.2. Methodology of work for Solar Photovoltaic Systems	11
2.1.3. Methodology of work for Wind Systems	13
3 Power Curves of Wind Turbines	17
3.1. <i>Methodology of work for Wind Systems</i>	17
3.2. <i>Wind turbine of 3.3 MW rated</i>	18
3.3. <i>Wind turbine of 2 MW rated</i>	21
3.4. <i>Wind turbine of 1 MW rated</i>	21
3.5. <i>Wind turbine of 0.5 MW rated</i>	22
3.6. <i>Wind turbine of 15 kW rated</i>	22
4 Reverse Osmosis and Desalinated Water Production	25
4.1. <i>Reverse Osmosis</i>	25
4.1.1. Basic configurations	26
4.2. <i>Design</i>	27
4.2.1. Reverse Osmosis membrane and rack designs	27
4.2.2. Seawater desalination plant design	27
4.2.3. Energy supply	28
4.3. <i>Part load operation</i>	28
4.3.1. Batch operation	29
4.3.2. Gradual capacity	29
4.3.3. Hybrid systems. Wind-PV	30
4.4. <i>Desalinated water production. Case of study</i>	30

5	Preliminary selection of Reverse Osmosis system designs	33
5.1	<i>Energy storage systems selection</i>	34
5.1.1	Small scale	41
5.2	<i>Gradual capacity methodology</i>	42
5.3	<i>Discussion of the results</i>	43
6	Impact of batteries in desalinated water production with solar photovoltaic systems	49
6.1	<i>Energy production</i>	50
6.1.1	Ecuador	50
6.1.2	Chile	52
6.2	<i>Water production</i>	56
6.2.1	Ecuador	57
6.2.2	Chile	57
6.3	<i>Water production for different Specific Energy Consumptions</i>	59
6.3.1	SEC=1 kWh/m ³	60
6.3.2	SEC=0.5 kWh/m ³	61
7	Impact of batteries in desalinated water production with wind systems	63
7.1	<i>Energy production</i>	63
7.1.1	Ecuador	63
7.1.2	Chile	66
7.2	<i>Water production</i>	69
7.2.1	Ecuador	70
7.2.2	Chile	71
7.3	<i>Water production for different Specific Energy Consumptions</i>	72
7.3.1	SEC=1 kWh/m ³	72
7.3.2	SEC=0.5 kWh/m ³	74
8	Generalisation to other Applications and Emplacements	77
8.1	<i>Photovoltaic Systems</i>	79
8.1.1	Ireland	79
8.1.2	Wales, United Kingdom	79
8.1.3	Brittany France, France	80
8.1.4	Alentejo, Portugal	81
8.1.5	Canary Islands, Spain	81
8.2	<i>Wind Systems</i>	82
8.2.1	Ireland	82
8.2.2	Wales, United Kingdom	83
8.2.3	Brittany France, France	83
8.2.4	Alentejo, Portugal	84
8.2.5	Canary Islands, Spain	85
8.3	<i>Discussion of the results</i>	85
9	Economic Assessment	87
9.1	<i>Levelised Cost of Energy</i>	87
9.1.1	Solar photovoltaics	88
9.1.2	Onshore wind	89
9.1.3	Capital Expenditure (CAPEX)	90
9.1.4	Ecuador and Chile regions	91
9.1.5	Atlantic region	92
9.2	<i>Levelised Cost of Water</i>	94
9.2.1	Ecuador and Chile regions	94
9.2.2	Atlantic region	95
9.3	<i>Optimisation of water cost</i>	96
10	Conclusions	97

Index of Tables

Table 2–1. Localisations selected for the preliminary study.	8
Table 2–2. METEONORM7 outputs.	10
Table 2–3. Localisations selected for the study.	10
Table 2–4 Table of PV inputs and outputs.	12
Table 2–5. Inputs of the wind system.	15
Table 2–6. Outputs of the wind systems.	15
Table 3–1. Inputs of the wind system.	18
Table 4–1. Main design parameters.	31
Table 4–2. Values of k ratio for large scale plants.	32
Table 4–3. Values of k ratio for small scale capacities.	32
Table 5–1. Water production for different k ratios.	33
Table 5–2. Useful energy from energy storage system in PV system of 3.3 MW when nominal consumption of the RO plant is 1500 kW, Cañar.	34
Table 5–3. Useful energy from energy storage system in wind system of 3.3 MW when nominal consumption of the RO plant is 1500 kW, Cañar.	34
Table 5–4. Useful energy from energy storage system in small PV (15 kW) installation when nominal consumption of the RO plant is 6 kW, Cañar.	41
Table 5–5. Useful energy from energy storage system in small wind installation (15 kW) when nominal consumption of the RO plant is 6 kW, Cañar.	41
Table 5–6. Battery capacity depending on the RO nominal consumption.	41
Table 5–7. Main design parameters.	43
Table 5–8. Gradual capacity steps.	43
Table 6–1. Localisations under study.	49
Table 6–2. Battery data.	49
Table 6–3. Energy production in Ecuador, with two hours of energy storage.	52
Table 6–4. Energy production in Chile, with two hours of energy storage.	56
Table 6–5. Values of k ratio for large scale plants.	56
Table 6–6. Water production with PV, SEC=2.14 kWh/m ³ .	59
Table 6–7. Water production with PV, SEC=1 kWh/m ³ .	60
Table 6–8. Water production with PV, SEC=0.5 kWh/m ³ .	61
Table 7–1. Energy production in Ecuador, with two hours of energy storage.	65
Table 7–2. Energy production in Chile, with two hours of energy storage.	68
Table 7–3. Values of k ratio for large scale plants.	69
Table 7–4. Values of k ratio for small scale capacities.	69

Table 7–5. Water production with Wind, SEC=2.14 kWh/m ³ .	71
Table 7–6. Water production with Wind, SEC=1 kWh/m ³ .	72
Table 7–7. Water production for a 15 kW wind turbine, SEC=1 kWh/m ³ .	73
Table 7–8. Water production with Wind, SEC=0.5 kWh/m ³ .	74
Table 7–9. Water production for a 15 kW wind turbine, SEC=0.5 kWh/m ³ .	74
Table 8–1. Localisations selected for the study	78
Table 8–2. Water production with PV in Ireland, SEC=2.03 kWh/m ³ .	79
Table 8–3. Water production with PV in Wales, SEC=2.03 kWh/m ³ .	79
Table 8–4. Water production with PV in Brittany France, SEC=2.03 kWh/m ³ .	80
Table 8–5. Water production with PV in Alentejo region, SEC=2.03 kWh/m ³ .	81
Table 8–6. Water production with PV in Canary Islands region, SEC=2.03 kWh/m ³ .	81
Table 8–7. Water production with wind in Ireland, SEC=2.03 kWh/m ³ .	82
Table 8–8. Water production with wind in Wales, SEC=2.03 kWh/m ³ .	83
Table 8–9. Water production with wind in Brittany France, SEC=2.03 kWh/m ³ .	83
Table 8–10. Water production with wind in Alentejo region, SEC=2.03 kWh/m ³ .	84
Table 8–11. Water production with wind in Canary Islands, SEC=2.03 kWh/m ³ .	85
Table 9–1. Discount rate values.	88
Table 9–2. Parameters used for the economical assessment.	88
Table 9–3. Capital costs of components.	90
Table 9–4. LCOE (€/kWh) values in Ecuador and Chile.	91
Table 9–5. LCOE (€/kWh) values in Atlantic region.	92
Table 9–6. LCOW (€/m ³) values in Ecuador and Chile.	94
Table 9–7. LCOW (€/m ³) values in Atlantic region.	95

Index of Figures

Figure 1-1. Global Water Demand for 2030 based on the optimistic scenario. [4]	1
Figure 1-2. World water use. [5]	2
Figure 1-3. Total desalination demand in 2030 for an optimistic scenario. [4]	2
Figure 1-4. Water demand projection in copper mining (2019-2030), Chile. [7]	3
Figure 2-1. Mining concessions maps of Ecuador and Chile.	7
Figure 2-2. Energy sources for desalination.	8
Figure 2-3. METEONORM7 first interface.	9
Figure 2-4. METEONORM7 interface to choose the parameters that are needed.	9
Figure 2-5. METEONORM7 outputs interface.	10
Figure 2-6. Exemplary loss diagram for a PV plant, as provided by PVSyst.	11
Figure 2-7. Exemplary graph of wind speed gathered by the meteorological station throughout January.	13
Figure 2-8. Power curve for VESTAS model selected.	14
Figure 3-1. Power curve for VESTAS model selected.	17
Figure 3-2. Power curve for VESTAS 112 3.3 MW IEC IIA.	18
Figure 3-3. Linear approximation of the power curve for VESTAS 112 3.3 MW IEC IIA between 3 and 5 m/s.	19
Figure 3-4. Linear approximation of the power curve for VESTAS 112 3.3 MW IEC IIA between 5 and 7 m/s.	19
Figure 3-5. Linear approximation of the power curve for VESTAS 112 3.3 MW IEC IIA between 7 and 12 m/s.	19
Figure 3-6. Example of energy production the first day of the year in Cañar.	20
Figure 3-7. Energy production in Cañar throughout the year.	20
Figure 3-8. Power curve for VESTAS 90 2 MW IEC IIA.	21
Figure 3-9. Power curve for ENERCON 58 1 MW IEC IIA.	21
Figure 3-10. Power curve for VESTAS 39 0.5 MW IEC IIA.	22
Figure 3-11. Power curve for ENBREEZE 15 KW WIND TURBINE.	22
Figure 4-1. On the left, two compartments divided by a semipermeable membrane. On the right, state of equilibrium.	25
Figure 4-2. Process of Reverse Osmosis.	26
Figure 4-3. Conceptual diagram of the basic SWRO process.	26
Figure 4-4. Conceptual diagram of two pass configuration.	26
Figure 4-5. Conceptual diagram of partial two pass configuration.	26
Figure 4-6. Conceptual diagram of two stages for high salinity configuration.	27
Figure 4-7. Energy collected with PV during the first five days of the year and useful energy in Cañar.	28

Figure 4-8. Gradual capacity SWRO plant in Pozo Izquierdo, Canarias (SDAWES Project, ITC). [22]	29
Figure 4-9. Exemplary cases of water composition in a number of plant locations.	30
Figure 4-10. System configuration scheme.	31
Figure 5-1. Sensibility analysis RES installations of 3.3 MW, Cañar.	34
Figure 5-2. Energy collected and energy stored in the battery during January in Cañar for PV systems.	37
Figure 5-3. Energy collected and energy stored in the battery during January in Cañar for wind systems.	40
Figure 5-4. Sensibility analysis RES installations of 15 kW, Cañar.	41
Figure 5-5. Gradual capacity configuration.	42
Figure 5-6. Water production for a PV system profile throughout the year in Cañar, for different system configurations.	44
Figure 5-7. Water production for a PV system profile throughout the year in Machala, for different system configurations.	44
Figure 5-8. Water production for a PV system profile throughout the year in Santiago, for different system configurations.	45
Figure 5-9. Water production for a PV system profile throughout the year in Valparaíso, for different system configurations.	45
Figure 5-10. Water production for a PV system profile throughout the year in Antofagasta, for different system configurations.	46
Figure 5-11. Summary of water production for a PV system profile, for different system configurations.	46
Figure 6-1. Comparison of the number of hours the RO plant is operating without and with batteries in Cañar and Machala.	50
Figure 6-2. Energy collected with wind and energy stored in the battery during January in Cañar and Machala.	51
Figure 6-3. Monthly useful energy profile in Ecuador, with two hours of energy storage.	52
Figure 6-4. Operation of the RO Plant during January in Santiago, Valparaíso and Antofagasta in Chile.	54
Figure 6-5. Comparison of the number of hours the RO plant is operating without and with batteries in Santiago, Valparaíso and Antofagasta in Chile.	55
Figure 6-6. Monthly useful energy profile in Chile, with two hours of energy storage.	56
Figure 6-7. Desalinated water production with batteries in Cañar, SEC=2.14 kWh/m ³ .	57
Figure 6-8. Desalinated water production with batteries in Machala, SEC=2.14 kWh/m ³ .	57
Figure 6-9. Desalinated water production with batteries in Santiago, SEC=2.14 kWh/m ³ .	58
Figure 6-10. Desalinated water production with batteries in Valparaíso, SEC=2.14 kWh/m ³ .	58
Figure 6-11. Desalinated water production with batteries in Antofagasta, SEC=2.14 kWh/m ³ .	58
Figure 6-12. Desalinated water production in all regions with and without energy storage given a k ratio, SEC=2.14 kWh/m ³ .	59
Figure 6-13. Desalinated water production in all regions with two hours of energy storage and without energy storage given a k ratio, SEC=0.5 kWh/m ³ .	60
Figure 6-14. Desalinated water production in all regions with two hours of energy storage and without energy storage given a k ratio, SEC=0.5 kWh/m ³ .	61
Figure 7-1. Comparison of the number of hours the RO plant is operating without and with batteries in Cañar.	63
Figure 7-2. Energy collected with wind and energy stored in the battery during January in Cañar and Machala.	64

Figure 7-3. Monthly useful energy profile in Ecuador, with two hours of energy storage.	65
Figure 7-4. Monthly useful energy profile in Ecuador for a 15 kW wind turbine, with two hours of energy storage.	66
Figure 7-5. Operation of the RO Plant during January in Antofagasta and Valparaíso, Chile.	66
Figure 7-6. Operation of the RO Plant during January in Antofagasta and Valparaíso, Chile.	67
Figure 7-7. Monthly useful energy profile in Chile, with two hours of energy storage.	68
Figure 7-8. Monthly useful energy profile in Chile for a 15 kW wind turbine, with two hours of energy storage.	69
Figure 7-9. Desalinated water production with batteries in Cañar, SEC=2.14 kWh/m ³ .	70
Figure 7-10. Desalinated water production with batteries in Machala, SEC=2.14 kWh/m ³ .	70
Figure 7-11. Desalinated water production with batteries in Antofagasta, SEC=2.14 kWh/m ³ .	71
Figure 7-12. Desalinated water production with batteries in Valparaíso, SEC=2.14 kWh/m ³ .	71
Figure 7-13. Desalinated water production with two hours of energy storage and without batteries, SEC=2.14 kWh/m ³ .	72
Figure 7-14. Desalinated water production with two hours of energy storage and without batteries, SEC=1 kWh/m ³ .	73
Figure 7-15. Desalinated water production with two hours of energy storage and without batteries for a 15 kW wind turbine, SEC=1 kWh/m ³ .	73
Figure 7-16. Desalinated water production with two hours of energy storage and without batteries, SEC=0.5 kWh/m ³ .	74
Figure 7-17. Desalinated water production with two hours of energy storage and without batteries for a 15 kW wind turbine, SEC=0.5 kWh/m ³ .	75
Figure 8-1. Map of the regions selected for the study.	77
Figure 8-2. Exemplary cases of water composition in several plant locations.	78
Figure 8-3. Desalinated water production with PV plant in Ireland with two hours of energy storage and without energy storage given a k ratio, SEC=2.03 kWh/m ³ .	79
Figure 8-4. Desalinated water production with PV plant in Wales with two hours of energy storage and without energy storage given a k ratio, SEC=2.03 kWh/m ³ .	80
Figure 8-5. Desalinated water production with PV plant in Brittany France with two hours of energy storage and without energy storage given a k ratio, SEC=2.03 kWh/m ³ .	80
Figure 8-6. Desalinated water production with PV plant in Alentejo regions with two hours of energy storage and without energy storage given a k ratio, SEC=2.03 kWh/m ³ .	81
Figure 8-7. Desalinated water production with PV plant in Canary Islands with two hours of energy storage and without energy storage given a k ratio, SEC=2.03 kWh/m ³ .	82
Figure 8-8. Desalinated water production with Wind plant in Ireland with two hours of energy storage and without energy storage given a k ratio, SEC=2.03 kWh/m ³ .	82
Figure 8-9. Desalinated water production with Wind plant in Wales with two hours of energy storage and without energy storage given a k ratio, SEC=2.03 kWh/m ³ .	83
Figure 8-10. Desalinated water production with Wind plant in Brittany France with two hours of energy storage and without energy storage given a k ratio, SEC=2.03 kWh/m ³ .	84
Figure 8-11. Desalinated water production with Wind plant in Alentejo regions with two hours of energy storage and without energy storage given a k ratio, SEC=2.03 kWh/m ³ .	84
Figure 8-12. Desalinated water production with Wind plant in Canary Islands with two hours of energy storage and without energy storage given a k ratio, SEC=2.03 kWh/m ³ .	85
Figure 9-1. Global weighted average LCOE and auction values 2010-2020.	89

Figure 9-2. Global weighted average LCOE and auction values 2010-2020.	89
Figure 9-3. LCOE (€/kWh) for every location in Ecuador and Chile.	91
Figure 9-4. LCOE (€/kWh) for every location in Europe.	92
Figure 9-5. Weighted average LCOE of newly commissioned utility-scale solar PV projects 2010-2020.	93
Figure 9-6. Weighted average LCOE of newly commissioned onshore wind projects 1984-2019.	93
Figure 9-7. LCOW (€/m ³) for every location in Ecuador and Chile.	95
Figure 9-8. LCOW (€/m ³) for every location in Europe.	96

Notation

RES	Renewable Energy Sources
RE	Renewable Energy
RO	Reverse Osmosis
PV	Photovoltaic
η_{PV}	Photovoltaic system efficiency
$E_{PV,a}$	Energy injected to the grid
I_{eff}	Effective irradiance
v	Speed
z	Height
z_0	Length roughness
P	Power
SWRO	Seawater Reverse Osmosis
BWRO	Brackish Water Reverse Osmosis
HID	Hybrid Interstage Design
ISD	Interstaged Design
HPP	High Pressure Pump
BP	Booster Pump
ERD	Energy Recovery Devices
SEC	Specific Energy Consumption
$P_{W,HPP}$	Power consumed by the High Pressure Pump
q_{vP}	Permeate volume flow
k	Ratio between the nominal consumption of the RO plant and the rated energy production of the RES plant
p_v	Pressure vessel
n	Number of membranes
S	Surface
LCOE	Levelised Cost of Energy
I_n	Investment cost in period n
M_n	Operations and maintenance expenditures in the year n
F_n	Fuel expenditures in year n
E_n	Electricity generation in the year n
N	Total number of periods
d	Discount rate
CAPEX	Capital Expenditure
LCOW	Levelised Cost of Water

1 INTRODUCTION

“Water is the driving force of all nature.”
 - Leonardo Da Vinci -

This first chapter aims to contextualise the project, as well as exposing the objectives to be met and the structure that will be followed.

Water and energy are indisputably two fundamental drivers in society. The demographic growth and climate change have caused an imbalance between available water and its demand, whether it is for consumption, agricultural sector or industry. [1]

1.1. Water scarcity

Water is the most abundant element in the planet Earth, yet not all of it is useful as from the 100% of existing water, only a 2.5% is fresh and the 97.5% remaining is seawater held by the oceans. The 69.7% of this fresh water is frozen into the polar icecaps, the 30% is difficult access groundwater and only the 0.3% is available for human consumption, which makes essential to understand the significance of desalination processes. [2]

The water global demand has been increasing at a rate of about 1% per year as a function of population growth, economic development and changing consumption patterns, among other factors, and it is a fact of a matter that it will continue to grow significantly over the next decades. Countries with emerging economies will be responsible for the vast majority of this growth as Figure 1-2 showcases. [3]

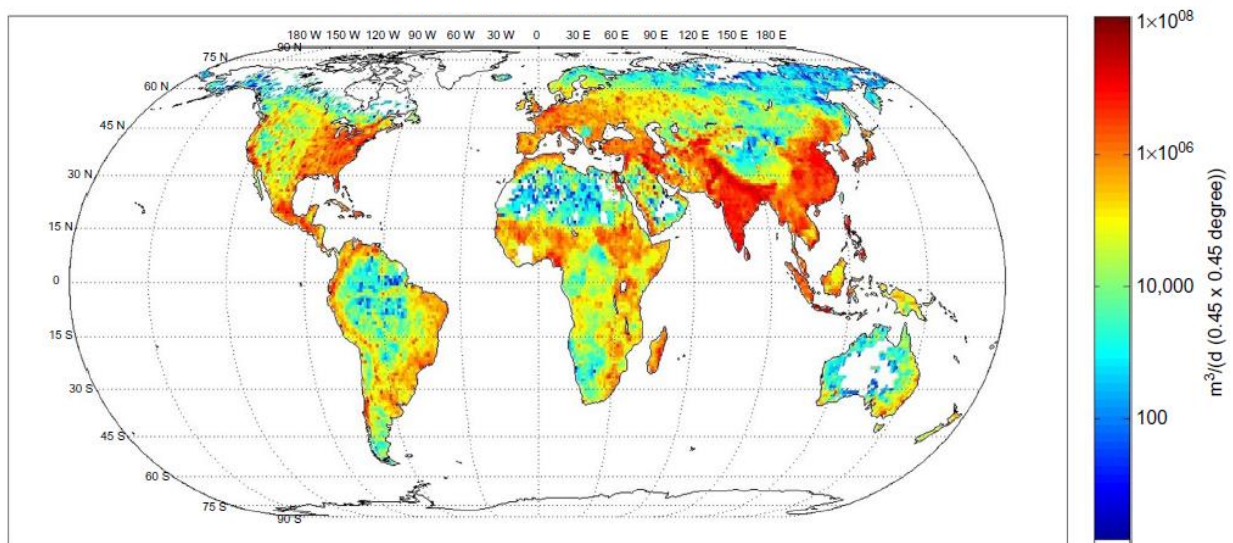


Figure 1-1. Global Water Demand for 2030 based on the optimistic scenario. [4]

In many parts of the world there are water resources with mineralisation that makes them unsuitable for industrial purposes. Freshwater is a scarce resource and water desalination enables to produce water suitable for any type of consumption from brackish or sea water, which offers the possibility of exploiting a source of water that otherwise would not be exploitable.

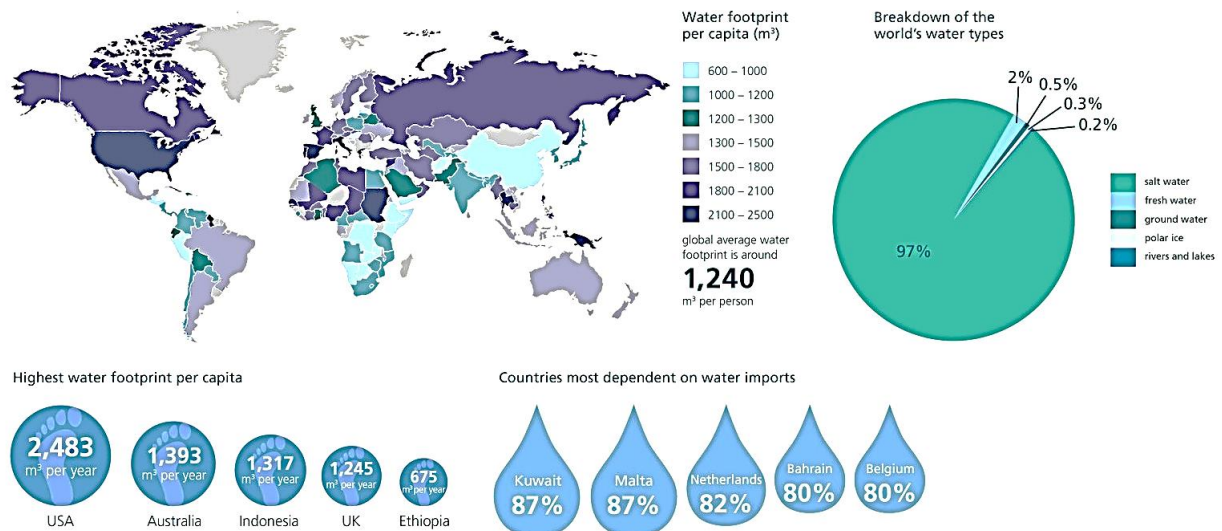


Figure 1-2. World water use. [5]

The development of renewable energy technologies during the last decades has been enhanced by the growing energy demand, the increasing interest in the search of independence from fossil fuels and preservation of the environment. As renewables are becoming increasingly main stream and technology prices continue to decline, these type of technologies are especially favourable for desalination applications, since they offer a sustainable alternative in regions where the wind or the sun are abundant resources and allow to consume in the same place of its generation, which diminishes energy losses, and, subsequently, the costs associated. [6]

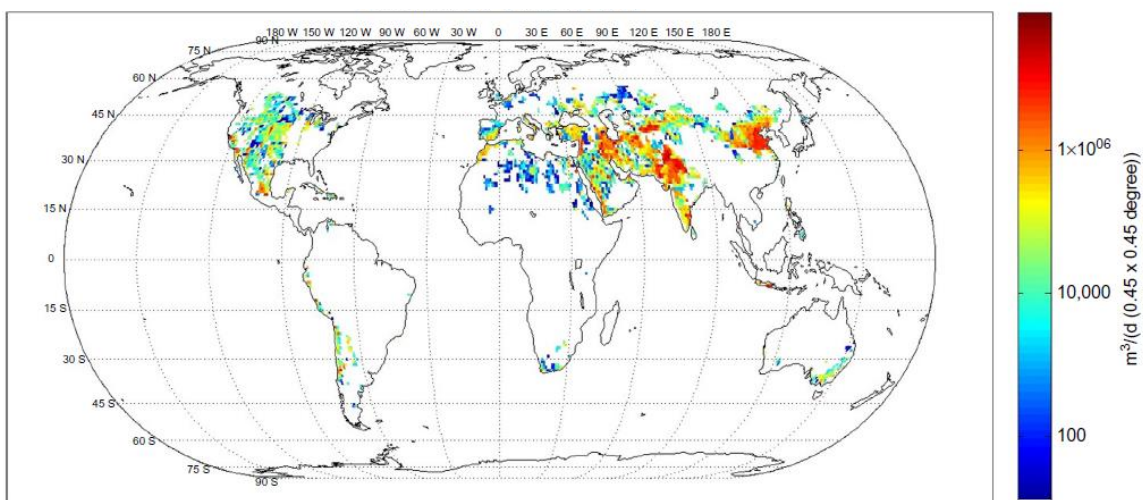


Figure 1-3. Total desalination demand in 2030 for an optimistic scenario. [4]

The framework of this project makes these technologies position as the first option. These non-conventional energy sources have demonstrated thus far to be competitive for desalination projects, the feasibility of photovoltaic and wind technologies will be examined.

1.2. Use of water in mining industry

Since this project is mainly focussed on mining industry, it is essential to understand the demand of water this specific industry generates. Water is mainly used in mining industry for transport of ore and waste in slurries and suspension, separation of minerals through chemical processes, physical separation of dust, cooling systems around power generation, suppression of dust (during mineral processing and around convey), washing equipment, dewatering of mines and employees' needs; it includes desalination and water treatments.

In most mining operations, water is sought from groundwater, streams, rivers and lakes, or through commercial water service suppliers. It is not uncommon that mines are located in areas with water scarcity which means that the previously mentioned water sources committed to human consumption. Water extraction becomes an issue as well, in many cases, especially with underground mining, considering that water needs to be pumped away from a mine site, which can reduce the levels of ground water, deplete surface water or cause pollution to local rivers.

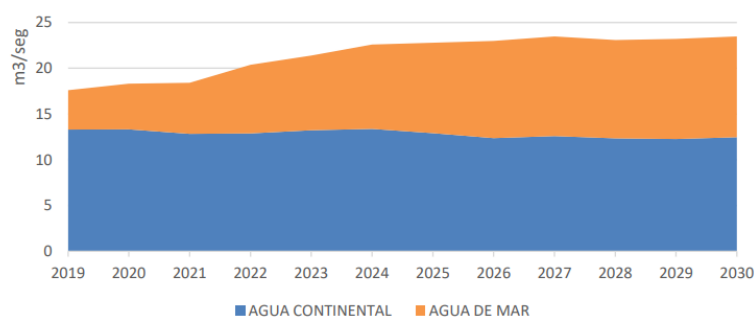


Figure 1-4. Water demand projection in copper mining (2019-2030), Chile. [7]

1.3. Context. REMIND

This Final Master thesis is included within the Project REMIND (Renewable Energies for Water Treatment and Reuse in Mining Industries), whose overall is to develop an innovative framework of interplay between Renewable Energy Sources (RES) and innovative Water Treatment Technologies in the logic of a sustainable growth for mining industries.

The novel paradigms explored are expected to drastically reduce the environmental impact due to extensive water and energy consumption, and to release of untreated wastewater during the production cycle of copper and gold. The REMIND collaborative network among European Union, Chile and Ecuador is in line with EU policy and strategy for raw materials supply; moreover, this partnership supports the economic and research efforts of Latin American countries towards a more eco-friendly and RES-driven development.

The bi-directional knowledge transfer activities implemented in REMIND aim to:

- Implement a rational use of water resources in the logic of circular economy.
- Promote a carbon-free technological approach (water-energy nexus) for reducing conventional energy resources requirements.
- Mitigate health environmental risk in two demonstration sites (mining districts of Antofagasta – CL and Regione de l’Oro – EC)
- Exploit the intersectorial cooperation between academia and industry by setting best practices for knowledge transfer in analogous contexts.

REMIND brings together 8 leading High Education Institutions and Large Companies from 4 Countries (Italy, Spain, Chile and Ecuador), and implements a multi-sectorial and transdisciplinary network that generates 64 secondments and 73 Knowledge Transfer Activities. [8]

1.4. Objectives

This Final Master thesis expands REMIND Project objectives considering another water treatment of great importance as water desalination is, by the achievement of the following objectives:

General objective:

- Analysis of photovoltaic and wind technologies for off grid installations (desalination and water treatments in mining) for different emplacements. The installed rated power considered ranges from small installations up to industrial capacity, being studied through cases of small power installed with 12 kW up to a representative case of industrial capacity systems with 3.3 MW.

Specific objectives:

- Assessment of photovoltaic and wind energy with energy storage for desalination application and water treatments in different localisations.
- Analysis of dedicated desalination designs that allows efficient part load operation as an alternative solution to the use of energy storage with high capacity.
- Costs assessment.
- Stablishing a design that ensures the minimization of costs.

1.5. Structure

Chapter 1 Introduction.	This chapter aims to provide a general vision of the project motivation, its context, as well as the objectives it pursues.
Chapter 2 Preliminary assessment.	The objective of this chapter is to introduce the methodology followed to calculate the energy production.
Chapter 3 Power curves of wind turbines.	This chapter aims to model the energy output for different wind turbines.
Chapter 4 Water treatments based on Reverse Osmosis: Desalination and mining wastewater treatment.	This chapter offers a general view of the fundamentals of Reverse Osmosis, as well as, the process followed to calculate water produced and specific energy consumption corresponding to a given system design, dealing with both water desalination and treatment of wastewater from mining industry.
Chapter 5 Preliminary selection of Reverse Osmosis system designs.	Considering off-design behaviour of Reverse Osmosis systems with candidate design configurations described in chapter 4, a preliminary selection of suitable designs will be performed concerning water desalination and mining wastewater treatment.
Chapter 6 Impact of batteries in desalinated water production in PV Systems.	Energy storage systems repercussion on desalinated water production profile for solar photovoltaic systems.
Chapter 7 Impact of batteries in desalinated water production in Wind Systems.	This chapter extends the topic discussed on Chapter 6 to Wind technology.

Chapter 8
Generalisation to other
Applications and
Emplacements.

The methodology used on previous chapters for mining facilities in Ecuador and Chile, is now applied for other water treatments and localisations.

Chapter 9
Economical assessment.

Study of LCOE and LCOW and final selection of suitable designs.

Chapter 10
Conclusions.

This chapter is a summary of the conclusions made on previous chapters, and a review of the accomplishments achieved.

2 PRELIMINARY ASSESSMENT

The objective of this chapter is to introduce the methodology followed in order to calculate the energy production for each of the cases that are under assessment, in other words, solar photovoltaic and wind technologies.

Desalination processes require large quantities of energy and, unfortunately, most large desalination plants around the world are driven by fossil fuels, which release greenhouse gases in addition to other hazardous emissions that contribute to climate change. Moreover, the need to develop new and alternate energy sources is becoming crucial for energy security and future sustainable development as the limited fossil fuel reserves are being depleted. Only about 1% of total desalinated water is currently based on energy from renewable sources. However, there is a large market potential for desalination systems powered by renewable energy sources worldwide. [9]

2.1. Selection criteria for localisations

The small and artisanal gold mining (SMAG) industry in certain regions of the world, in particular Latin America, is comprised of a myriad of small facilities in remote, off-grid areas, with no supply of electricity or fuels [10]. The study focusses on mining regions, for which the density of mining operations was first studied in order to establish those emplacements that were going to be studied in Chile and Ecuador.

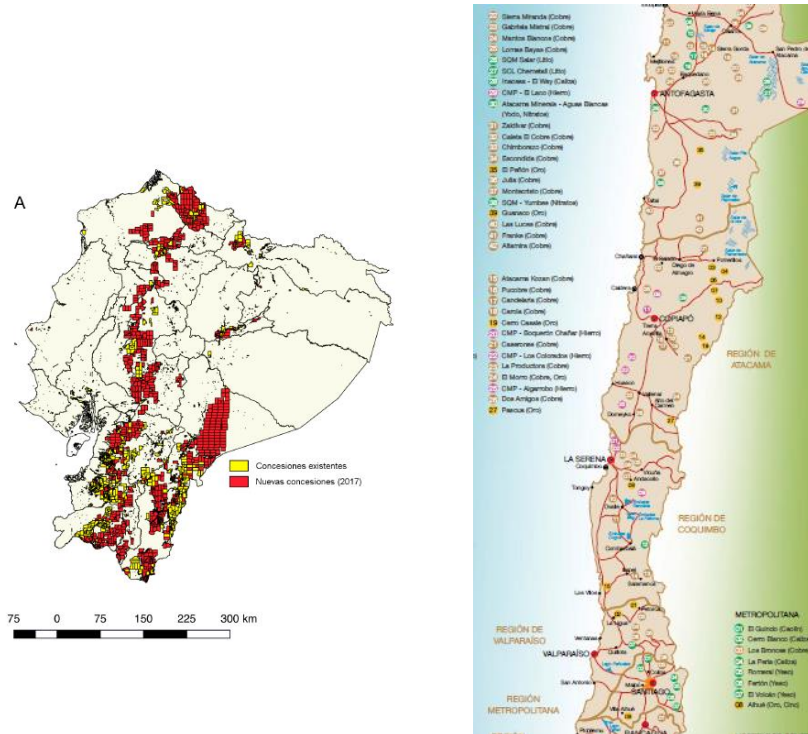


Figure 2-1. Mining concessions maps of Ecuador and Chile. ^{1 2}

¹https://www.google.com/search?q=concesiones+mineras+ecuador&source=lnms&tbn=isch&sa=X&ved=0ahUKewiG_6zEnbXkAhUI3OAKHcsyAQ0Q_AUIEyC&biw=1366&bih=657#imgrc=6-3kzP1Qom5RHM:

²<https://www.cochilco.cl/SIAC/Paginas/Mapa-Minero-de-Chile.aspx>

In the preliminary assessment the foregoing maps were evaluated to decide those localisations where the feasibility of PV and Wind systems was going to be studied.

Table 2–1. Localisations selected for the preliminary study.

ECUADOR	CHILE
Cañar	Antofagasta
Chimborazo	Copiapó
Machala	La Serena
Riobamba	Santiago
San Gabriel	Valparaíso

2.2. Renewable energy systems

Selecting the most suitable renewable energy-driven desalination technology depends on several factors such as the size of the plant, the salinity of the feed water and required product, remoteness, existence of access to an electricity grid, technical infrastructure and the RES and its availability, potential and exploitation cost. There are several combinations of desalination and RE technologies, which are particularly promising with regard to their economic and technological feasibility. [11]

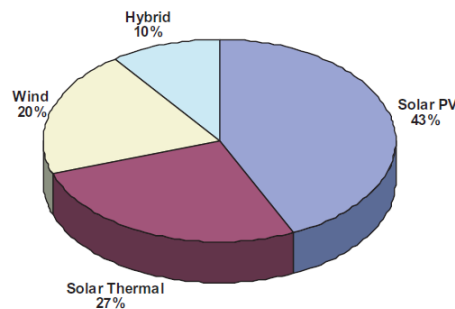


Figure 2-2. Energy sources for desalination.³

Since the assessment focusses on solar and wind as energy sources, the first step in order to develop the project was gathering of the weather data needed. METEONORM7 was the Software used for this purpose.

2.1.1 METEONORM 7

The information about the availability of solar and wind energy is obtained from METEONORM version 7 [12], building on some of the existing weather stations and creating additional sets for other locations through interpolation. This software produces hourly meteorological datasets, from which the following information is taken for the analysis: horizontal global radiation, horizontal diffuse radiation, normal direct radiation, global radiation on the tilted surface, diffuse radiation on the tilted surface, ambient temperature, wind direction, wind speed and atmospheric pressure.

METEONORM [13] is a meteorological database that contains climatological data for solar engineering applications for every region of the globe. It generates typical years interpolating long term monthly means, these typical years represent an average year of the selected period of time, as it is shown in Figure 2-2.

METEONORM7 is fundamentally a method for the calculation of solar radiation on arbitrarily orientated surfaces at any desired location which enables the study of power production with solar source, nonetheless it also generates information about wind speed that can be used to estimate the wind power production for a given wind turbine.

³Source <https://www--sciencedirect--com.us.debiblio.com/science/article/pii/S0038092X03002585?via%3Dihub#FIG1>



Figure 2-3. METEONORM7 first interface.

The fixed database in METEONORM 7 contains approx. 6200 cities, 8325 weather stations and 1200 DRY (Design Reference Year) sites. For weather stations, monthly average values are stored and hourly values are generated accordingly. For cities, the monthly average values (long term averages) are interpolated and then the hourly values generated. In order to collect the solar and wind resources' data when the location from which the data are required is far from a weather station, additional new ones can be created -user defined sites-, and the data from neighbouring weather station will be interpolated.

METEONORM generates hourly weather data, from which the analysis concerns about the following hourly information: horizontal global radiation, horizontal diffuse radiation, normal direct radiation, global radiation on the tilted surface, diffuse radiation on the tilted surface, ambient temperature, wind direction, wind speed and atmospheric pressure. The interface shown in Figure 2-3 allows the user select which parameters the Software is going to generate and the units in which they would be expressed.

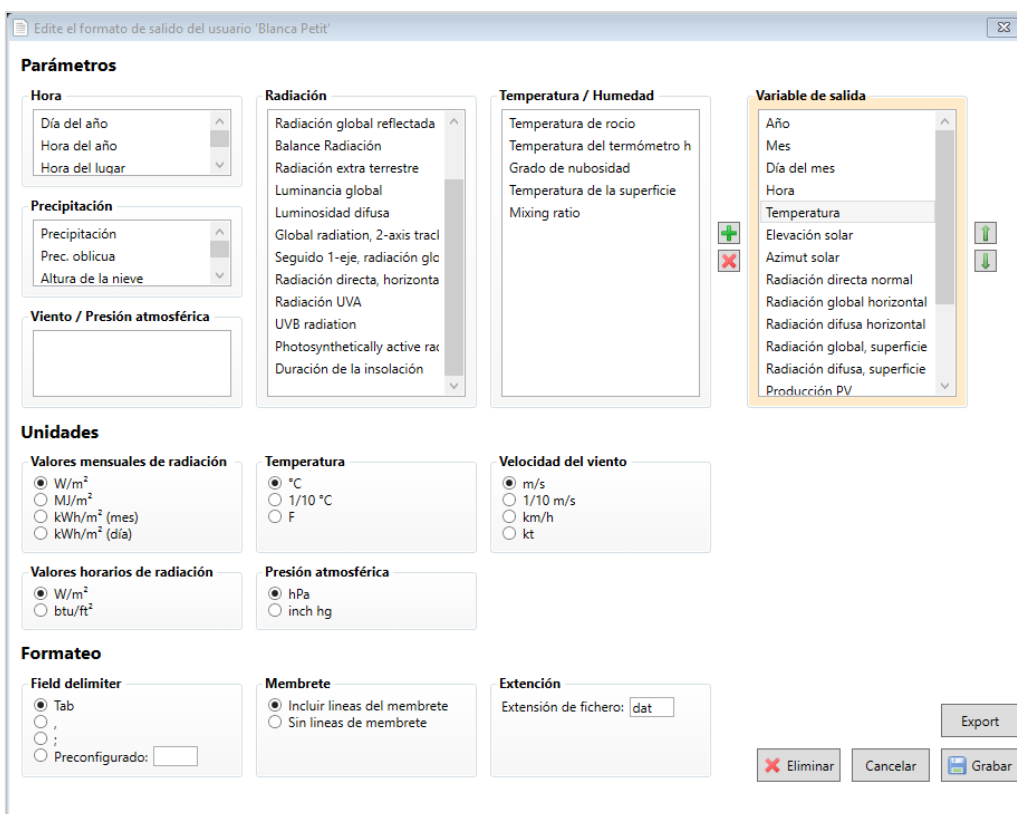


Figure 2-4. METEONORM7 interface to choose the parameters that are needed.

The results, as it was mentioned beforehand, do not represent a real historic year but a hypothetical year, which statistically represents a typical year at the selected location.

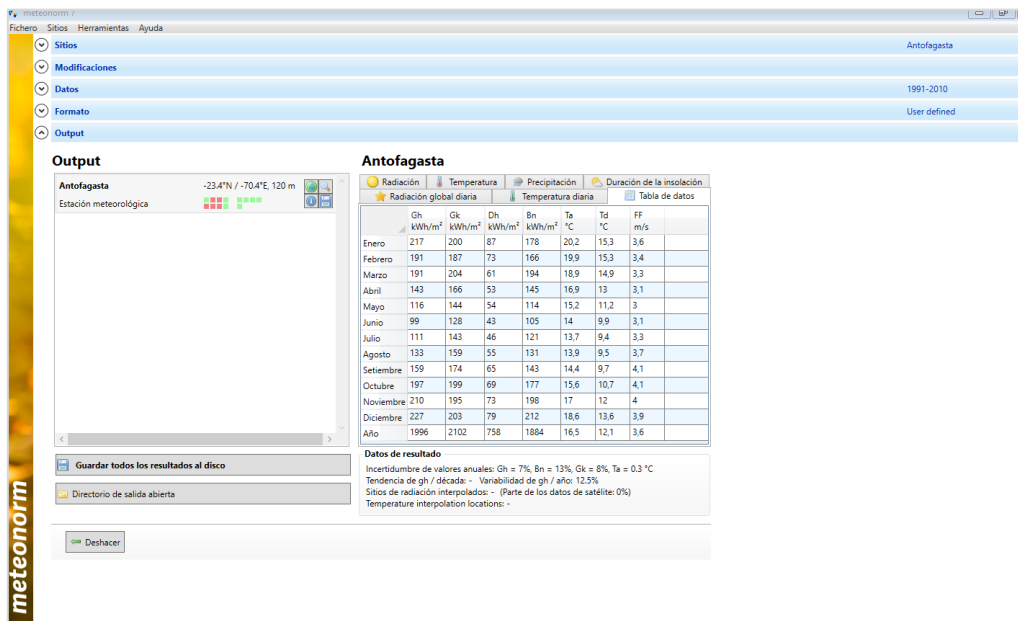


Figure 2-5. METEONORM7 outputs interface.

Table 2–2. METEONORM7 outputs.

Data generated with METEONORM7	
Solar data	Wind data
Normal Direct Radiation, G_{bn} [W/m ²]	Wind direction
Global Horizontal Radiation, G_{gh} [W/m ²]	Wind speed [m/s]
Diffuse Horizontal Radiation, G_{dh} [W/m ²]	Atmospheric pressure [hPa]
Global radiation on tilted Surface, G_{gk} [W/m ²]	
Diffuse radiation on tilted Surface, G_{dk} [W/m ²]	
Ambient Temperature, T_a [°C]	

Once the weather data from METEONORM was gathered, it was noted that there were emplacements where the solar and wind resources were more abundant, therefore it was decided that the study would be focussed on these localisations that seemed to be more representative, listed in the ensuing table:

Table 2–3. Localisations selected for the study.

ECUADOR	CHILE
Cañar	Antofagasta
Machala	Santiago
	Valparaíso

Some combinations are more suited for large-scale desalination plants, whereas others are more appropriate for small-scale applications. The following subsections describe the methodology adopted to study the production of electricity by means of RE resources along with the main assumptions made to analyse the water production capacity of the associated renewable energy technologies.

2.1.2 Methodology of work for Solar Photovoltaic Systems

Photovoltaic installations produce electricity directly from solar radiation. The devices responsible for the conversion of solar radiation to electric energy are photovoltaic cells, which are in association with each other by means of what are called photovoltaic modules.

Studies prove Solar photovoltaic (PV) powered reverse osmosis (RO) to be one of the most promising forms of RE powered desalination, especially when it is used in remote areas [14]. The potential combination of PV with RO has generated growing interest because of the simplicity of both technologies. The compatibility of RO with solar PV power and other RE forms has been greatly enhanced by the appearance of efficient and reliable energy recovery pumps, which recycle the hydraulic energy of the reject brine to assist pumping the feed water. Many installations have been demonstrated throughout the world especially in rural areas for small desalination capacities in the range of 1–5 m³/day based on electro dialysis and reverse-osmosis processes. The advantages of PV energy are reported as: environmental-friendly, no air or sound pollution, minimum maintenance and constant power generation efficiency throughout lifetime. [15]

Once presented PV power systems compatibility with RO the methodology followed for the assessment will be presented in the following paragraphs. The analysis will be developed through PVSyst Software, a program that allows the study, simulation and data analysis of photovoltaic installations. [16]

The system simulation calculates monthly energy distribution throughout the year, the main results are described on the foregoing lines:

- The total energy production [MWh/y] is essential for the evaluation of the PV system’s profitability.
- The Performance Ratio (PR [%]) which is and indicator of the quality of the system itself, independently of the incoming irradiance, expressed as the quotient of the system final yield and the reference yield (energy production if the system were always running at "nominal" efficiency).
- The specific energy [kWh/kWp] is an indicator of production based on the available irradiation (location and orientation).

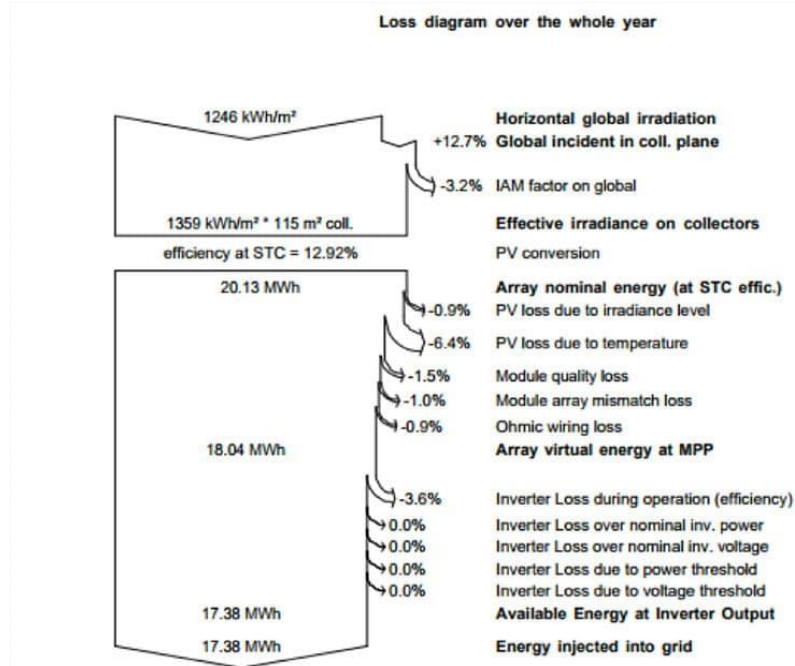


Figure 2-6. Exemplary loss diagram for a PV plant, as provided by PVSyst.

The process can be summarised and easily described in three major steps:

- Specify the desired power or available area.
- Choose the PV module from the internal database.
- Choose the inverter from the internal database.

Once followed the previous steps PVSyst proposes an array or system configuration, that allows to conduct a preliminary simulation.

In order to model the performance of photovoltaic installations, realistic energy efficiencies (η_{PV}) are first calculated. These are indeed obtained by simulation of photovoltaic (PV) systems carried out with PVSyst [16]. The main input data to the software are the available solar irradiance and ambient temperature (the impact of temperature on panel efficiency is included in the calculations) along with the peak power expressed in [Wp], which is the highest power output that can be obtained from the system in the most favourable conditions –power production at given test conditions-. With this information, the software provides the annual yield [MWh/year], specific generation capacity [kWh/kWp] –figure of merit of the potential of the system–, performance ratio [%], as well as all the main variables used and the area needed to produce the rated output of the plant.

Finally, the energy flows presented in the Sankey diagram shown in Figure 2.5 can be translated into a global system efficiency (η_{PV}) enabling the calculation of the hourly yield of the PV modules from the effective irradiance on the tilted panels (I_{eff}), ambient temperature and technical features of the PV field. To this end, hourly values provided by METEONORM 7 were used.

$$\eta_{PV} = \frac{E_{PV,a} [kWh/m^2]}{I_{eff} [kWh/m^2]} \quad (2-1)$$

It is also noted that, for the simulation (i.e., for the calculation of η_{PV}), neither blocking obstacles nor nearby shading elements such as buildings or trees were taken into consideration. The impact of this assumption on the annual yield is estimated at less than 2%, according to the simulations with PVSyst.

Table 2–4 Table of PV inputs and outputs.

Inputs	Outputs (monthly values)
Localisation.	Effective irradiance on collectors.
Solar modules orientation.	Array nominal energy.
Desired power or available area.	Available energy at inverter output.
Photovoltaic modules.	Energy injected into grid.
Inverter.	
Obstacle profile, nearby shadows.	

2.1.3 Methodology of work for Wind Systems

Wind energy can be considered as a product of solar energy as well. The Earth is exposed to the Sun heat, but its inclination and geometry cause a non-uniform heating, but much more accentuated in the equatorial region than in the poles, and these gradients originate air circulation across the globe.

Wind power is an exceptional candidate for powering a desalination unit, especially in remote areas with suitable wind speed. Excellent work on wind and RO systems has been done by the Instituto Tecnológico de Canarias (ITC) within several projects such as AERODESA and SDAWES (Sea Desalination Autonomous Wind Energy System). The SDAWES project installed eight RO units of 25 m³/day capacity each with specific consumption of 7.2 kW h/m³. Additionally, a wind/RO system without energy storage was developed and tested within the JOULE Program (OPRODES-JORCT98-0274) in 2001 by the University of Las Palmas. The typical capacity of the implemented wind/RO units ranged from 50 to 2000 m³/day. [17]

The output of a wind turbine depends on the specifications of the system and on the available wind speed, with ambient temperature playing a secondary role. The latter dataset is obtained from METEONORM which, as described previously, provides hourly time series of wind speed distribution.

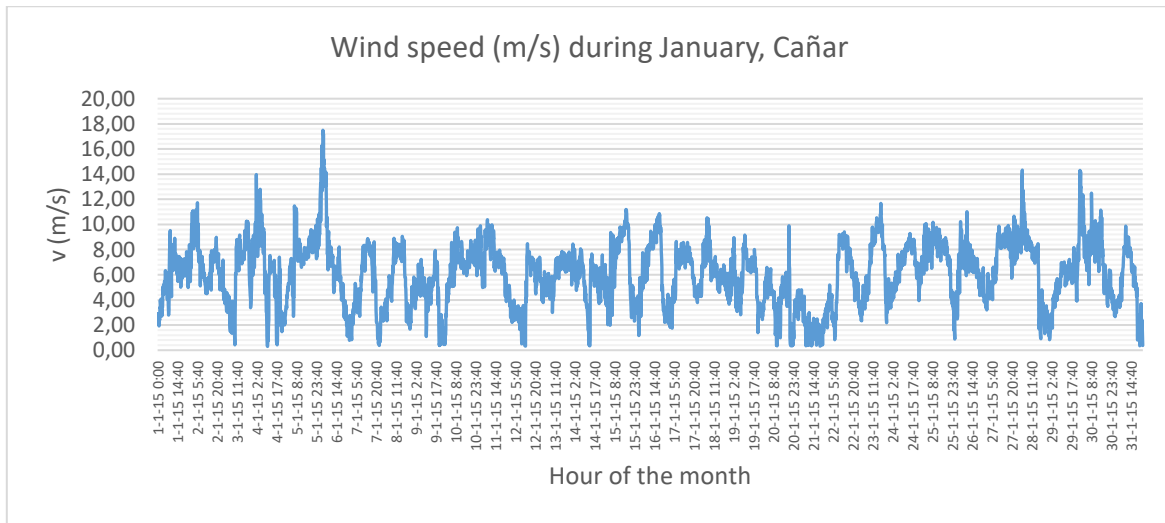


Figure 2-7. Exemplary graph of wind speed gathered by the meteorological station throughout January.

This information about wind speed provided by METEONORM is given at a height of 10 meters above sea level (z_{ref}) and must be corrected to the height at which the hub of the turbine is standing (z). This is done through extrapolation with the following logarithmic equation [18]:

$$v(z) = v(z_{ref}) \frac{\ln\left(\frac{z}{z_0}\right)}{\ln\left(\frac{z_{ref}}{z_0}\right)} \quad (2-2)$$

Where:

- $v(z)$ is wind speed at 80 m [m/s].
- $v(z_{ref})$ is the wind speed provided by METEONORM at 10 m [m/s].
- z is the height of the hub of the wind turbine [m].
- z_0 is the roughness length 0.2 of the field [m].
- z_{ref} is the height whereby measures are taken [m], in this case 10 m.

The following figure, Figure 2-8, showcases the Power curve of one of the chosen wind turbines, VESTAS, V112 3.3 MWTM IEC IB, a performance map of the wind turbine yielding the power output for a given wind speed. Three different regions can be distinguished as it can be seen in the figure:

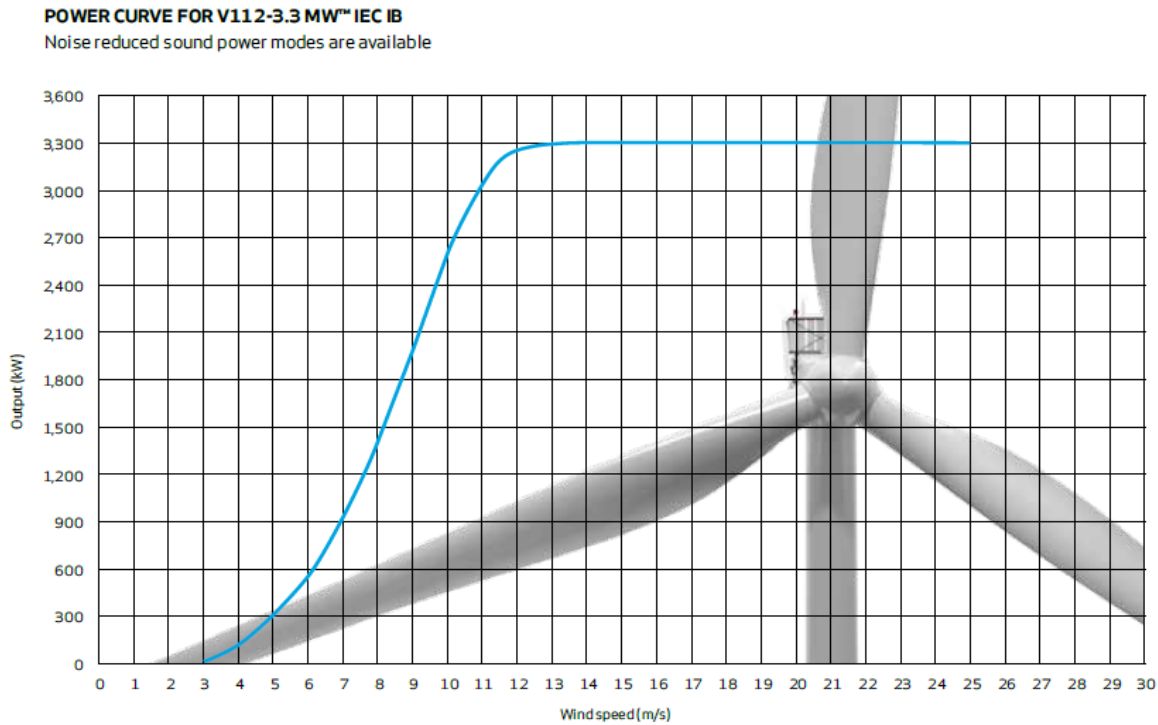


Figure 2-8. Power curve for VESTAS model selected. ⁴

For the calculation of a wind system production we will work with Excel worksheets, in lieu of making use of a specific Software. Once the wind speed at the height of interest is calculated, the power curve can be approximated as follows if the *cut-in* ($v_{w,in}$) and nominal ($v_{w,nom}$) wind speeds are known:

$$P(v) \begin{cases} P = 0 & v_w < v_{w,in} \\ P = m \cdot v + n & v_{w,in} \leq v_w \leq v_{w,rated} \\ P = P_{rated} & v_w > v_{w,rated} \end{cases} \quad (2-3)$$

Where:

- P is power output of the wind turbine [kW].
- v is the wind speed [m/s].
- v_w is the corrected wind speed at the hub.
- $v_{w,in}$ is the cut-in wind speed below which the turbine is not able to produce power.
- $v_{w,rated}$ is the wind speed above which the turbine cannot increase the output because of the limited capacity of the electric generator.
- m and n are coefficients of the linear function fitting the power curve.

With this approximation, the hourly or monthly yield throughout the year can be calculated.

The following tables present a brief summary of the parameters needed to study the energy production profile derived from wind resource, as well as the main results.

⁴Source manufacturer.

Table 2–5. Inputs of the wind system.

Inputs	
Hourly wind data	Provided by the weather station.
Wind turbine power curve	Supplied by the manufacturer.
Wind turbine hub height	Hypothesis.
Roughness length	Hypothesis: Area with roughness length equal to 0.2 m.

Table 2–6. Outputs of the wind systems.

Outputs
Power generated hourly (MWh)
Power generated monthly (MWh)
Energy generated monthly (MWh)

3 POWER CURVES OF WIND TURBINES

This chapter aims to model the energy output for different wind turbines. The concept of power curve and the methodology used for its modelling will be explained, allowing the calculation of the energy production profile for any turbine.

3.1 Methodology of work for Wind Systems

The following figure, Figure 3-1, showcases the Power curve of the chosen wind turbine, VESTAS, V112 3.3 MWTM IEC IB, a performance map of the wind turbine yielding the power output for a given wind speed. Three different regions can be distinguished:

- In the first one, the wind speed is low and the torque the wind exercises on the blades is not enough to make them rotate, which implies that the turbine will not produce power.
- As the wind speed increases and overcomes the cut-in wind speed, electrical power will be generated reaching the rated power output, 3.3 MW.
- Above the cut-out wind speed, even though the power available in the wind, the operating conditions are not safe for the integrity of the wind turbine, through control strategies, the pitch turns then 90 degrees ceasing the aerodynamic load on its blades as well as the electric production, the cost of producing energy under the conditions in this region outweighs the benefits.

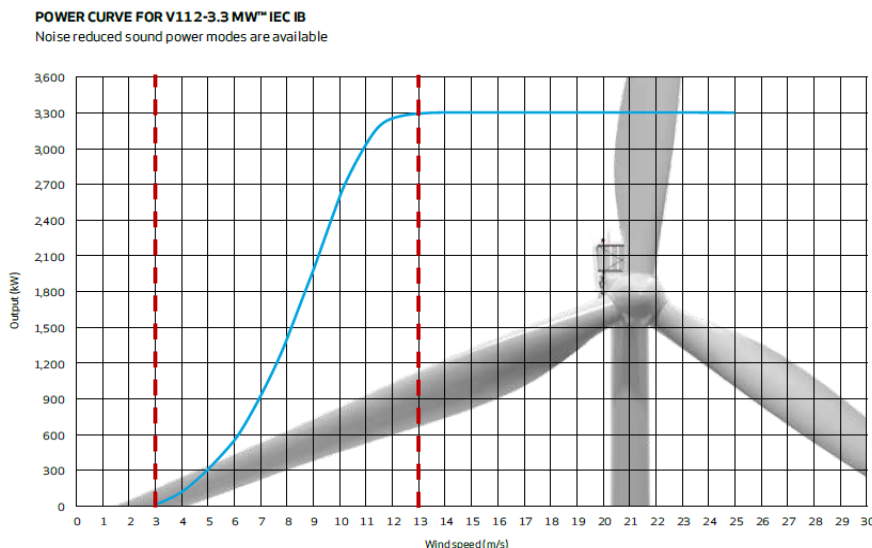


Figure 3-1. Power curve for VESTAS model selected.⁵

Modularity in PV can, in fact, be obtained effortlessly by adding or removing PV modules (effective area), nevertheless, when calculating wind energy production, it is fundamental to highlight the importance of the wind turbine selected, because depending on the height of the hub the results of the wind speed will vary and so will the power curve, as evidenced in previous chapter (equation 2-2). Once the wind speed is known the power curve can be calculated taking into account the cut-in (v_{on}) and cut-out (v_a) wind speed:

⁵Source manufacturer.

$$P(v) \begin{cases} P = 0 & v < v_{on} \\ P = mx + n & v_{on} < v < v_a \\ P = cte & v_a < v \end{cases} \quad (3-1)$$

The range of the energy needed can vary, consequently, the study was made for four different wind turbines with different rated power.

Table 3-1. Inputs of the wind system.

Wind turbines	
3.3 MW	VESTAS, V112/3000
2 MW	VESTAS, V90/2000
1 MW	ENERCON, E58/1000
0.5 MW	VESTAS, V39/500

3.2 Wind turbine of 3.3 MW rated

To begin, Figure 3-2 showcases the Power curve of the chosen wind turbine, VESTAS, V112 3.3 MW IEC IB, it is the starting point for the process of obtaining the energy profile throughout the year.

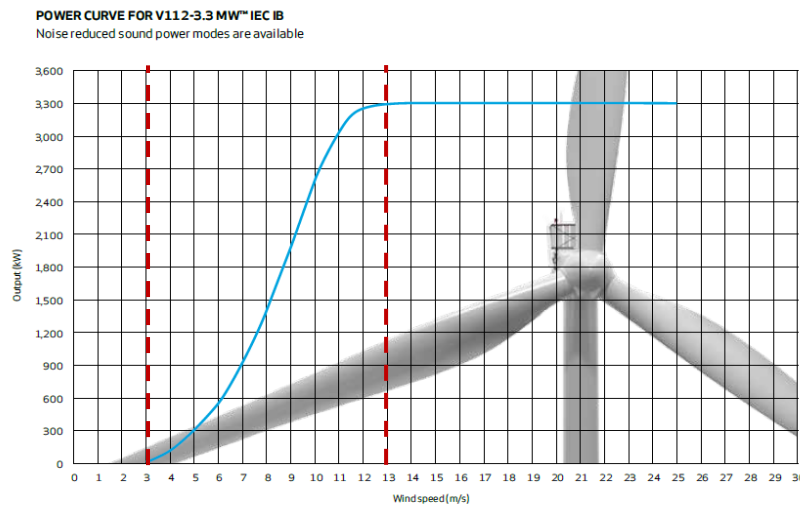


Figure 3-2. Power curve for VESTAS 112 3.3 MW IEC IIA.

Regarding what was explained in section 2.3.2. on the previous chapter, the power curve can be divided in three different regions and defined as a piecewise function, so the power the wind turbine generates depending on the wind speed can be calculated:

$$P(v) \begin{cases} P = 0 & v < 3 \text{ m/s} \\ P = mx + n & 3 \text{ m/s} < v < 12 \text{ m/s} \\ P = cte & 12 \text{ m/s} < v \end{cases} \quad (3-2)$$

Given the function in equation (3-2) the focus is on the region between 3 and 12 m/s as it does not follow the same linear trend as a whole. To this end, this region of the power curve is sectioned once again in three which permits establishing equations that reflect a more substantive interpretation of the power curve by adding trend lines for each segment. Hereunder, an example of the process:

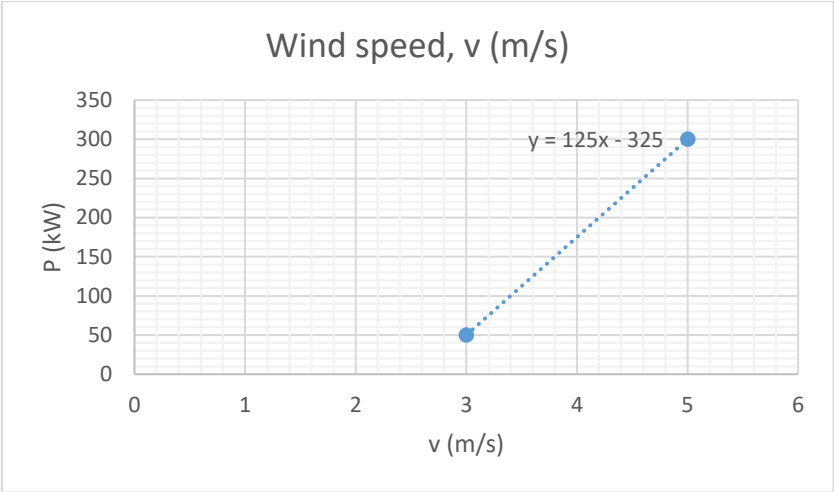


Figure 3-3. Linear approximation of the power curve for VESTAS 112 3.3 MW IEC IIA between 3 and 5 m/s.

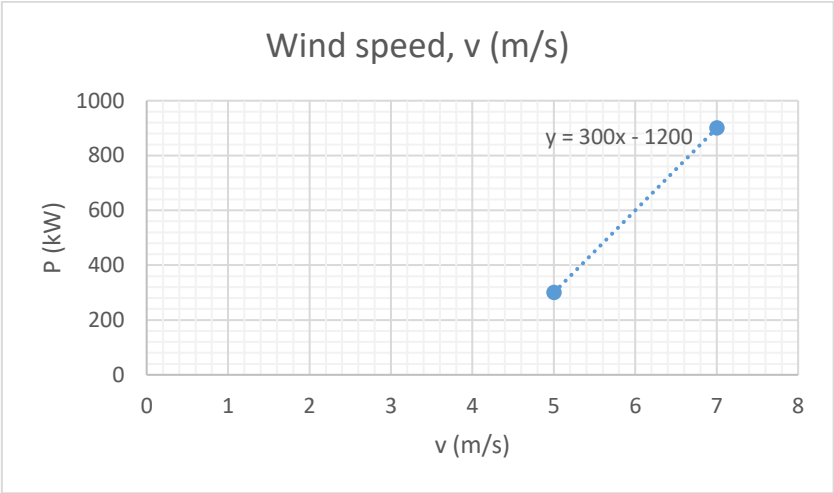


Figure 3-4. Linear approximation of the power curve for VESTAS 112 3.3 MW IEC IIA between 5 and 7 m/s.

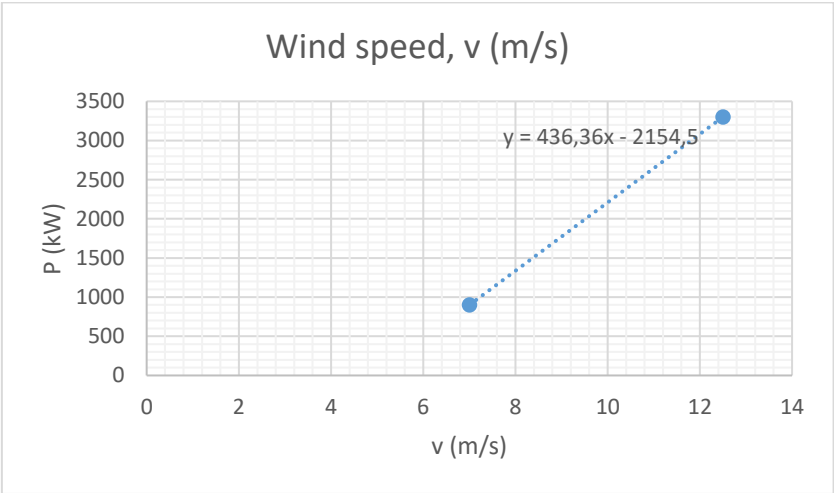


Figure 3-5. Linear approximation of the power curve for VESTAS 112 3.3 MW IEC IIA between 7 and 12 m/s.

Hence, the resulting function is:

$$P(v) \begin{cases} P = 125v - 325 & 3 \text{ m/s} < v < 5 \text{ m/s} \\ P = 300v - 1200 & 5 \text{ m/s} < v < 7 \text{ m/s} \\ P = 436.36v - 2154.4 & 7 \text{ m/s} < v < 12 \text{ m/s} \end{cases} \quad (3-3)$$

Implementing this piecewise function and adding up the results, the energy production throughout the year, for each month can be calculated. As Figure 3-6 shows, thanks to the equation the energy production for each hour is obtained and the sum of all those hours gives the resulting production for each month, as can be seen in Figure 3-7.

Year	Month	Day	Hour	v(10m)	v(80m)	P (kW)	E (kWh)
2005	1	1	1	1,9	2,9	0,0	0,0
2005	1	1	2	1,4	2,1	0,0	0,0
2005	1	1	3	1,2	1,8	0,0	0,0
2005	1	1	4	1,5	2,3	0,0	0,0
2005	1	1	5	1,4	2,1	0,0	0,0
2005	1	1	6	1,8	2,8	0,0	0,0
2005	1	1	7	1,4	2,1	0,0	0,0
2005	1	1	8	2,2	3,4	96,2	96,2
2005	1	1	9	1,8	2,8	0,0	0,0
2005	1	1	10	3,7	5,7	500,0	500,0
2005	1	1	11	3	4,6	249,3	249,3
2005	1	1	12	2,8	4,3	211,0	211,0
2005	1	1	13	3,2	4,9	287,6	287,6
2005	1	1	14	3,7	5,7	500,0	500,0
2005	1	1	15	3	4,6	249,3	249,3
2005	1	1	16	4,4	6,7	821,6	821,6
2005	1	1	17	3,2	4,9	287,6	287,6
2005	1	1	18	3,7	5,7	500,0	500,0
2005	1	1	19	2,8	4,3	211,0	211,0
2005	1	1	20	3	4,6	249,3	249,3
2005	1	1	21	3	4,6	249,3	249,3
2005	1	1	22	2	3,1	57,9	57,9
2005	1	1	23	1,5	2,3	0,0	0,0
2005	1	1	24	1,3	2,0	0,0	0,0

Figure 3-6. Example of energy production the first day of the year in Cañar.

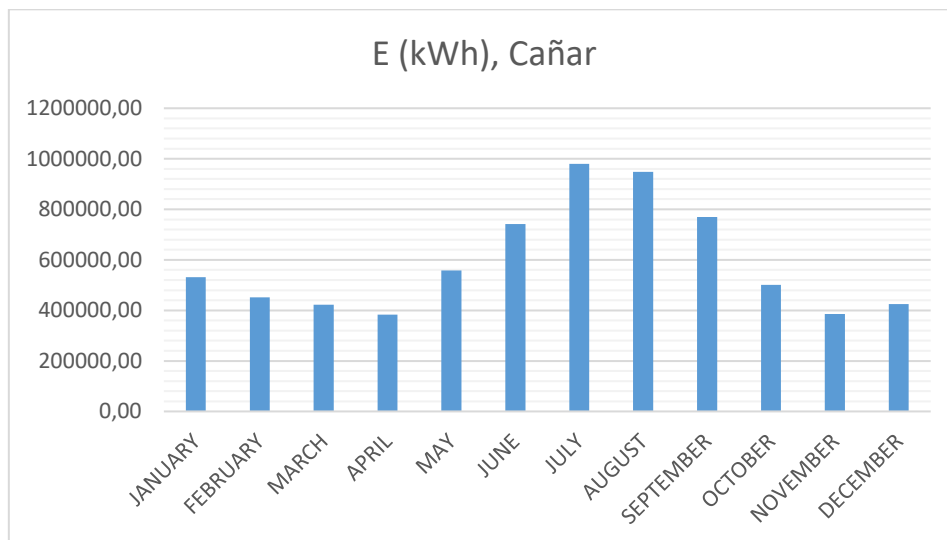


Figure 3-7. Energy production in Cañar throughout the year.

The following sections present the results of the methodology beforehand detailed for different wind turbines ranging from 15 kW to 3.3 MW.

3.3 Wind turbine of 2 MW rated

The steps with a different wind turbine proceed very much in the same way as previously described. First, given a power curve, as shown on Figure 3-8, three main segments are selected and their trend lines modelled.

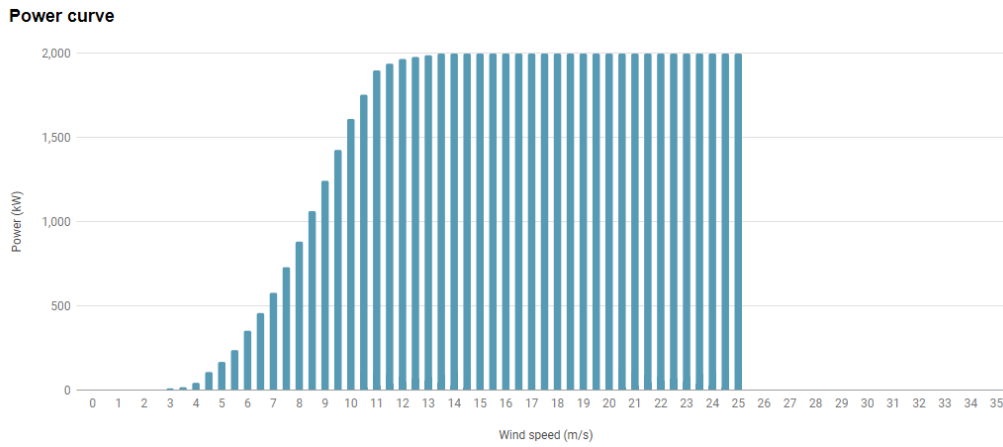


Figure 3-8. Power curve for VESTAS 90 2 MW IEC IIA.⁶

The resulting piecewise function for this wind turbine is:

$$P(v) \begin{cases} P = 80v - 230 & 3 \text{ m/s} < v < 5 \text{ m/s} \\ P = 205v - 855 & 5 \text{ m/s} < v < 7 \text{ m/s} \\ P = 254.55v - 1201.8 & 7 \text{ m/s} < v < 12 \text{ m/s} \end{cases} \quad (3-4)$$

3.4 Wind turbine of 1 MW rated

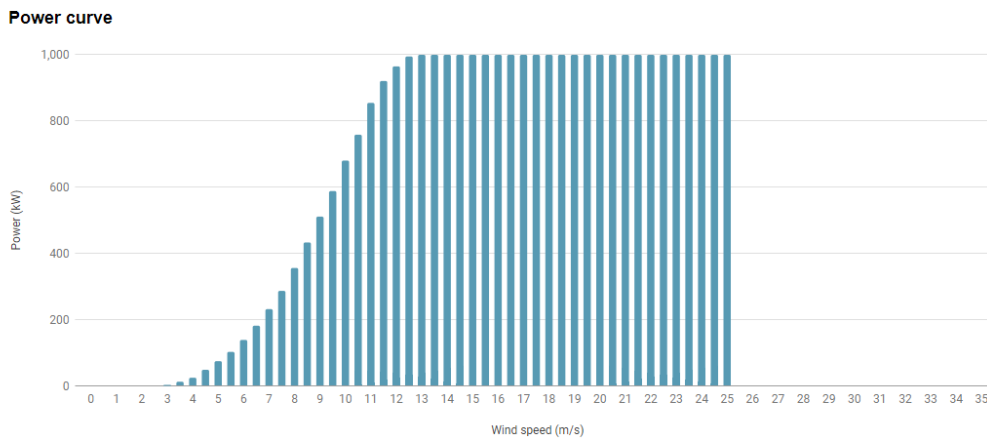


Figure 3-9. Power curve for ENERCON 58 1 MW IEC IIA.⁷

In this case, the function to represent the second region of the power curve is:

$$P(v) \begin{cases} P = 36.5v - 106.5 & 3 \text{ m/s} < v < 5 \text{ m/s} \\ P = 78.5v - 316.5 & 5 \text{ m/s} < v < 7 \text{ m/s} \\ P = 138.55v - 736.82 & 7 \text{ m/s} < v < 12 \text{ m/s} \end{cases} \quad (3-5)$$

⁶ Source https://www.thewindpower.net/turbine_es_32_vestas_v90-2000.php

⁷ Source https://www.thewindpower.net/turbine_en_218_enercon_e58-1000.php

3.5 Wind turbine of 0.5 MW rated

Lastly, in the case of a wind turbine with 0.5 MW of rated power, it is only necessary to fragment this section of the curve in two:

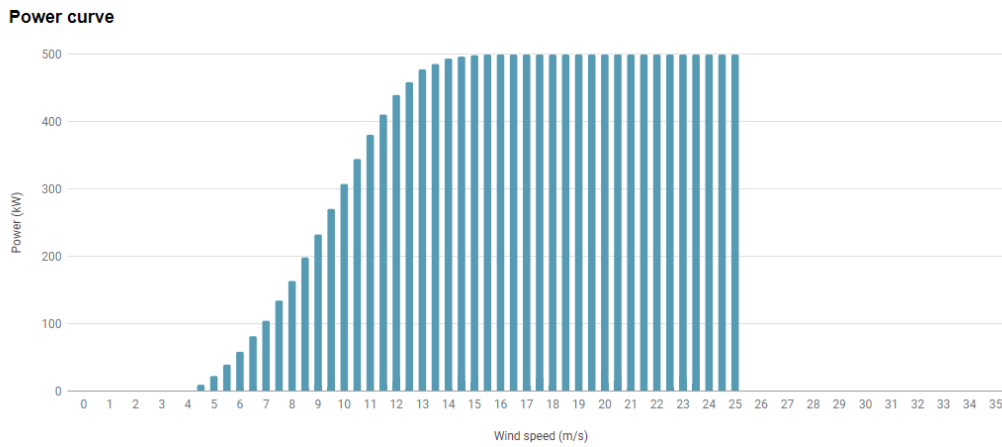


Figure 3-10. Power curve for VESTAS 39 0.5 MW IEC IIA.⁸

Therefore, the resulting function is:

$$P(v) = \begin{cases} P = 36.5v - 106.5 & 4 \text{ m/s} < v < 7 \text{ m/s} \\ P = 78.5v - 316.5 & 7 \text{ m/s} < v < 13.5 \text{ m/s} \end{cases} \quad (3-6)$$

3.6 Wind turbine of 15 kW rated

Analyses of SWRO powered by wind energy have been normally focused only on small scale desalination, for this reason, the performance of a small wind turbine of 15 kW will also be studied.

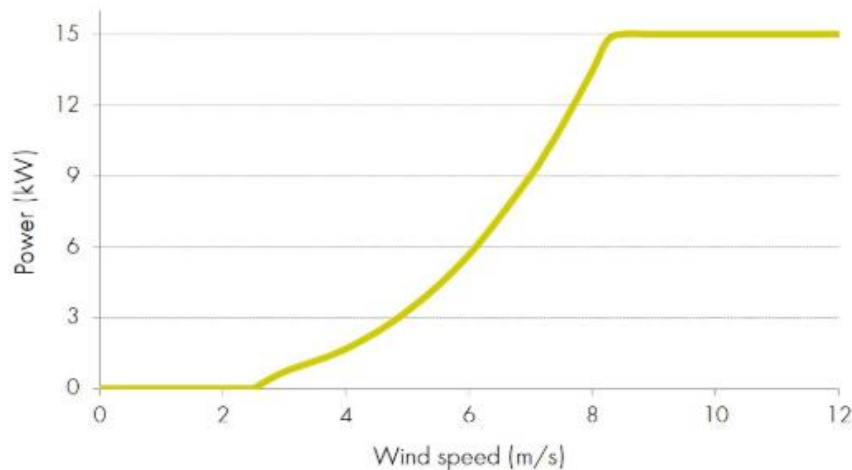


Figure 3-11. Power curve for ENBREEZE 15 KW WIND TURBINE.⁹

⁸ Source https://www.thewindpower.net/turbine_en_169_vestas_v39-500.php

⁹ Source <http://enbreeze.com/en/enbreeze15kw/>

In the case of smaller turbines, more precision was put into the calculations in order not to waste energy, therefore, the out coming function has more segments:

$$P(v) \begin{cases} P = v - 2.5 & 2.5 \text{ m/s} < v < 4 \text{ m/s} \\ P = 1.5v - 4.5 & 4 \text{ m/s} < v < 5 \text{ m/s} \\ P = 3v - 12 & 5 \text{ m/s} < v < 6 \text{ m/s} \\ P = 6v - 33 & 6 \text{ m/s} < v < 7 \text{ m/s} \\ P = 5.45v - 29.18 & 7 \text{ m/s} < v < 8 \text{ m/s} \end{cases} \tag{3-7}$$

4 REVERSE OSMOSIS AND DESALINATED WATER PRODUCTION

This chapter offers an overall view on desalination definitions and processes and explains the methodology followed in order to find the desalinated water produced and specific energy consumption corresponding to a given system design, dealing with both water desalination and treatment of wastewater from mining industry.

4.1 Reverse Osmosis

Reverse Osmosis (RO) is a demineralisation process that relies on a semi-permeable membrane to effect the separation of dissolved solids from a liquid. The semipermeable membrane allows the pass of liquid and some ions but retains the bulk of dissolved solids. The primary application of RO is water-based systems, even though other liquids may be used as solvents.

Reverse Osmosis relies on the natural phenomenon known as osmosis, a natural process where water flows through a semipermeable membrane from a solution with a low concentration of dissolved solids to a solution where the concentration of dissolved solids is high.

Given a cell divided into two compartments by a semipermeable membrane, as Figure 4-1 displays, where one compartment has a solution with low concentration of dissolved solids and the other contains a solution with high concentration of dissolved solids. The water and some ions are allowed by the membrane to pass through it, but most of the dissolved solids are unable to pass as the membrane is impermeable to them. Water will flow from the side with the lowest concentration to the other in the process of Osmosis, process that would only stop once the pressure difference created by the higher height of compartment 1 makes equal the chemical potential of the solvent in both compartments.

At this point, the equilibrium between both sides has been reached, being equal in both compartments the temperature and the chemical potential of the solvent and being different, salt concentration, pressure and chemical potential of solutes.

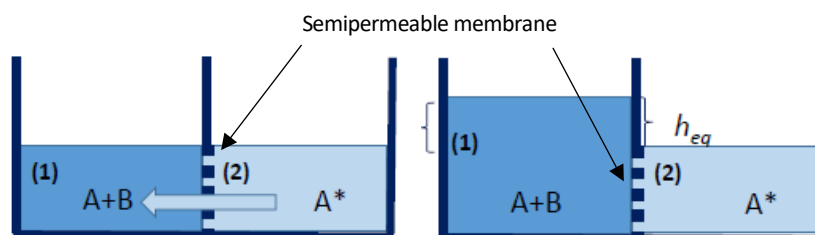


Figure 4-1. On the left, two compartments divided by a semipermeable membrane. On the right, state of equilibrium. ¹⁰

Once introduced Osmosis, Reverse Osmosis is the process that takes place when a pressure higher than the osmotic pressure is applied on the compartment with the high concentration; this pressure forces water to flow in the opposite direction through the membrane, this way the water in one of the compartments is demineralised and the dissolved solids concentrated.

¹⁰ Source Lourdes García Rodríguez.

The pressure needed to achieve reverse osmosis is significantly higher than the osmotic pressure due to the added resistance of the membrane. [19]

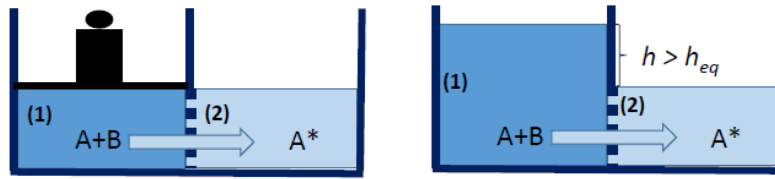


Figure 4-2. Process of Reverse Osmosis. ¹¹

4.1.1 Basic configurations

The simplest system for seawater desalination is a train configuration comprised of one single stage and a single pass, as Figure 4-3 shows.

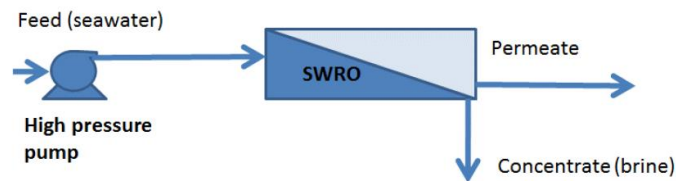


Figure 4-3. Conceptual diagram of the basic SWRO process. ¹²

A second pass can be installed consisting of a Brackish Water Reverse Osmosis (BWRO) rack for processing the permeate that the pass generates, it is a common practise to connect the concentrate from the second pass to the feed of the first pass, since it is less concentrated than seawater.

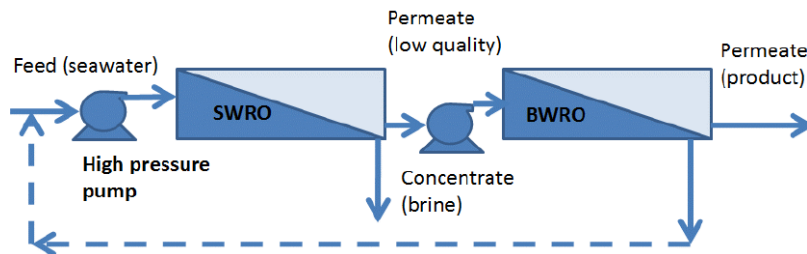


Figure 4-4. Conceptual diagram of two pass configuration. ¹³

Split partial of the product permeate from the first stage is sometimes performed and permits processing a fraction of the first pass permeate resulting in a reduction of the energy consumption.

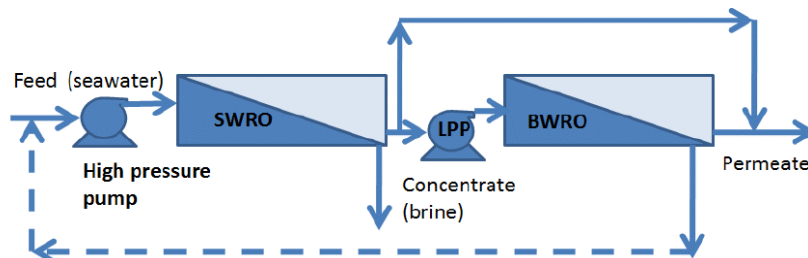


Figure 4-5. Conceptual diagram of partial two pass configuration. ¹⁴

¹¹ Source Lourdes García Rodríguez.

¹² Source Lourdes García Rodríguez.

¹³ Source Lourdes García Rodríguez.

¹⁴ Source Lourdes García Rodríguez.

A second stage is normally added to desalinate the brine.

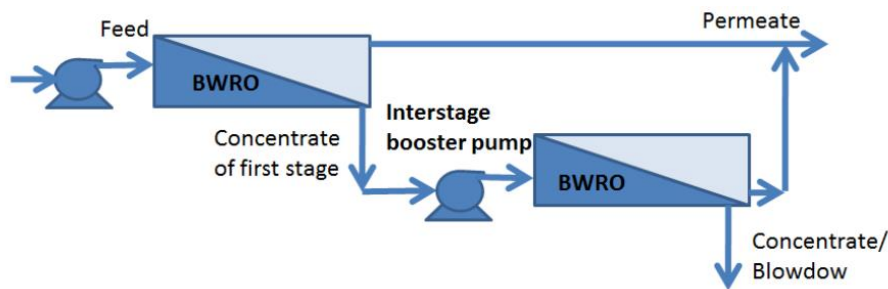


Figure 4-6. Conceptual diagram of two stages for high salinity configuration.¹⁵

4.2 Design

The following sections describe the different tendencies on Reverse Osmosis design depending on which factor they affect:

- RO membrane and rack design.
- SWRO desalination plant designs.
- Energy supply.

4.2.1 Reverse Osmosis membrane and rack designs

When designing a Reverse Osmosis plant, it is desirable to achieve greater filtration surface within the same volume. Eight –inch membrane elements have been the industrial standard size, during the past years it has been evaluated the possibility of introducing RO elements of larger diameter as a new standard.

Hybrid Interstage Design (HID) or Interstaged Design (ISD) permits using different nominal flux elements within the same pressure vessel, the first membrane in the pressure vessel is the most prone to fouling, due to highest flux that passes through it, consequence of the lower osmotic pressure. For this reason, membranes with lower permeability are required, in order to decrease the permeate flux which results in better salt rejection, thus allowing better product quality. This design has several advantages such as greater efficiency and energy savings with given product quality requirement and given membrane area.

Increasing the number of membranes within the pressure vessel is another option that ensures better performance and lower investment costs in some specific cases, this, however, cannot be done indefinitely, and at the present, seven and eight elements are the best options in conventional plants.

4.2.2 Seawater desalination plant design

Energy Recovery Devices perform the energy transfer from the brine to the feed. In these days either, pressure exchangers (also referred to as isobaric chambers) or turbochargers are used. Turbochargers normally act as high pressure booster pumps, pressurizing the pump discharge. On the contrary, energy recovery systems based on pressure exchangers and the iSave turbocharger operate in parallel to the high pressure pump. They process only a fraction of the stream coming from the seawater pre-treatment system. After passing through the pressure exchangers a booster pump is required, before being blended with the outgoing stream of the high pressure pump. On the other hand, the iSave turbocharger has an internal energy consumption, so no external booster pump is required.

A second pass (Figure 4-4) is normally needed when the water quality requirements are high, so the second pass allows to treat the permeate from the first pass.

The split partial is based on collecting permeate from both first and second pass, processing only a fraction of the product from the first pass in the second (Figure 4-5).

¹⁵ Source Lourdes García Rodríguez.

4.2.3 Energy supply

Desalination processes have high costs and high energy consumption, the biggest concerns that limit its use. However, this main drawback, its high energy consumption, is the biggest driving force towards Renewable Energy Systems, as they seem to be a reliable source for plants in isolated regions with no electricity grid available and difficulties in fossil fuel supply.

Promotion of large-capacity desalination plants driven, either totally or partially, by RES is essential to the sustainability of fresh water production. The high capital costs of RES make efficiency of the desalination process a key issue. RO is indisputably the dominant technology in the desalination market, for this reason, the retrofit of existing RO plants through incorporation of a RES could be a key idea in avoiding electrical consumption from the grid during peak hours. In principle, the use at the present time.

It is important, for the operation of RES powered plants, to have a suitable process insensitive to repeated start up and shutdown cycles caused by changing weather conditions or alternatively, system configurations that allow continuous operation as far as possible.

4.3 Part load operation

The preliminary assessment considered that the RO plant would only operate each and every time the hourly energy production reached the nominal consumption of the plant, which means that the energy produced when the RO plant is not operating and the energy surplus were therefore neglected and not utilized. To illustrate this point Figure 4-7 shows that, up until now, only the energy in the shaded area was useful, neglecting a considerable quantity of potential energy.

When the RO plant is operating out of design conditions, the energy produced by the power source does not reach to the nominal consumption of the plant, what is called part load operation. At this point of the assessment, it is time to make improvements and start analysing different options to minimise the energy not used and optimise part load operation.

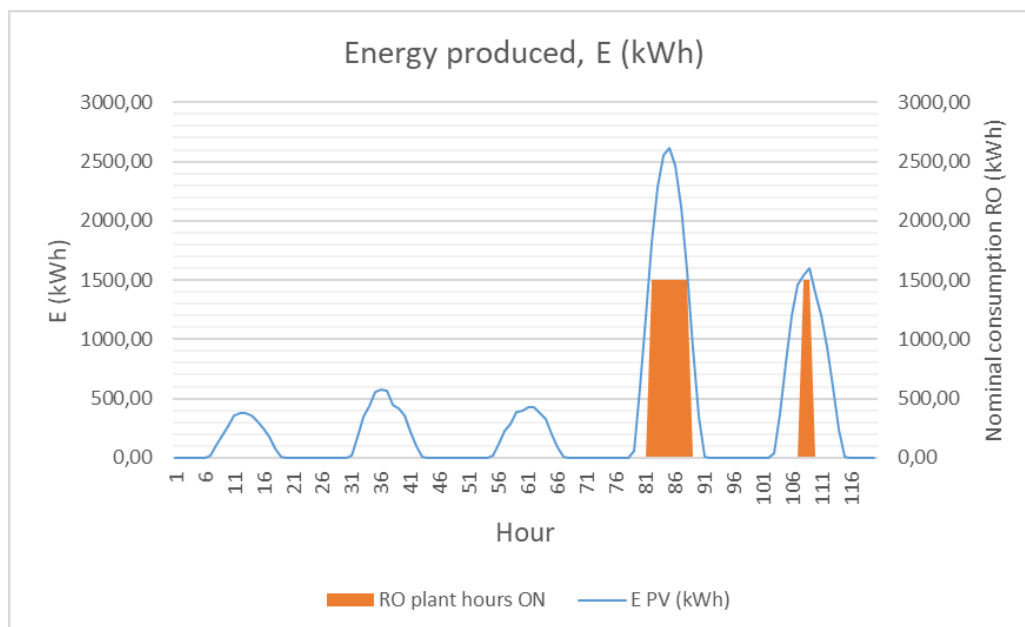


Figure 4-7. Energy collected with PV during the first five days of the year and useful energy in Cañar.

Electricity storage is still a challenge, so combining power generation and water desalination can also be a cost-effective option for electricity storage when generation exceeds demand [9]. The following sections analyse various methods of operation that result in an increase of the desalinated water production.

4.3.1 Batch operation

The desalination systems that have been most developed to operate in batches of small capacity are electro dialysis (García-Rodríguez, 2003), for brackish water desalination, and membrane distillation, used for seawater desalination (Blanco-Gálvez et al., 2009a). This mode allows design of small-capacity systems without the need of energy storage, and is applicable coupled with a single renewable or hybrid energy systems, including microgrids.

4.3.2 Gradual capacity

RO systems can operate at partial load with high efficiency, this operating mode can avoid or minimise capital costs related to energy storage. The main objectives of gradual operation are to increase efficiency outside nominal conditions and to lower the power requirement to permit longer and cheaper operation of the desalination unit. Gradual capacity systems can either consist of:

- A number of RO trains with different capacities operated in parallel, which are able to operate independently and could be connected or disconnected depending on the available energy (Figure 4-8).
- Adapting the RO plant energy consumption to variable input power changing its operating parameters. These adaptations have two main drawbacks; the product quality is strongly affected by operational conditions and the availability of energy recovery devices capable of operating in variable conditions has, historically, been limited. [20] [21]

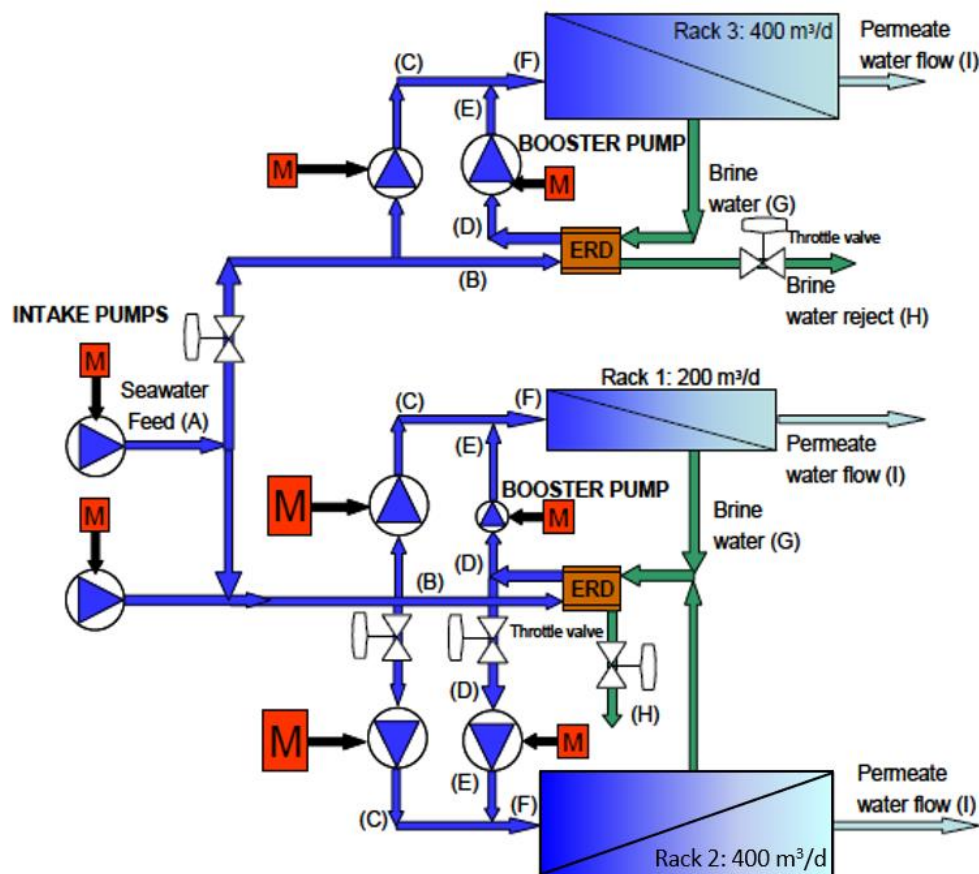


Figure 4-8. Gradual capacity SWRO plant in Pozo Izquierdo, Canarias (SDAWES Project, ITC). [22]

4.3.3 Hybrid systems. Wind-PV

The combination of different energy sources, known as hybridisation, in this case of solar and wind resources, may as well be a design option to consider in order to reduce intermittent operation and lengthen operation time and therefore, water production, and especially in areas where both resources are abundant as Ecuador and Chile's regions have proved to be.

It is necessary to perform a study of the localisations since both sources, wind and solar, must be available at the same time. The variability in power generation, as well the operation and maintenance become an issue, as more complex control and monitoring systems are required. Nonetheless, energy production is higher and costs may be reduced. [23]

4.4 Desalinated water production. Case of study

One of the objectives of this Master Thesis is to determine ranges of desalinated water production in the regions under study. To this end, using the Software Q+ (LGChem), realistic specific energy consumption for a Reverse Osmosis plant located in Pacific Ocean area can be defined. To define water composition Wilf 2007 [24] was taken as reference:

Constituent	Mediterranean	Persian Gulf	Red Sea	Caribbean	Pacific	Atlantic	Canary Islands
Temperature	14°C, 28°C	16°C, 34°C	16°C, 26°C	26°C	20°C	20°C	22°C
pH	8.1	7.0	7.8	8.2	8.0	8.0	7.8
Ca ⁺ , ppm	483	478	500	477	440	410	464
Mg ⁺ , ppm	1557	1672	1540	1160	1300	1302	1526
Na ⁺ , ppm	12200	14099	13300	11322	10200	10812	11700
K ⁻ , ppm	481	530	490	386	380	389	429
CO ₃ ⁻ , ppm	5	4.2	2.3	2.3	2.0	2.0	3.2
HCO ₃ ⁻ , ppm	162	154	126.8	137	170	143	204
SO ₄ ²⁻ , ppm	3186	3314	3240	2600	3000	2713	3059
Cl ⁻ , ppm	22599	24927	23180	20034	18500	19441	21344
F ⁻ , ppm	1.4	-	-	-	-	-	-
NO ₃ ⁻ , ppm	-	-	-	-	-	-	-
B ⁺ , ppm	5	5	5.3	5.3	4.5	4.5	4.5
SiO ₂ , ppm	1.6	-	-	-	-	-	-
TDS, ppm	40686	45199	42389	36149	34000	35240	38739

Figure 4-9. Exemplary cases of water composition in a number of plant locations.¹⁶

One crucial factor designing RES driven RO is minimising power demand, this can mainly be achieved by the incorporation of Energy Recovery Devices, since the Specific Energy Consumption (SEC) can be reduced, resulting in minor energy generation requirements and energy storage, and thus investment costs.

For this reason, the configuration selected for this assessment is comprised of a single stage, a decision influenced by the fact that the salinity in the Pacific Ocean is relatively low. It consists of a High Pressure Pump (HPP), an Energy Recovery Device (ERD), Booster Pump (BP) and the Reverse Osmosis rack. It includes an Energy Recovery Device (in Figure 4-10 based on pressure exchangers, Isobaric Chamber) to perform the energy transfer from the brine to the feed.

¹⁶ Wilf, M., & Awerbuch, L. (n.d.). The Guidebook to membrane desalination technology : reverse osmosis, nanofiltration and hybrid systems, process, design, applications and economics / . Balaban Desalination Publications.

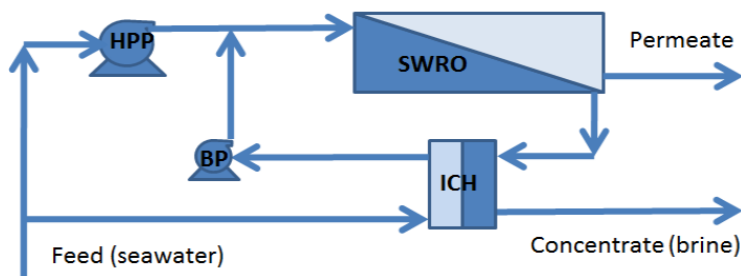


Figure 4-10. System configuration scheme.¹⁷

Table 4-1. Main design parameters.

Design parameters	
ERD	Isobaric Chamber
High pressure side differential	0.7 bar
Leakages	5%
Recovery	45%
Pump Efficiency	85%
Number of membranes	7
Elements	LG SW 440 SR

Having in mind the previous scheme (Figure 4-10), considering the water composition of the Pacific for the feed water (Figure 4-9) and the specifications listed in Table 5-1 for the components of the RO train, the specific energy consumption SEC (equation 4-1) can be instantly obtained thanks to the Software Q+, which simulations determine:

$$SEC = \frac{\sum P_{W,HPP}}{q_{VP}} = \frac{P_{HPP} + P_{BP}}{q_{VP}} = 2.14 \frac{kWh}{m^3} \quad (4-1)$$

Where:

- $P_{W,HPP}$ is the power consumed by the High Pressure Pump [kW].
- $P_{W,BP}$ is the power consumer by the Booster Pump [kW].
- q_{VP} is the permeate volume flow [m³/h].

Once the specific energy consumption for the RO plant located in Pacific Ocean is known, an estimated value of water production capacity can be obtained, regarding hourly energy production profile, as it will be assessed further on, in Chapters 5 and 6.

For the purpose of studying energy production and desalinated water production, a parameter that expresses the ratio between the nominal consumption of the RO plant, understood as the power consumption of the plant at operating nominal conditions, and the rated energy production of the PV plant is defined, thus, the results will be homogenised:

$$k = \frac{\text{Nominal power consumption of the RO plant}}{\text{Rated power production of the RES plant}} \quad (4-2)$$

¹⁷ Source Lourdes García Rodríguez.

Tables 4-1 and 4-2 present each value of this denominated k ratio for the different cases studied given the nominal consumption of the RO plant and the rated energy production, each of them considering two options: without and with energy storage systems:

Table 4–2. Values of k ratio for large scale plants.

Nominal consumption of the RO plant (kW)	Rated energy production of the plant (kW_{installed})	k value
1500	3300	0,4545
1000	3300	0,3030
500	3300	0,1515

Since the performance of a small wind turbine has also been analysed as outlined on Chapter 4, k ratio values will also be defined for this small scale capacity plants with rated energy production of 15 kW, again each of them considering two options: without and with energy storage systems:

Table 4–3. Values of k ratio for small scale capacities.

Nominal consumption of the RO plant (kW)	Rated energy production of the plant (kW_{installed})	k value
6	15	0,4000
4	15	0,2667
2	15	0,1333

These two tables may seem like extreme cases, nonetheless, RO systems are modular, therefore smaller capacity designs, such as the ones displayed in Table 4-3 must be taken into account. On the other hand, bigger installations such as those showed in Table 4-2 to wit some Megawatts and completely standardised designs, are in fact the same designs, but multiplying for a factor the nominal capacity.

5 PRELIMINARY SELECTION OF REVERSE OSMOSIS SYSTEM DESIGNS

Considering part load behaviour of Reverse Osmosis systems with candidate design configurations described in Chapter 4, this chapter performs a preliminary selection of suitable designs concerning water desalination and mining wastewater treatment.

Fluctuations on the available power can lead to start and stop cycles of the RO unit which can make operation pressure and flow inside the pressure vessels vary. The performance of the RO unit would decrease considerably due to these rapid pressure variations, resulting in lower production and lower quality of the product water, shorter lifetime and higher operation and maintenance costs. For this reason, the selection of the system design will be mainly based on minimising, as much as possible, oscillations on available power.

Reverse Osmosis plants can only produce desalinated water if the power required is available, RO plants can operate separately:

- Feed water pumping.
- Productive nucleus of desalination process.
- Product pumping to the consumption point.

The preliminary assessment considered that if the power was sufficient desalinated water would be produced, if there was an excess it would be utilised for auxiliary pumping, if the producer power did not allow water production, but it allows to operate any of the pumping auxiliaries, these would operate.

For this assessment the configuration selected is comprised of a single stage, as mentioned in Chapter 4, it includes Energy Recovery Devices (in Figure 4-10 based on pressure exchangers, Isobaric Chamber) to perform the energy transfer from the brine to the feed.

Three different design configurations are going to be evaluated:

- Water production for nominal conditions: Case of k ratio equal to 0.4545 (Table 5-1).
- Water production with gradual capacity: For five production steps of the RO plant; 1000, 800, 600, 400 and 200 m³/h.
- Water production with energy storage: Case of k ratio equal to 0.4545 and two hours of energy storage (Table 5-1).

Table 5-1. Water production for different k ratios.

Nominal consumption of the RO plant (kW)	Rated energy production of the plant (kW _{installed})	k value	Water production (m ³ /h)
1500	3300	0,4545	700,93
1000	3300	0,3030	467,29
500	3300	0,1515	233,64

5.1 Energy storage systems selection

In order to select the size of the batteries, in other words, the hours of energy storage they have, a sensitivity analysis shall be performed.

Figure 5-1 (on the following pages) shows the energy production profile of the PV systems and the performance of the battery bank in Cañar, Figure 5-2 is The dashed line represents the energy production profile, the solid line represents the energy that is stored in the battery and finally, the red line stands for the number of hours the RO plant is able to operate when the system includes energy storage. Tables 5-2 and 5-3 present the results obtained from the sensibility analysis for PV and installations respectively:

Table 5–2. Useful energy from energy storage system in PV system of 3.3 MW when nominal consumption of the RO plant is 1500 kW, Cañar.

	0,5 h 750 kW	1 h 1500 kW	1,5 h 2250 kW	2 h 3000 kW	2,5 h 3750 kW	3 h 4500 kW
E (kWh)	7.323.209,14	7.678.844,46	7.716.227,37	7.716.230,62	7.716.230,62	7.716.230,62
E (kWh/kW_p)	2.219,15	2.326,92	2.338,25	2.338,25	2.338,25	2.338,25

Table 5–3. Useful energy from energy storage system in wind system of 3.3 MW when nominal consumption of the RO plant is 1500 kW, Cañar.

	0,5 h 750 kW	1 h 1500 kW	1,5 h 2250 kW	2 h 3000 kW	2,5 h 3750 kW	3 h 4500 kW
E (kWh)	9.582.190,36	10.248.673,76	10.428.100,17	10.428.100,17	10.428.100,17	10.428.100,17
E (kWh/kW_r)	2.903,69	3.105,66	3.160,03	3.160,03	3.160,03	3.160,03

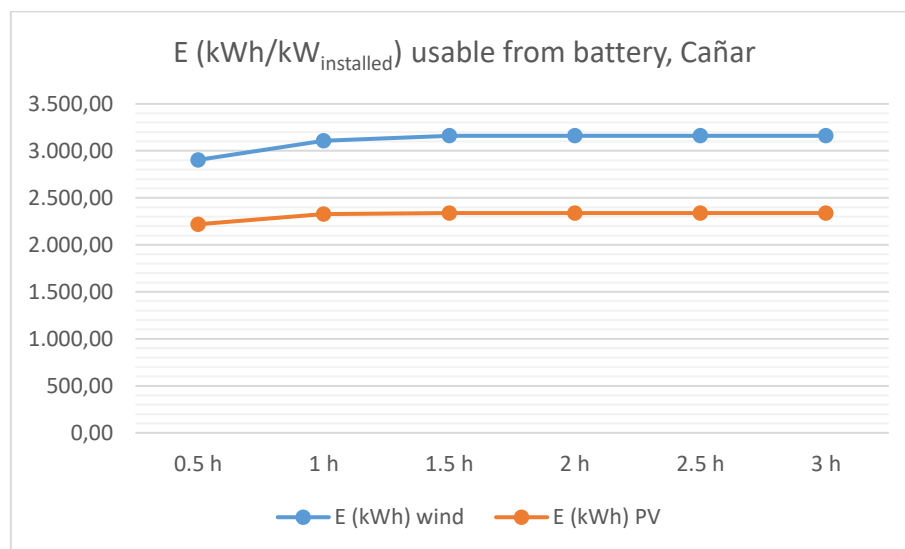
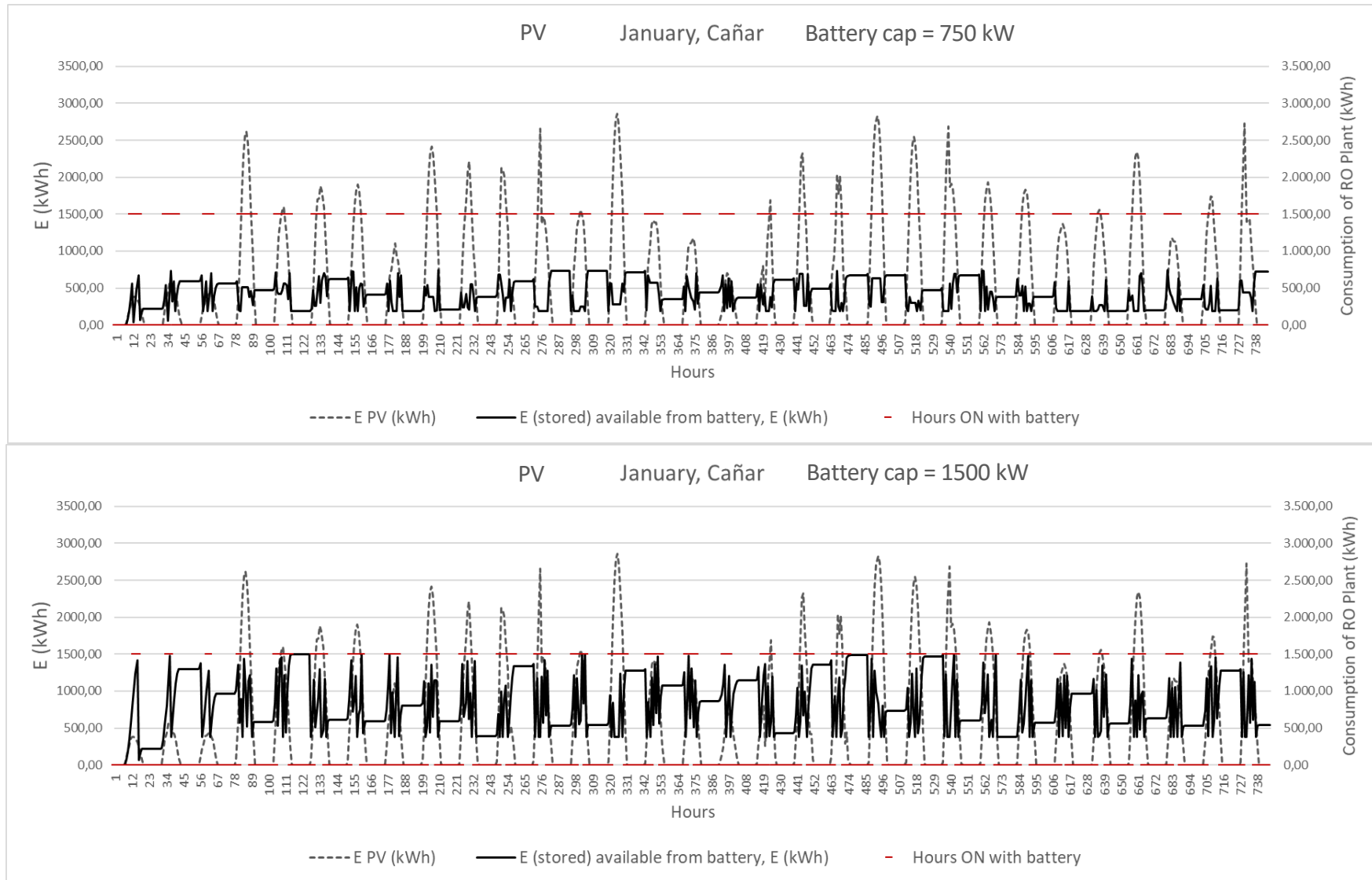
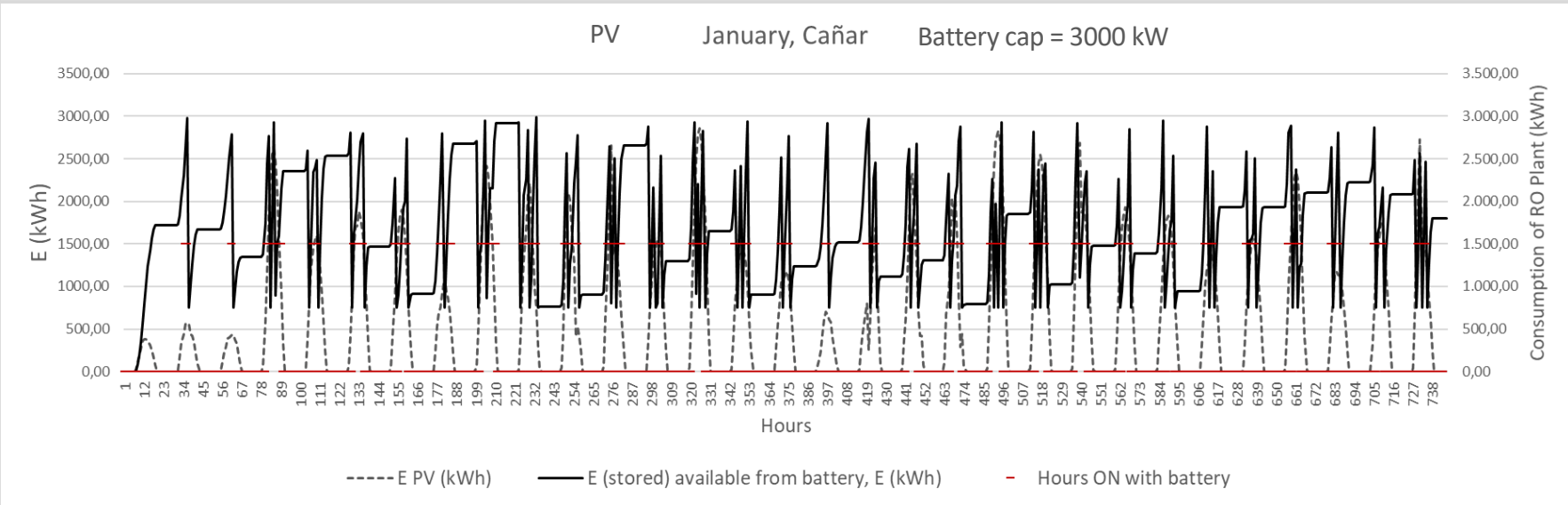
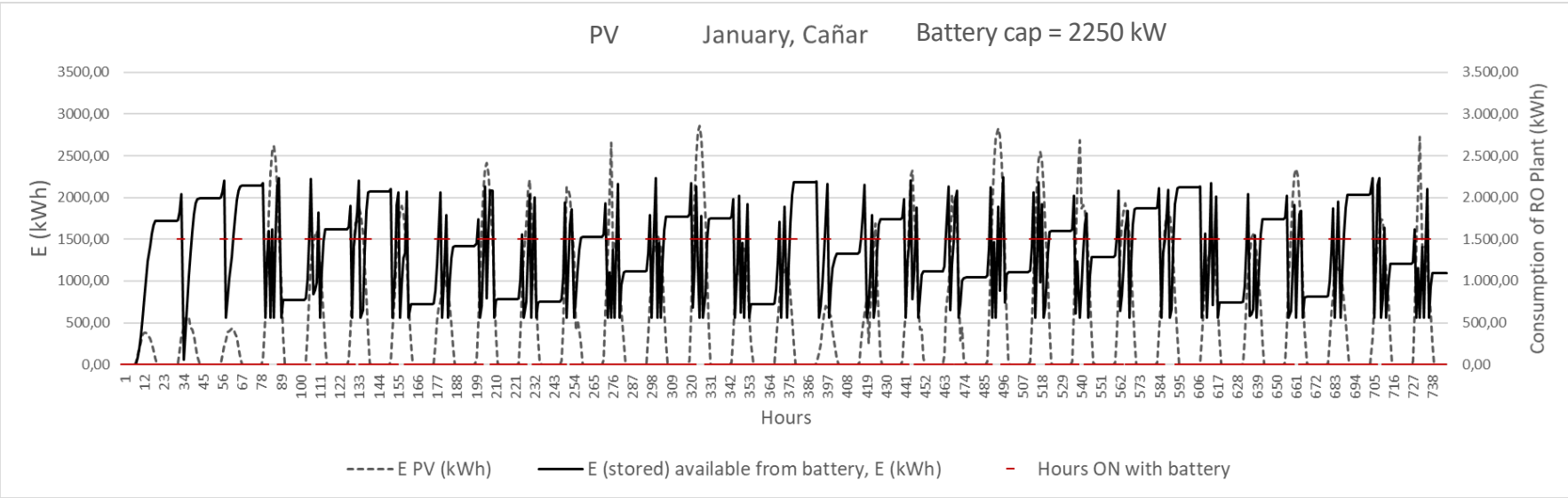


Figure 5-1. Sensibility analysis RES installations of 3.3 MW, Cañar.

Once 3000 kW of storage capacity is reached, the energy that can be used to operate the RO does not increase, for this reason, energy storage will be twice the nominal consumption of the RO plant, since using higher capacity batteries would mean over-dimensioning the system. Moreover, it can be stated that this the decision will be the optimal in economic terms, since the highest rate of useful energy is ensured, nonetheless, at the lowest capital cost.





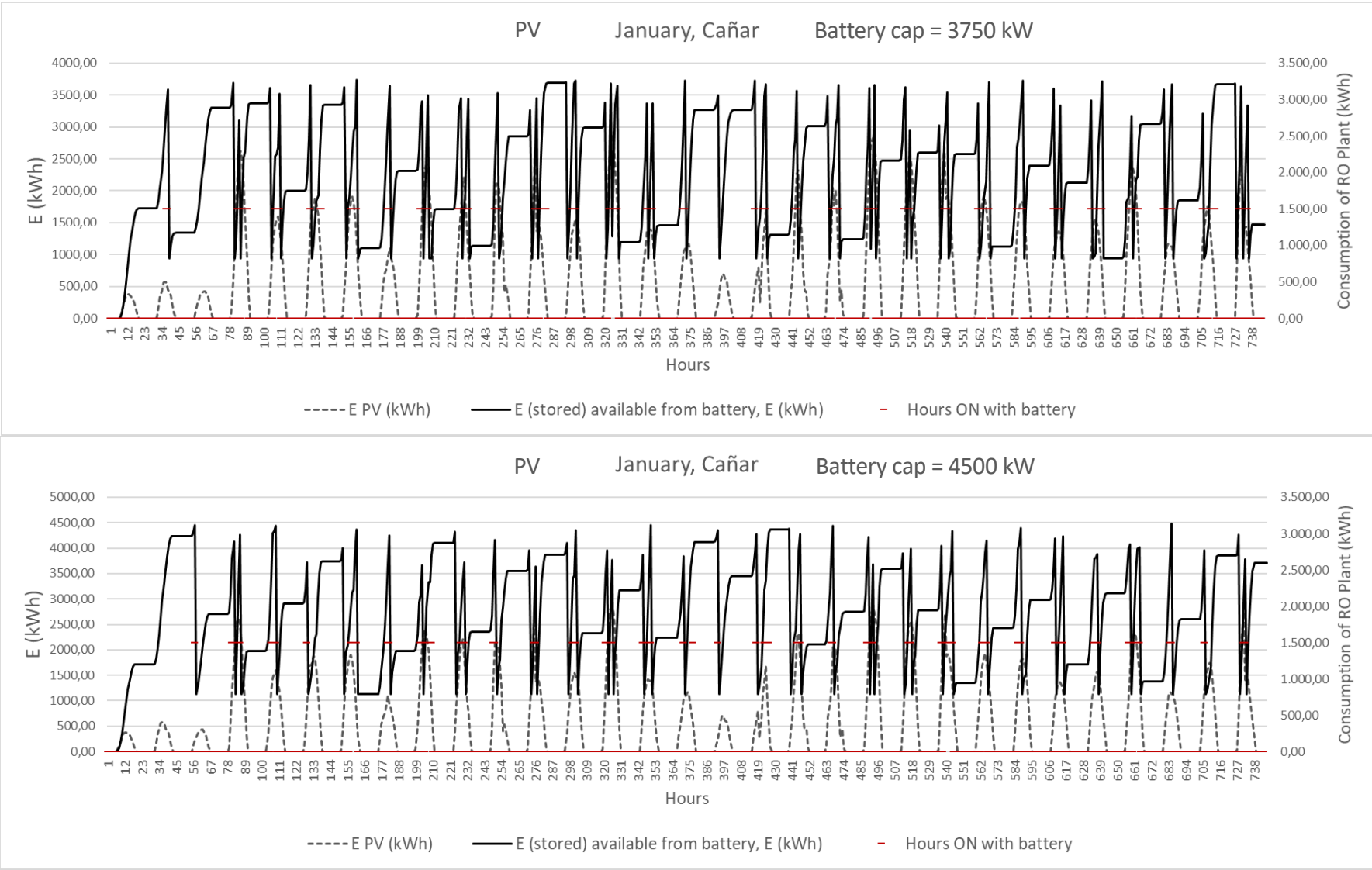
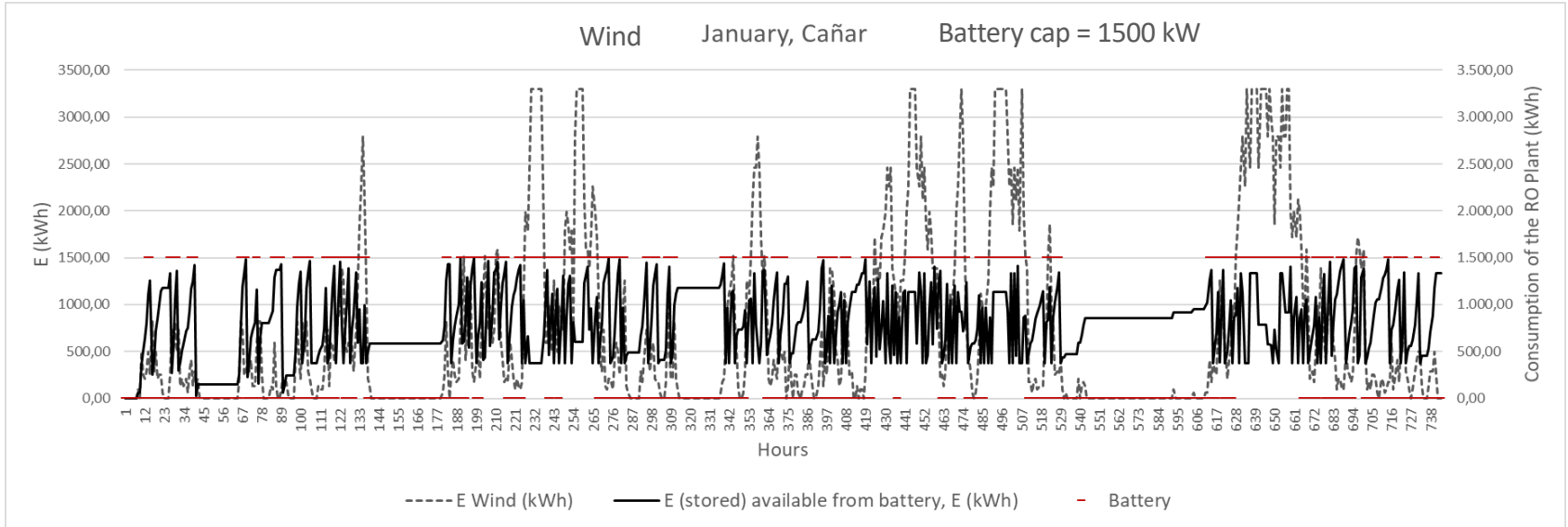
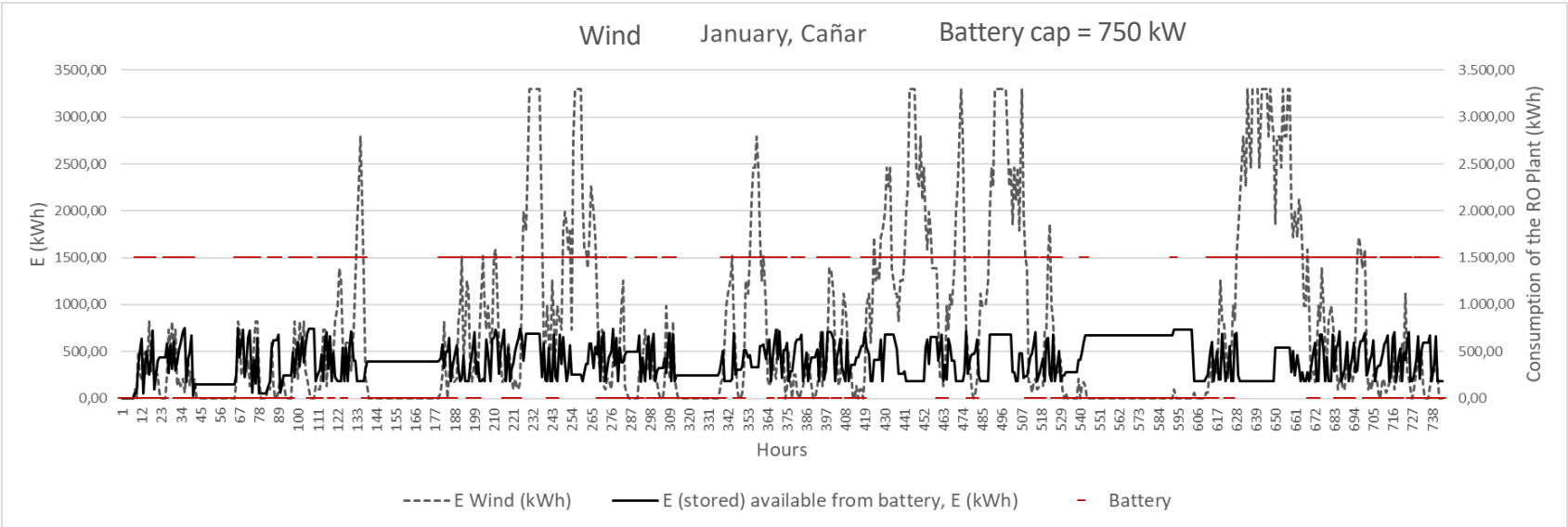
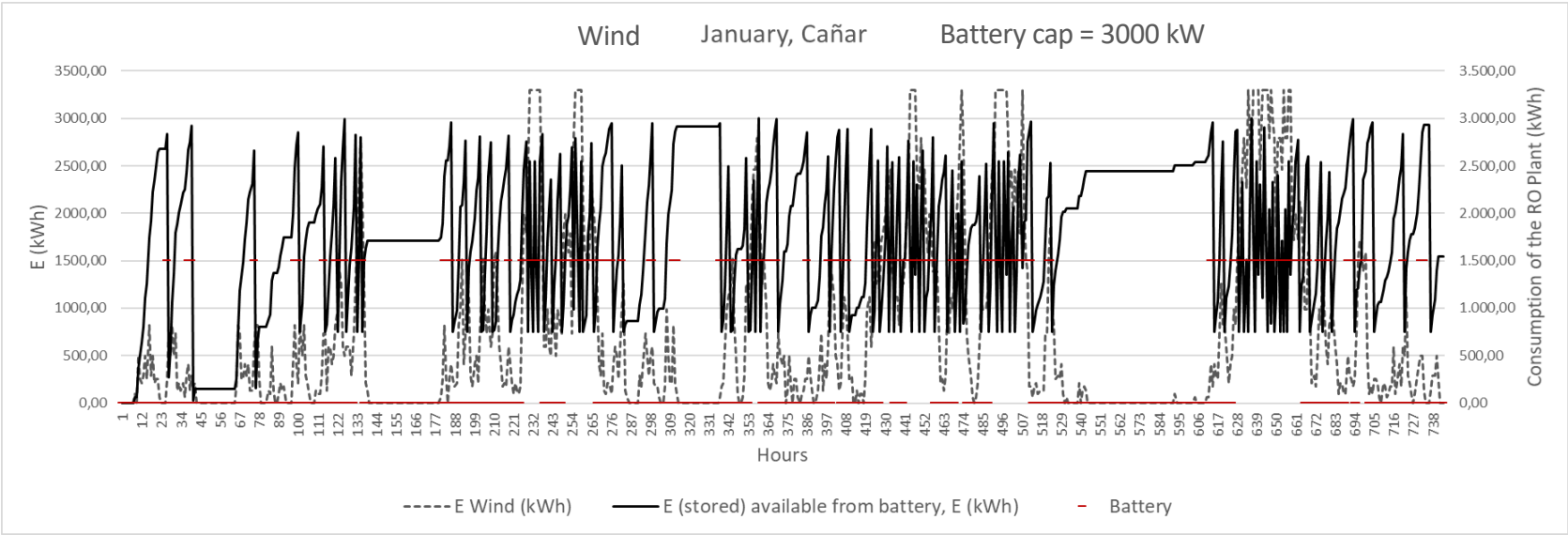
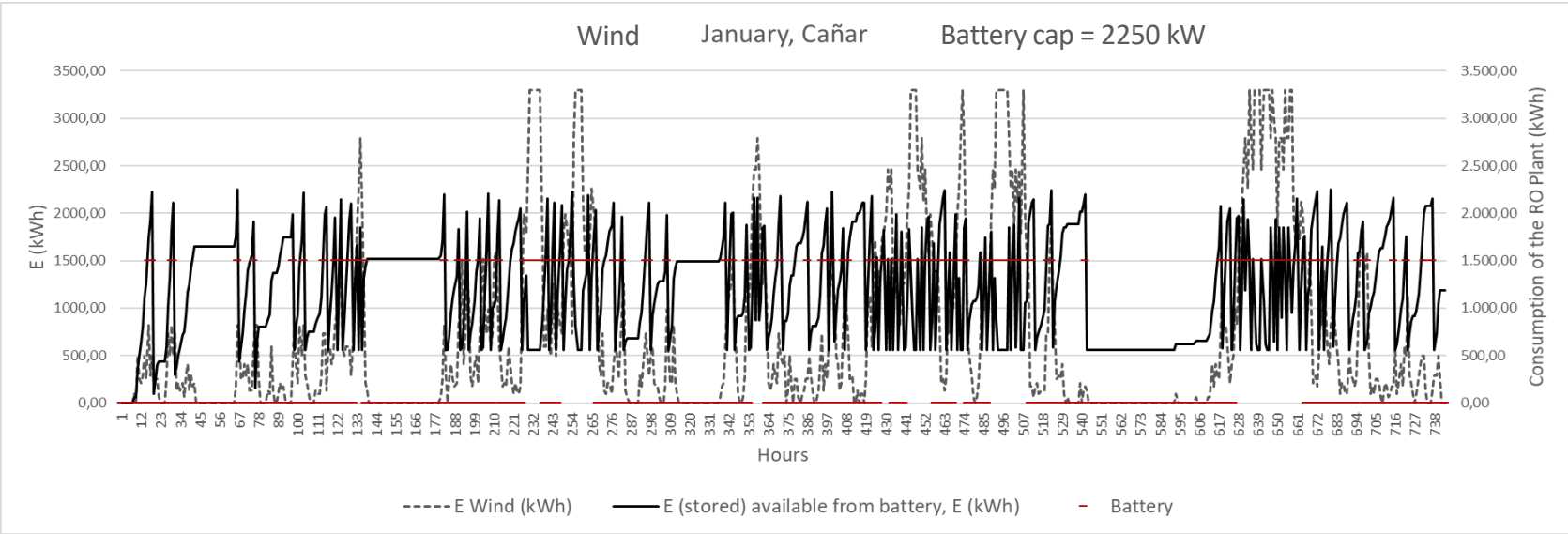


Figure 5-2. Energy collected and energy stored in the battery during January in Cañar for PV systems.





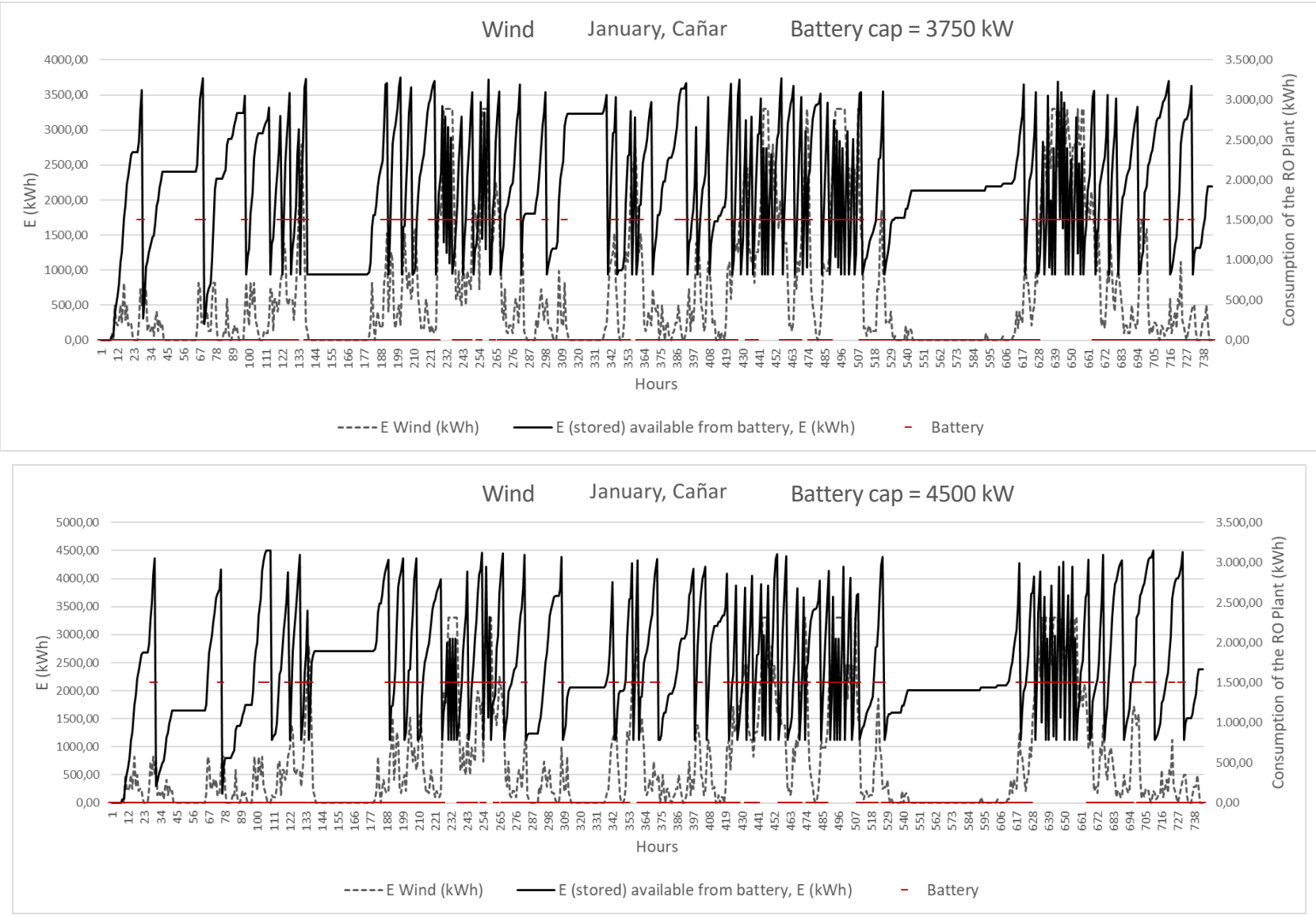


Figure 5-3. Energy collected and energy stored in the battery during January in Cañar for wind systems.

5.1.1 Small scale

Table 5–4. Useful energy from energy storage system in small PV (15 kW) installation when nominal consumption of the RO plant is 6 kW, Cañar.

	0,5 h 3 kW	1 h 6 kW	1,5 h 9 kW	2 h 12 kW	2,5 h 15 kW	3 h 18 kW
E (kWh)	32.613,72	34.722,67	35.344,30	35.366,27	35.366,27	35.366,27
E (kWh/kW_p)	2.174,25	2.314,84	2.356,29	2.357,75	2.357,75	2.357,75

Table 5–5. Useful energy from energy storage system in small wind installation (15 kW) when nominal consumption of the RO plant is 6 kW, Cañar.

	0,5 h 3 kW	1 h 6 kW	1,5 h 9 kW	2 h 12 kW	2,5 h 15 kW	3 h 18 kW
E (kWh)	40.666,25	44.394,21	47.249,61	47.249,61	47.249,61	47.249,61
E (kWh/kW_p)	2.711,08	2.959,61	3.149,97	3.149,97	3.149,97	3.149,97

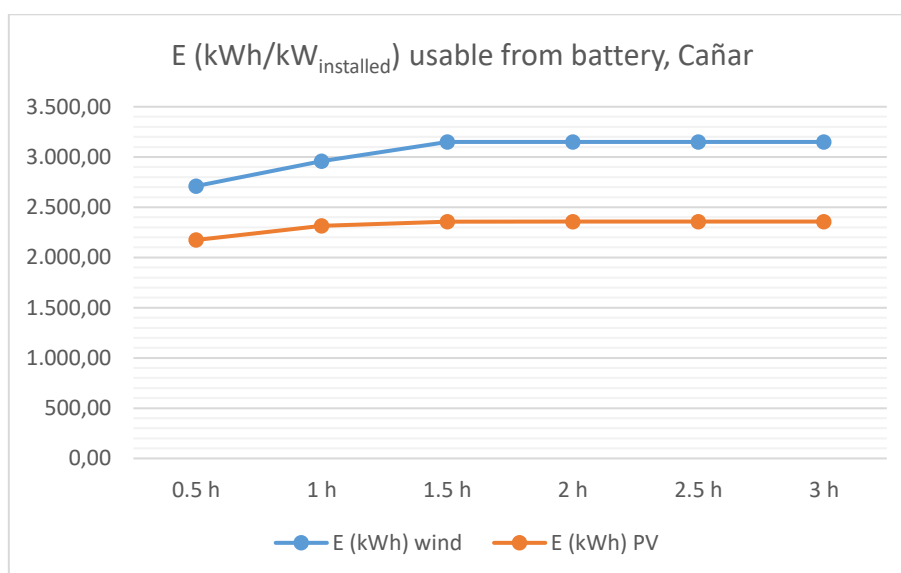


Figure 5-4. Sensibility analysis RES installations of 15 kW, Cañar.

Results for small utilities are remarkably similar to the ones obtained on the previous case with large installations, for this reason, to unify criteria, it was decided that the capacity of the batteries would be twice the nominal consumption of the RO plant:

Table 5–6. Battery capacity depending on the RO nominal consumption.

Nominal consumption of the RO plant (kW)	Batteries capacity (kW)
1500	3000
1000	2000
500	1000
6	12
4	8
2	4

5.2 Gradual capacity methodology

This gradual capacity system consists of 3 different racks operated in parallel, that will operate independently and could be connected or disconnected depending on the available energy, such as the one displayed on the Figure 5-5, but with higher water production. It is essential to understand that the more RO units operating, the higher the SEC, for this reason the SEC for each operation step must be determined.

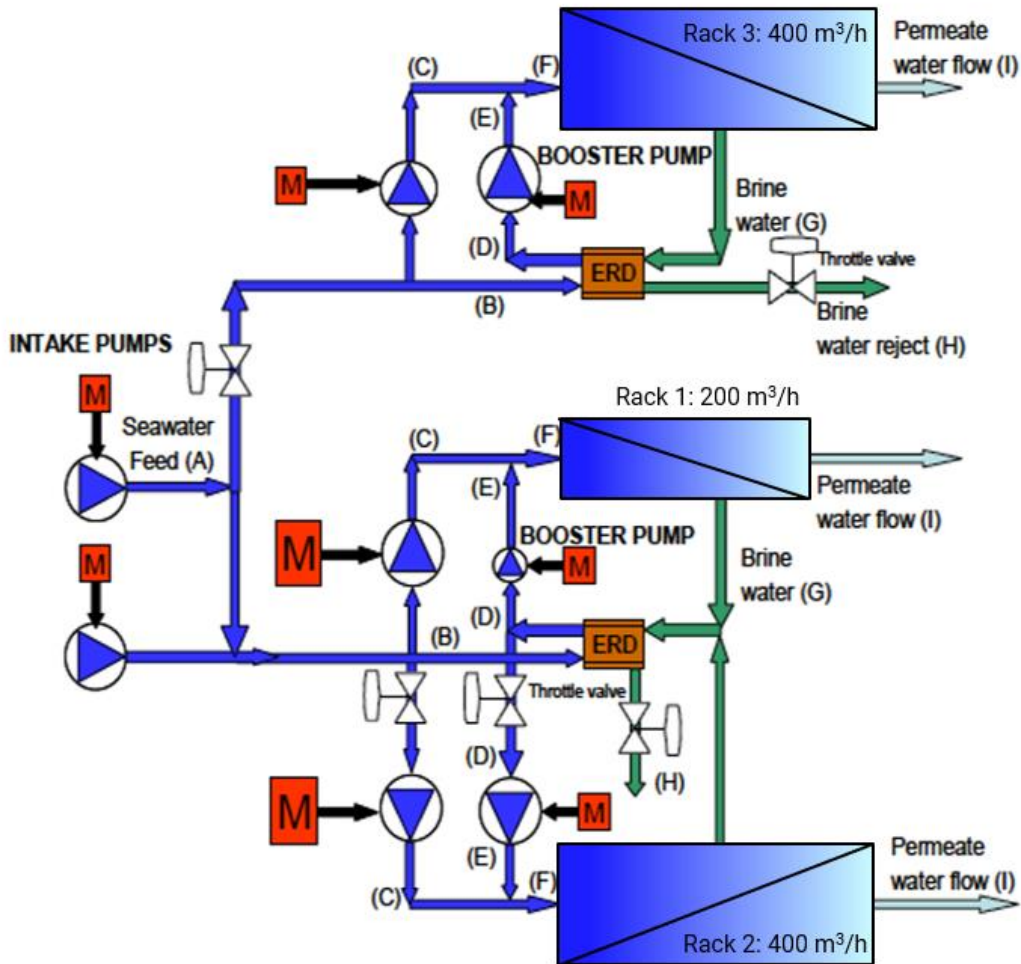


Figure 5-5. Gradual capacity configuration.

To calculate the SEC for each step of water production it is necessary first to determine the number of pressure vessels of the RO plant.

$$Flux \left[\frac{l}{m^2 \cdot h} \right] = \frac{Feed\ water \left[\frac{m^3}{h} \right] \cdot Recovery \cdot 1000}{pv \cdot n \cdot S [m^2]} \quad (5-1)$$

Where:

- pv is the number of pressure vessels.
- n is the number of membranes per pressure vessel.
- S is the effective surface of each membrane [m^2].

The main design parameters used to simulate the RO plant in Q+ are the same as those used in Chapter 4:

Table 5–7. Main design parameters.

Design parameters	
ERD	Isobaric Chamber
High pressure side differential	0.7 bar
Leakages	5%
Recovery	45%
Pump Efficiency	85%
Number of membranes	7
Elements	LG SW 440 SR (440 ft ² = 41 m ²)

In order to ensure having an average flux of 14 lmh [24] in the first pass, the feed that flows per each pressure vessel can be cleared from Equation 5-2:

$$\begin{aligned}
 1 \text{ pv} \cdot \frac{7 \text{ membranes} \cdot 41 \text{ m}^2}{1 \text{ PV}} \cdot \frac{14 \frac{\text{l}}{\text{h}} \text{ of permeate}}{1 \text{ m}^2} \cdot \frac{1 \frac{\text{m}^3}{\text{h}} \text{ of feed water}}{0.45 \frac{\text{m}^3}{\text{h}} \text{ of permeate}} & \quad (5-2) \\
 = 8.93 \frac{\text{m}^3}{\text{h}} \text{ of feed water per pv} &
 \end{aligned}$$

Knowing the feed per pressure vessel and the total feed water needed, the following estimation of the number of pressure vessels required presented in equation 5-3 can be made, which results for each capacity step are presented in Table 5-3:

$$n \text{ pv} = \frac{\text{feed m}^3/\text{h}}{\text{feed per pv m}^3/\text{h}} \quad (5-3)$$

Table 5–8. Gradual capacity steps.

Desalinated water production (m³/h)	Feed water (m³/h)	Number of pressure vessels	SEC (kWh/m³)	Nominal consumption of the RO plant (kW)
200	444.44	50	2.15	430
400	888.89	100	2.15	860
600	1333.33	149	2.15	1296
800	1777.78	199	2.16	1728
1000	2222.22	249	2.16	2160

5.3 Discussion of the results

Analysing Figure 5-6, it could be claimed that the method that allows a higher rate of water production is gradual capacity. The option of installing gradual capacity seems to be the design with best results in most adverse months, except for January and December, when even surpassing the water production with gradual capacity, the difference between productions is negligible.

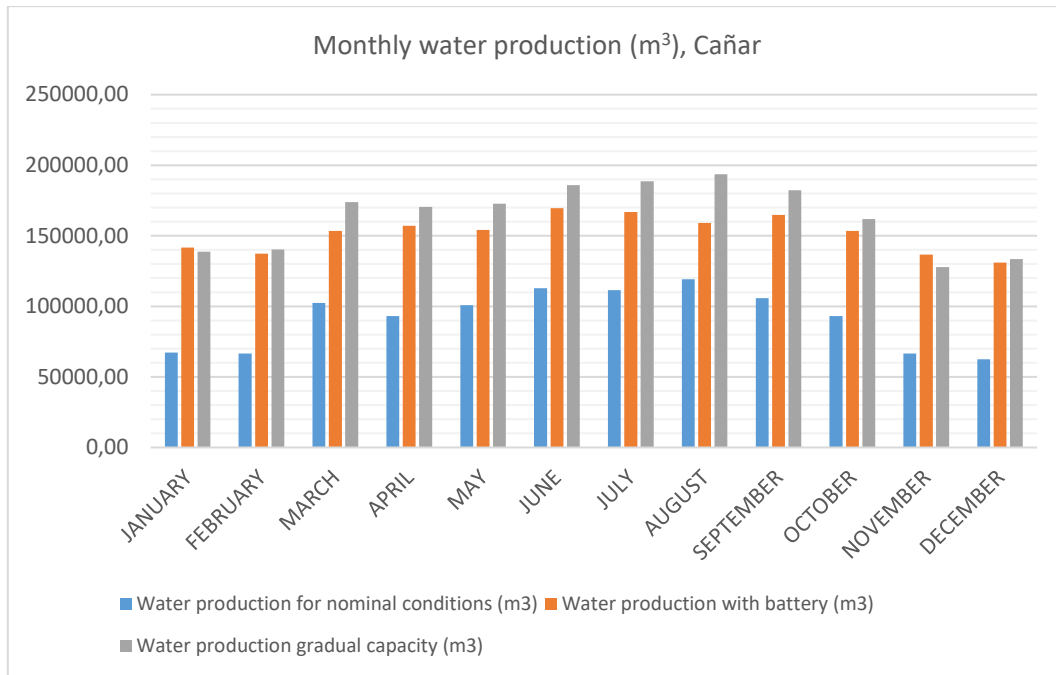


Figure 5-6. Water production for a PV system profile throughout the year in Cañar, for different system configurations.

The logical reasoning expressed on the previous paragraph could be interpolated for the other localisations, but in fact, as graphs showcased in the following Figures (from 5-6 to 5-10) display, the location causes great variation in the results.

Gradual capacity is visibly the design that guarantees the largest production of desalinated water throughout the year in some locations such as Cañar (Figure 5-6) or Machala (Figure 5-7), regardless, energy storage in batteries becomes a competitive option some months (between October and February).

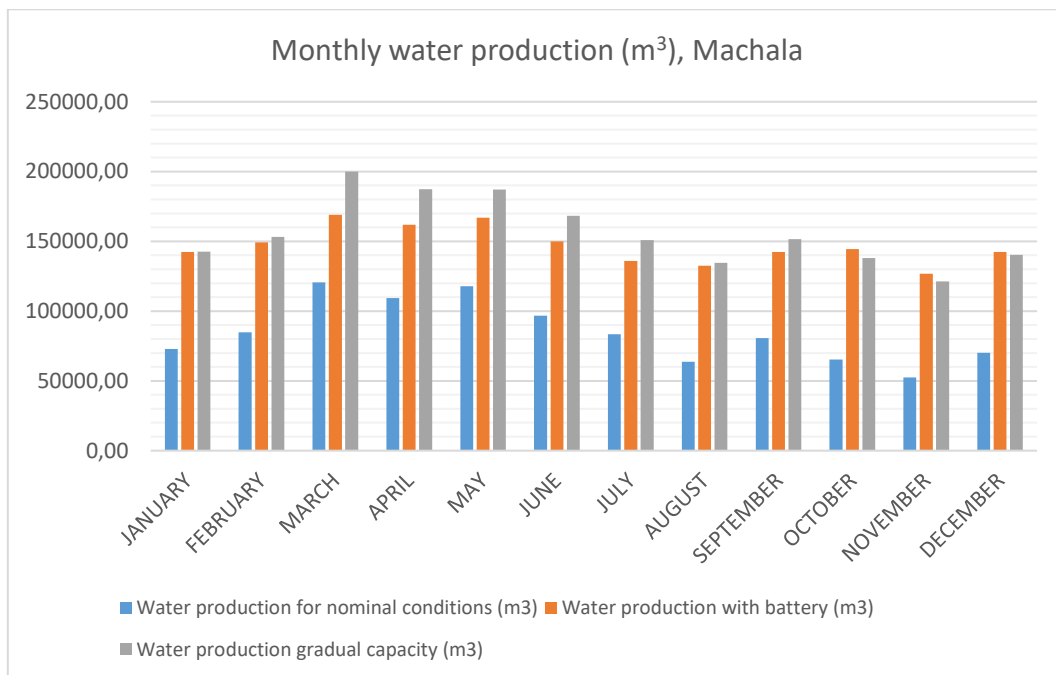


Figure 5-7. Water production for a PV system profile throughout the year in Machala, for different system configurations.

In the cases of Santiago (Figure 5- 8) and Valparaíso (Figure 5-9) energy storage can result in truly little water production or a production that exceeds the one achieved with gradual capacity, depending on the month. Being the second case, Valparaíso, as Figure 5-9 shows, more pronounced than the former, Santiago.

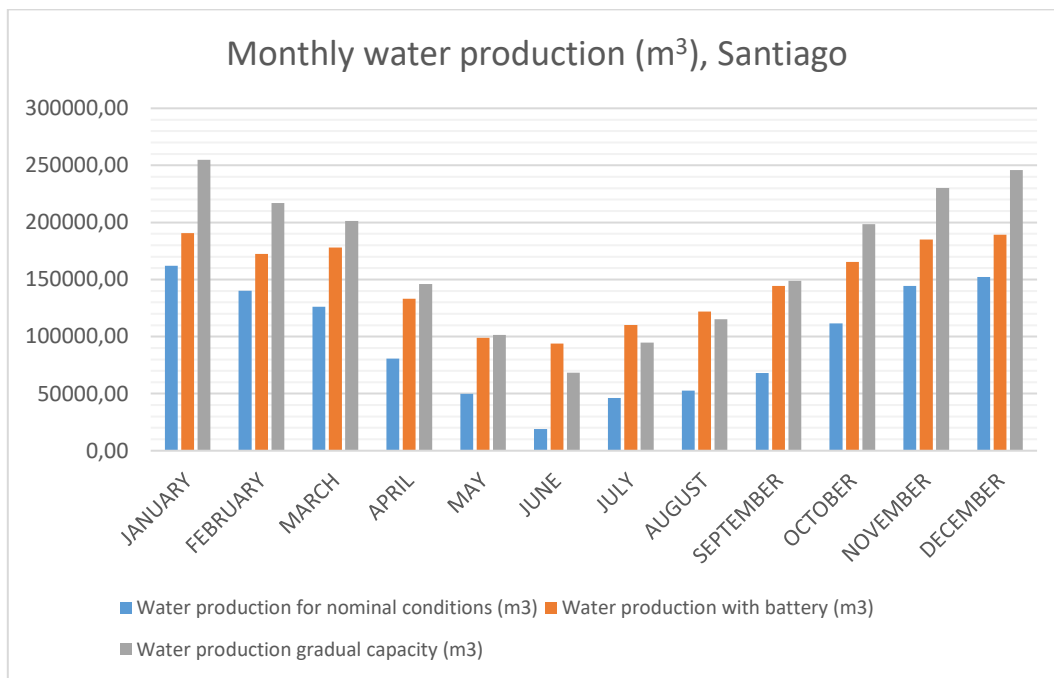


Figure 5-8. Water production for a PV system profile throughout the year in Santiago, for different system configurations.

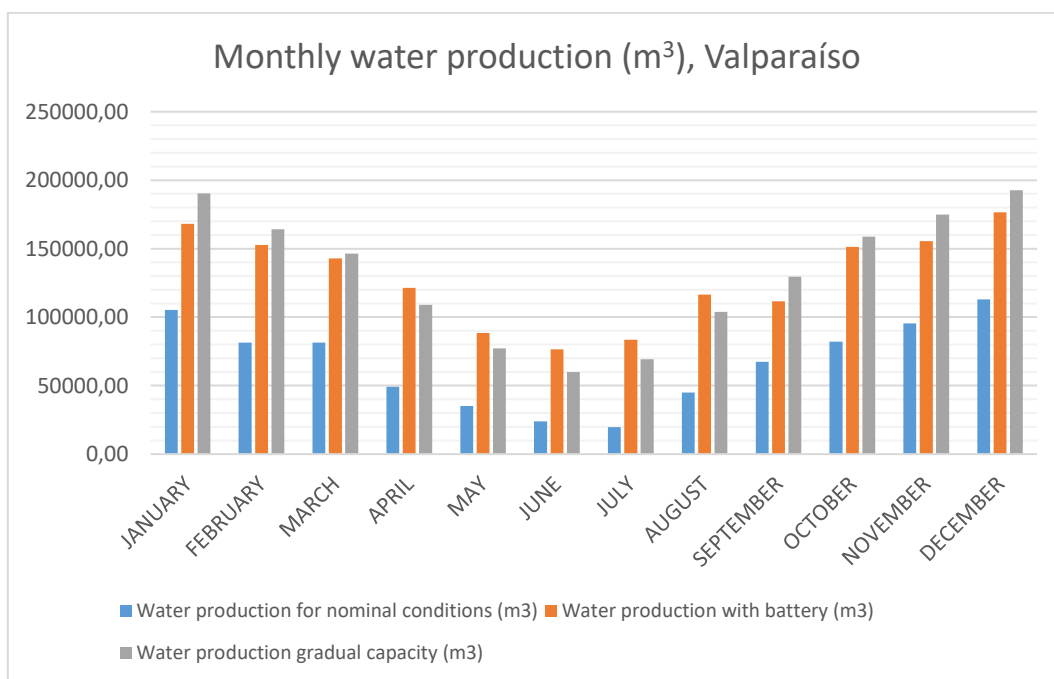


Figure 5-9. Water production for a PV system profile throughout the year in Valparaíso, for different system configurations.

On the other hand, the case of Antofagasta, demonstrates that energy storage systems may be preferable in some locations reaching the same results as gradual capacity in some months and exceeding it the rest of the year.

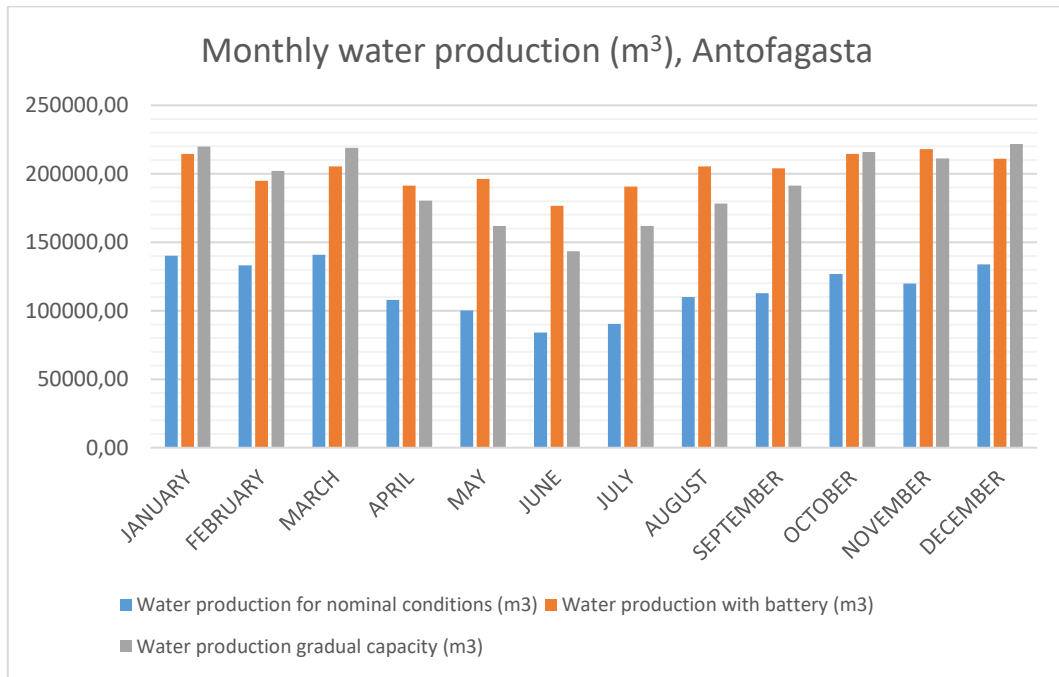


Figure 5-10. Water production for a PV system profile throughout the year in Antofagasta, for different system configurations.

The following Figure, Figure 5-11, is a summary of water production in the case of PV systems for each location.

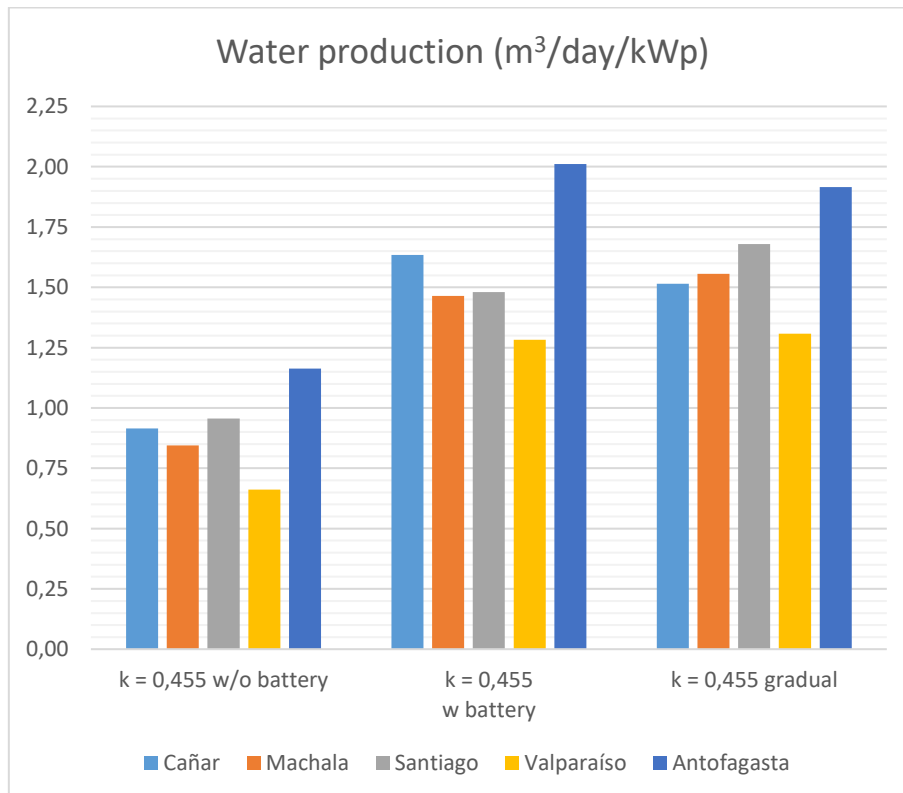


Figure 5-11. Summary of water production for a PV system profile, for different system configurations.

In conclusion, even though with gradual capacity the energy loss associated to charge and discharge of the batteries is eliminated, and therefore the energy can be better exploited, the results make clear that a decision on whether to choose between energy storage and gradual capacity cannot be made taking into consideration only production. The selection of these systems is highly influenced by their capital costs and the emplacement, and an economical assessment must be performed in order to conclude their feasibility, in other words; the costs and the region where the plant is located will be the decisive parameters when selecting the best design.

6 IMPACT OF BATTERIES IN DESALINATED WATER PRODUCTION WITH SOLAR PHOTOVOLTAIC SYSTEMS

The main drawbacks of renewable energy sources are their unpredictability, their intermittency owing to dependence on seasonal changes and the fact that their production might be de-coupled from the actual demand.

Energy storage is an issue of great importance for the development of renewable energy. At present, it is one of the greatest technical and commercial barriers due to the integration of RES, especially for those off-grid systems powered by intermittent solar or wind energy. Studies related to hybrid wind–photovoltaic battery power generation are mainly focused on modelling, capacity allocation, optimal design, economic evaluation, among others [25]. Energy storage systems are adopted to compensate the mismatch between the injections of a photovoltaic power plant and the day-ahead market power schedule.

Taking into consideration batteries in the case of photovoltaic technology, the number of operating hours of the RO Plant in a year can be prolonged in time, which translates to more desalinated water production. In other words, the first measure of improvement is the introduction of batteries as energy storage systems to exploit the energy surplus unutilized, to increase the annual useful energy.

The energy demand of desalination depends on a range of factors including recovery, pre-treatment design, the type of distillation process or SWRO membranes used, the efficiency of pumps and motors, the type and efficiency of the energy recovery system installed (if any), environmental conditions and the product water specifications.[25] For the study, this demand will be fixed and there will be three cases of nominal consumption for the RO Plant, comparing the production of desalinated water in the absence of batteries and including them.

The localisations under study chosen are no other than Santiago, Valparaíso and Antofagasta in Chile and Cañar and Machala in Ecuador. For the purpose of the analysis, the battery size is considered to be twice the RO plant consumption and the efficiency is considered to be 60%, since the energy loss in a battery is likely to be around 35% and 40%. Depth of discharge is the percentage ratio between the actual available capacity and the nominal capacity of the battery, this parameter influences the duration and efficiency of the battery and ranges from 70 to 80%.

Table 6–1. Localisations under study.

Ecuador	Chile
Cañar	Santiago
Machala	Valparaíso
	Antofagasta

Batteries of RES systems are subjected to frequent charging and discharging process. Gel type lead acid batteries are used for remote applications which require maintenance free operation.

Table 6–2. Battery data.

Concept	Value
Efficiency	60%
Depth of Discharge	75%

To begin with the assessment energy production with RE coupled with energy storage systems will be analysed, first in Ecuador and secondly in Chile. Lastly, the water production will be studied.

6.1 Energy production

6.1.1 Ecuador

Figure 6-1 (on the following page) shows the energy production profile of the PV systems and the performance of the battery bank. The dashed line represents the energy production profile, the solid line represents the energy that is stored in the battery and finally, the red line stands for the number of hours the RO plant is able to operate when the system includes energy storage.

First of all, it should be noted the energy that the PV system can produce represented stands for the hourly production whereas the energy available from the battery represents the energy stored, which means that is a cumulative value. It is noticeable that, as expected, the energy production pattern is repeated every day with a marked peak which coincides with those hours of the day where the solar radiation reaches its highest level, between 14.00 and 16.00 h, and remains constant and equal to zero at night.

Figure 6-2 represents the number of hours the RO plant is able to operate thanks to the energy supply of the PV systems; in pale blue when the system does not include energy storage and in black when the PV system incorporates battery.



Figure 6-1. Comparison of the number of hours the RO plant is operating without and with batteries in Cañar and Machala.

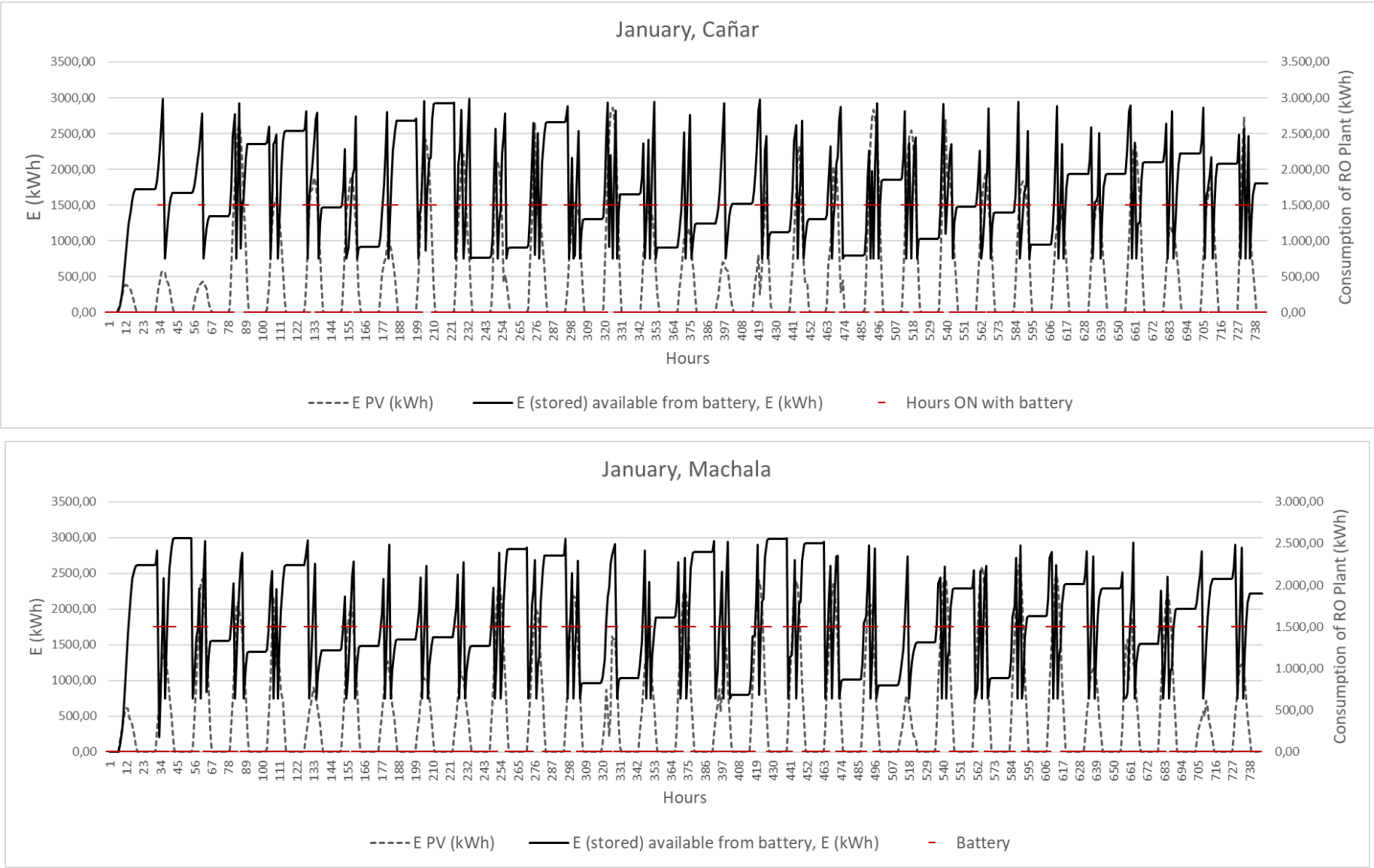


Figure 6-2. Energy collected with PV and energy stored in the battery during January in Cañar and Machala.

Figure 6-3 shows the effect of the energy storage systems in Cañar and Machala throughout the year. It can be noted the use of batteries implies indeed a major increase of useful energy, which is in fact, roughly four times the energy production of the system when all the energy surplus is neglected. On table 6-4 below the exact values of production can be observed, both Figure 6-4 and Table 6-4 demonstrate that the PV system proves to have a higher efficiency with the battery-based system.

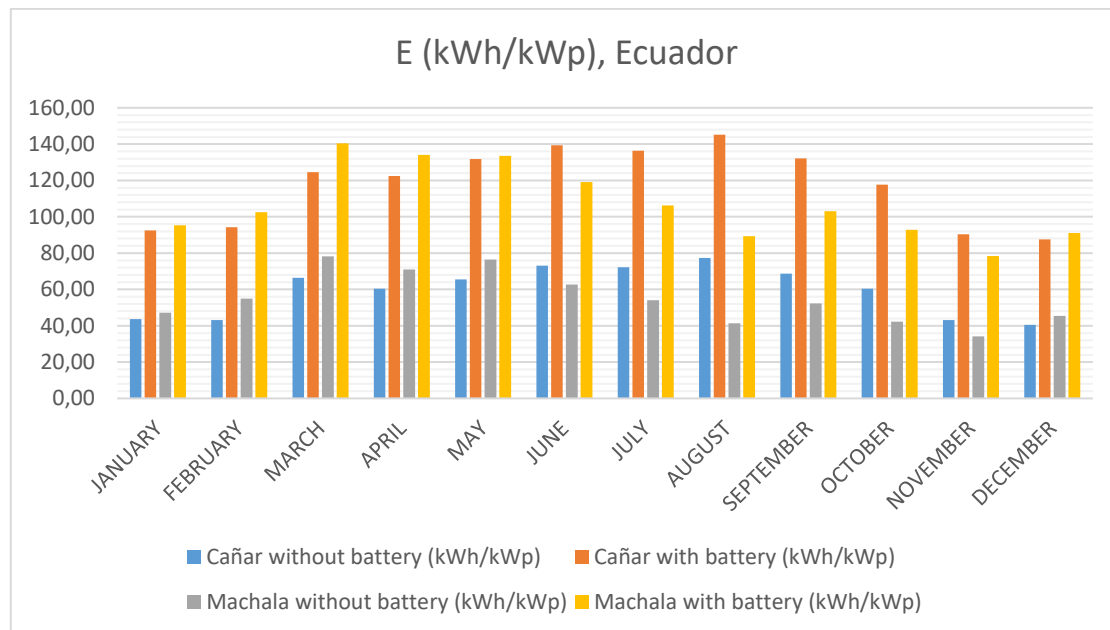


Figure 6-3. Monthly useful energy profile in Ecuador, with two hours of energy storage.

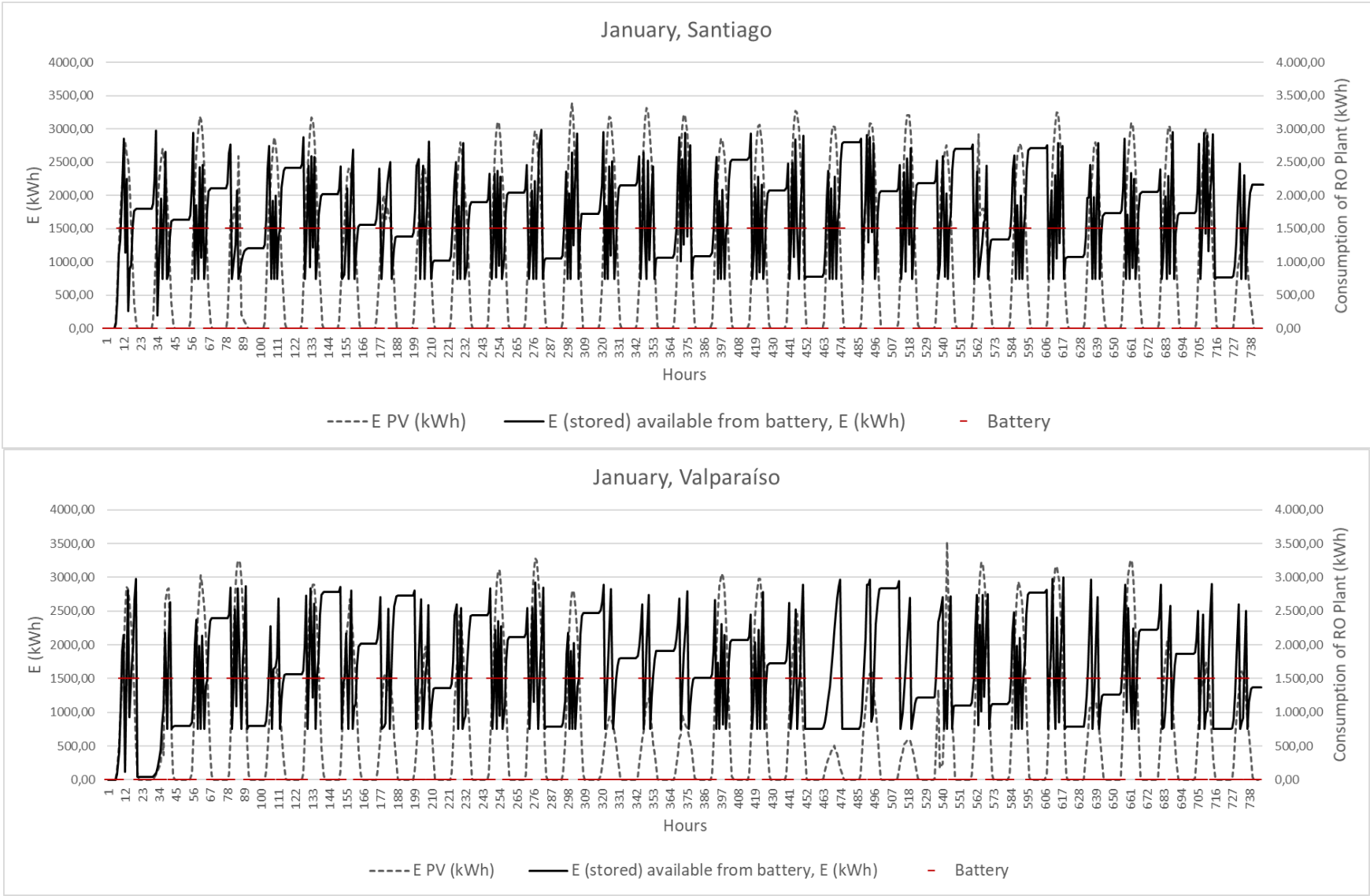
Table 6-3. Energy production in Ecuador, with two hours of energy storage.

MONTH	Energy production in Ecuador (kWh/kWp)			
	CAÑAR		MACHALA	
	Cañar without battery	Cañar with battery	Machala without battery	Machala with battery
JANUARY	43,64	92,53	47,27	95,32
FEBRUARY	43,18	94,32	55,00	102,54
MARCH	66,36	124,49	78,18	140,45
APRIL	60,45	122,53	70,91	134,14
MAY	65,45	131,79	76,36	133,49
JUNE	73,18	139,30	62,73	119,06
JULY	72,27	136,43	54,09	106,17
AUGUST	77,27	145,16	41,36	89,36
SEPTEMBER	68,64	132,13	52,27	103,09
OCTOBER	60,45	117,65	42,27	92,84
NOVEMBER	43,18	90,36	34,09	78,30
DECEMBER	40,45	87,51	45,45	91,15

6.1.2 Chile

The same process was followed then, for the regions located in Chile, and again, the results achieved were remarkably similar.

In Figure 6-4 it is showed the energy production profile of the PV systems and the performance of the battery bank. The same pattern explained in Figure 6-2 appears.



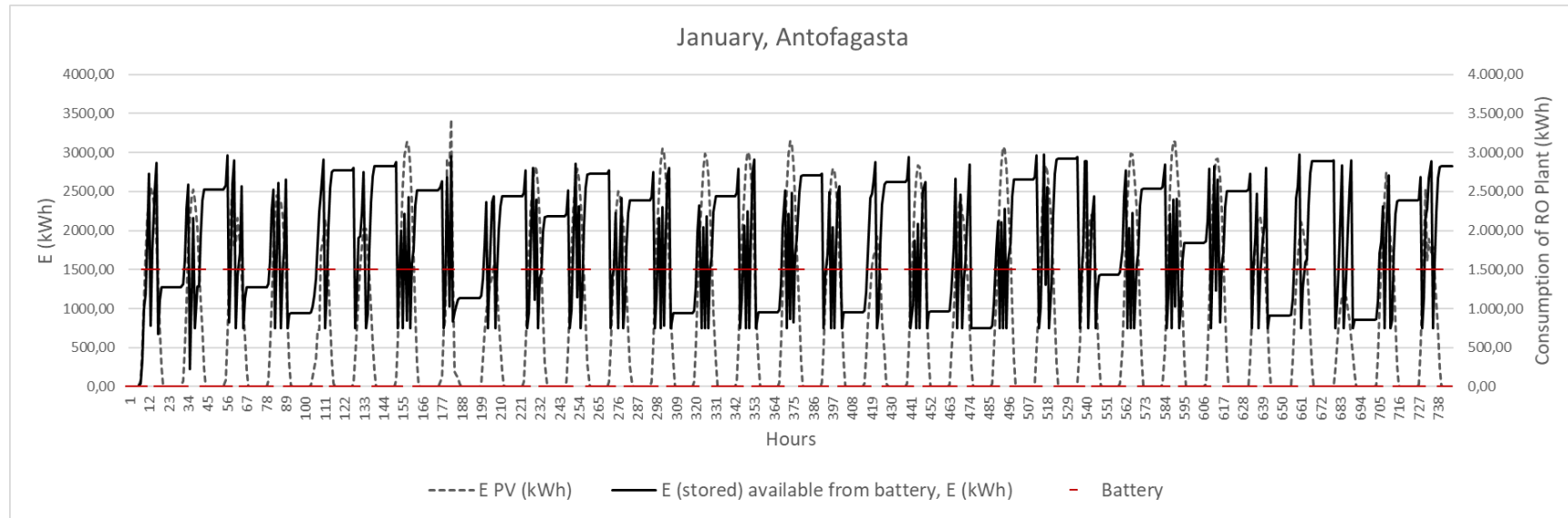


Figure 6-4. Operation of the RO Plant during January in Santiago, Valparaíso and Antofagasta in Chile.

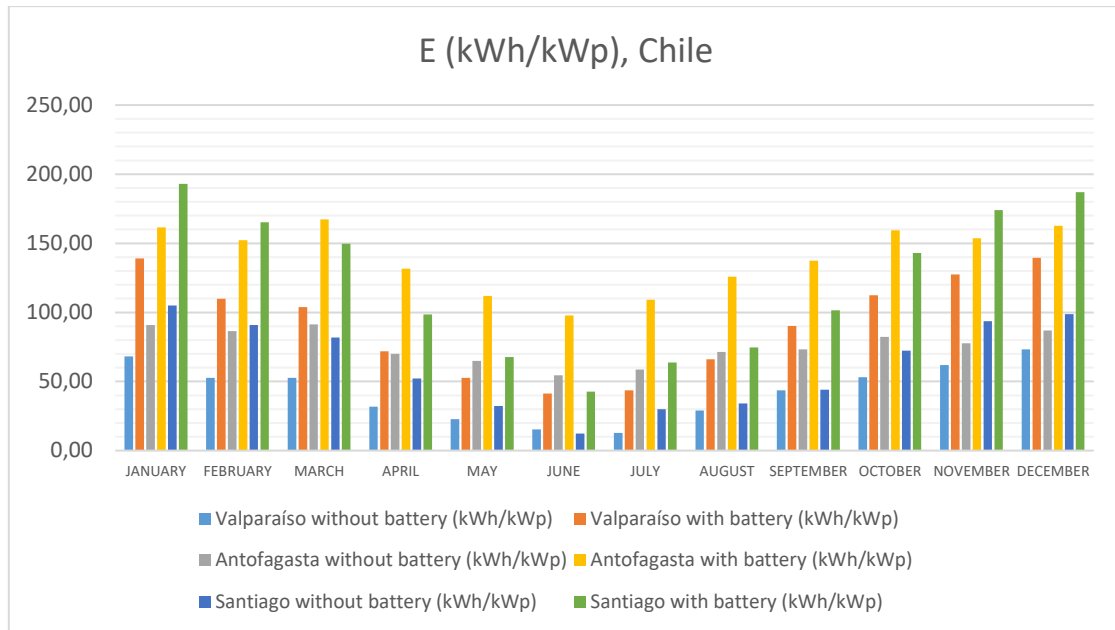


Figure 6-6. Monthly useful energy profile in Chile, with two hours of energy storage.

Table 6-4. Energy production in Chile, with two hours of energy storage.

Energy production in Chile (kWh/kWp)						
	SANTIAGO		VALPARAÍSO		ANTOFAGASTA	
MONTH	Santiago without battery	Santiago with battery	Valparaíso without battery	Valparaíso with battery	Antofagasta without battery	Antofagasta with battery
JANUARY	105,00	193,08	68,18	138,98	90,91	161,48
FEBRUARY	90,91	165,14	52,73	109,85	86,36	152,26
MARCH	81,82	149,67	52,73	103,87	91,36	167,38
APRIL	52,27	98,43	31,82	71,75	70,00	131,53
MAY	32,27	67,70	22,73	52,71	65,00	111,85
JUNE	12,27	42,79	15,45	41,35	54,55	97,81
JULY	30,00	63,84	12,73	43,66	58,64	109,09
AUGUST	34,09	74,70	29,09	66,17	71,36	125,73
SEPTEMBER	44,09	101,49	43,64	90,08	73,18	137,34
OCTOBER	72,27	143,03	53,18	112,33	82,27	159,32
NOVEMBER	93,64	174,03	61,82	127,47	77,73	153,60
DECEMBER	98,64	187,07	73,18	139,54	86,82	162,75

6.2 Water production

The water production will be described as a function of the earlier described in Chapter 4 (section 4.4. Desalinated water production. Case of study), k ratio, which expresses the ratio between the nominal consumption of the RO plant and the rated energy production of the PV plant:

Table 6-5. Values of k ratio for large scale plants.

Nominal consumption of the RO plant (kW)	Rated energy production of the plant (kW _p)	k value
1500	3300	0,4545
1000	3300	0,3030
500	3300	0,1515

6.2.1 Ecuador

Figures 6-7 and 6-8 showcase the improvement in water production in Cañar and Machala. On the one hand, it is remarkably visible that the investment on batteries in the case of k ratio equal to 0.152 does not result in significant enhancements compared to the other ratios.

On the other hand, the batteries do represent such an evident improvement for the other two cases. When the system does not count with batteries the water production profile of the plants with k ratios 0.455 and 0.303 is practically the same, adding them, the case of k ratio 0.455 is the one that produces more water. This means that more remarkable enhances are obtained for bigger k ratios.

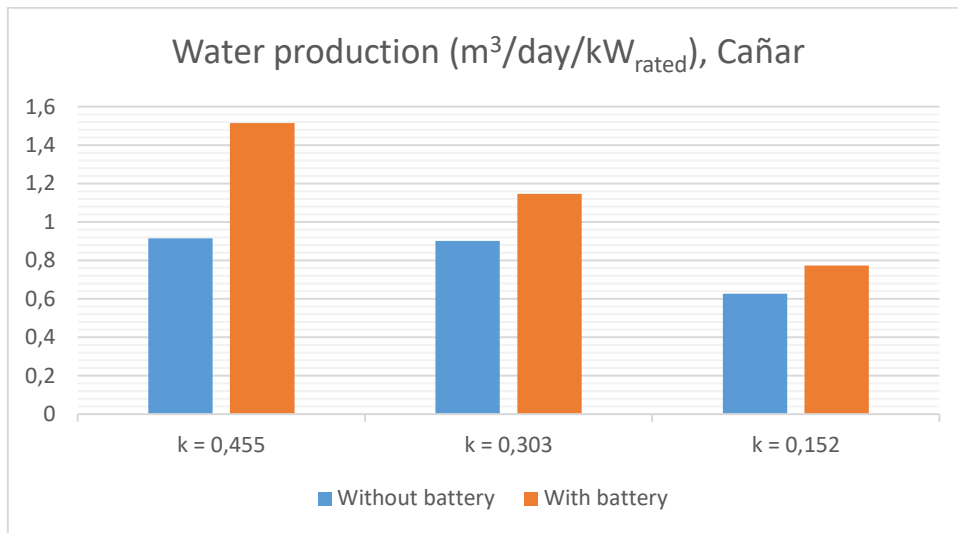


Figure 6-7. Desalinated water production with batteries in Cañar, SEC=2.14 kWh/m³.

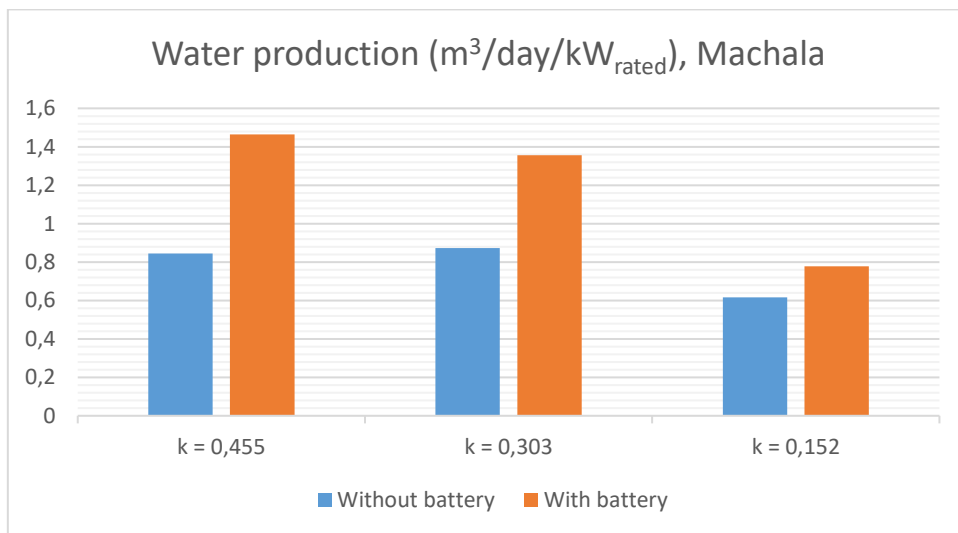


Figure 6-8. Desalinated water production with batteries in Machala, SEC=2.14 kWh/m³.

6.2.2 Chile

The cases Santiago, Valparaíso and Antofagasta, as Figures 6-9, 6-10 and 6-11 display are analogous; the bigger the k ratio, the better improvements in water production profile are obtained adding energy storage systems, remarkably noticeable in the case of Valparaíso (Figure 6-10).

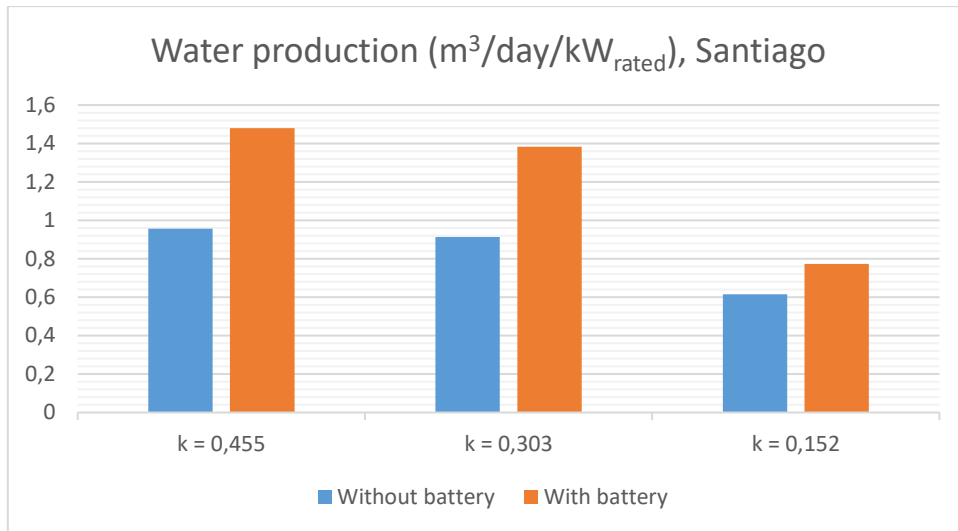


Figure 6-9. Desalinated water production with batteries in Santiago, SEC=2.14 kWh/m³.

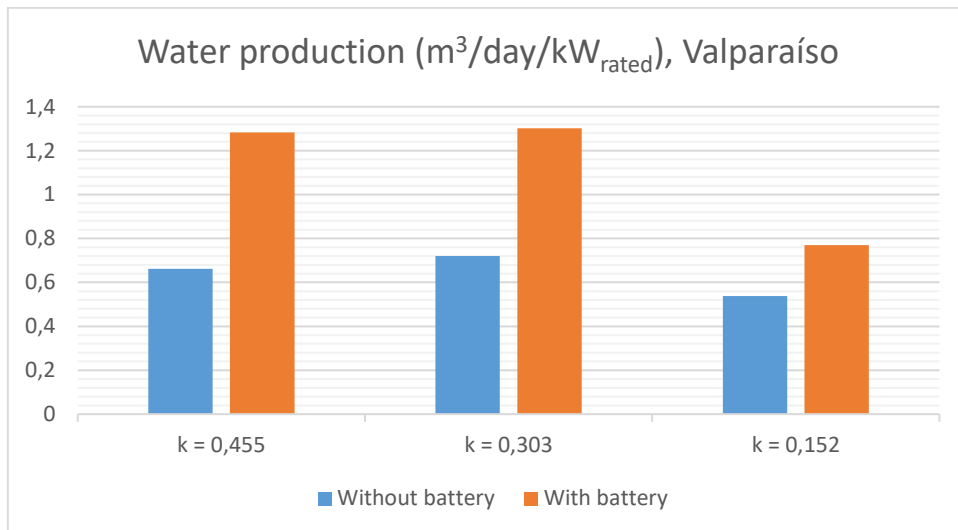


Figure 6-10. Desalinated water production with batteries in Valparaíso, SEC=2.14 kWh/m³.

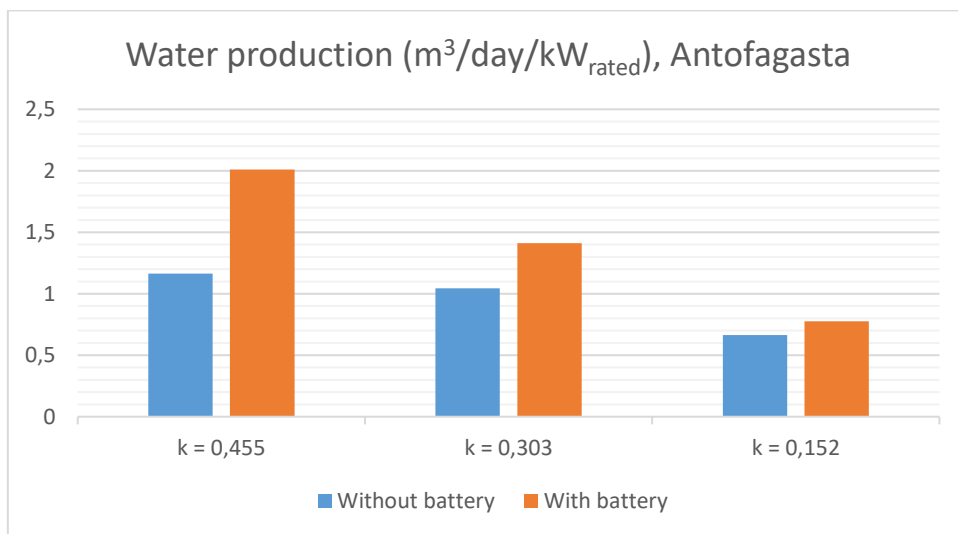


Figure 6-11. Desalinated water production with batteries in Antofagasta, SEC=2.14 kWh/m³.

Table 6-6 and Figure 6-12 summarise what has been exposed throughout the chapter, giving ranges of cubic meters of desalinated water produced per kW rated of the energy source in a day.

Table 6–6. Water production with PV, SEC=2.14 kWh/m³.

		Water production (m ³ /day/kW _{rated})					
		k = 0,455		k = 0,303		k = 0,152	
		k = 0,455 w/o battery	k = 0,455 w battery	k = 0,303 w/o battery	k = 0,303 w battery	k = 0,152 w/o battery	k = 0,152 w battery
Chile	Cañar	0,91	1,52	0,90	1,15	0,63	0,77
	Machala	0,84	1,46	0,87	1,36	0,62	0,78
Ecuador	Santiago	0,96	1,48	0,91	1,38	0,62	0,77
	Valparaíso	0,66	1,28	0,72	1,30	0,54	0,77
	Antofagasta	1,16	1,41	1,04	1,35	0,66	0,78

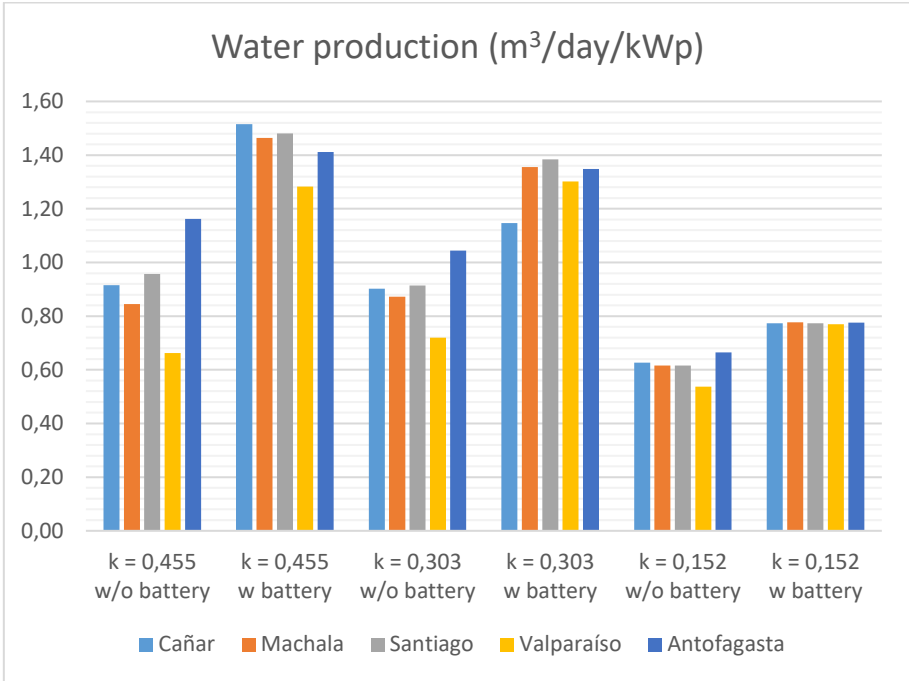


Figure 6-12. Desalinated water production in all regions with and without energy storage given a k ratio, SEC=2.14 kWh/m³.

6.3 Water production for different Specific Energy Consumptions

The Specific Energy Consumption (SEC) becomes much lower when the water treatment is set for effluents or brackish water instead of desalination of water directly pumped from the sea. The next sections present the assessment of water production when the SEC has the values of 1 kWh/m³ and 0.5 kWh/m³.

6.3.1 SEC=1 kWh/m³

The water production for this Specific Energy Consumption doubles and even surpasses the values obtained previously.

Table 6–7. Water production with PV, SEC=1 kWh/m³.

		Water production (m ³ /day/kW _{rated})					
		k = 0,455		k = 0,303		k = 0,152	
		k = 0,455 w/o battery	k = 0,455 w battery	k = 0,303 w/o battery	k = 0,303 w battery	k = 0,152 w/o battery	k = 0,152 w battery
Chile	Cañar	1,96	3,24	1,93	2,45	1,34	1,66
	Machala	1,81	3,13	1,87	2,90	1,32	1,66
Ecuador	Santiago	2,05	3,17	1,96	2,96	1,32	1,65
	Valparaíso	1,42	2,74	1,54	2,79	1,15	1,65
	Antofagasta	2,49	3,02	1,04	1,35	1,42	1,66

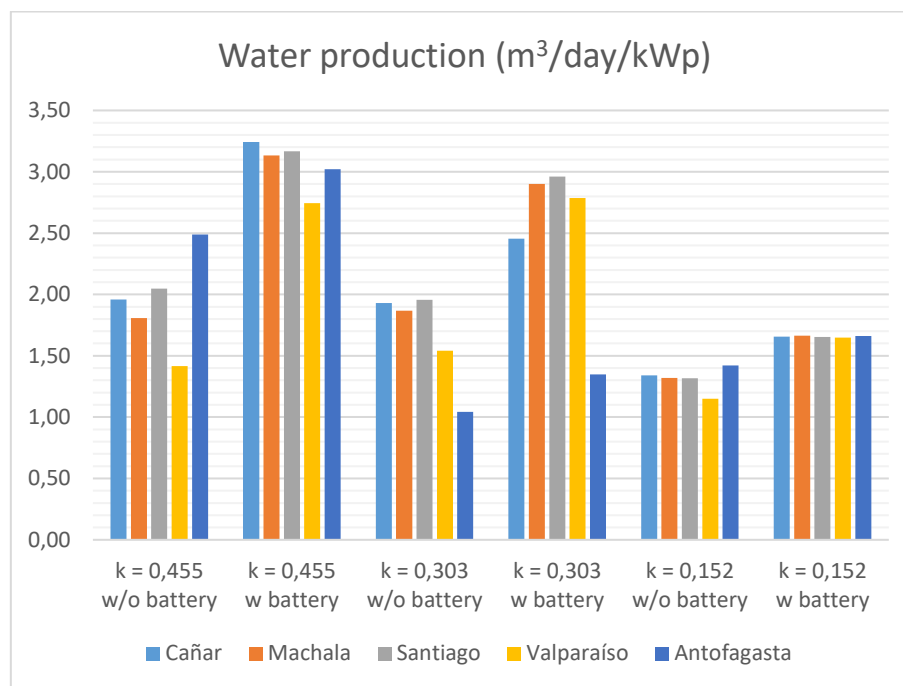


Figure 6-13. Desalinated water production in all regions with two hours of energy storage and without energy storage given a k ratio, SEC=0.5 kWh/m³.

6.3.2 SEC=0.5 kWh/m³

The water production is a direct function of the Specific Energy Consumption; for this case, where the SEC is half the SEC on the previous section, the production is the twice the one obtained for SEC=1 kWh/m³.

Table 6–8. Water production with PV, SEC=0.5 kWh/m³.

		Water production (m ³ /day/kW _{rated})					
		k = 0,455		k = 0,303		k = 0,152	
		k = 0,455 w/o battery	k = 0,455 w battery	k = 0,303 w/o battery	k = 0,303 w battery	k = 0,152 w/o battery	k = 0,152 w battery
Chile	Cañar	3,92	6,49	3,86	4,91	2,68	3,31
	Machala	3,62	6,27	3,73	5,80	2,64	3,33
Ecuador	Santiago	4,09	6,34	3,91	5,92	2,64	3,31
	Valparaíso	2,83	5,49	3,08	5,57	2,30	3,30
	Antofagasta	4,98	6,04	1,04	1,35	2,84	3,32

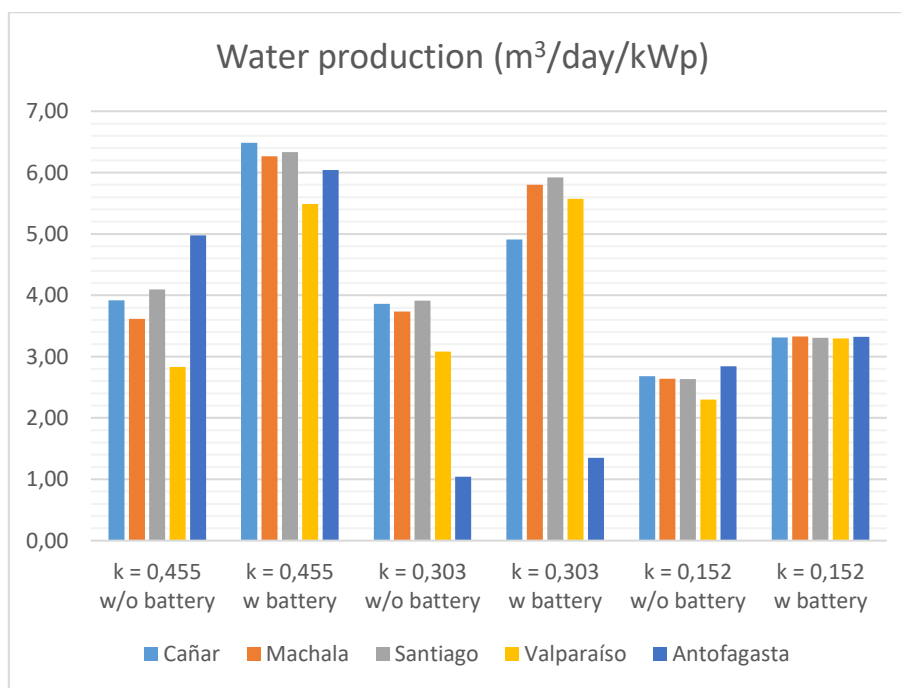


Figure 6-14. Desalinated water production in all regions with two hours of energy storage and without energy storage given a k ratio, SEC=0.5 kWh/m³.

The conclusions that may be extracted from the results are clear and expected; water production is a direct function of the Specific Energy Consumption, the lower the Specific Consumption of the process, the higher the water production the RO plant may offer as the energy required to operate is lower.

7 IMPACT OF BATTERIES IN DESALINATED WATER PRODUCTION WITH WIND SYSTEMS

This chapter, extends the topic discussed on the previous chapter to Wind technology, so that the energy production and the desalinated water produced will be studied.

7.1 Energy production

7.1.1 Ecuador

Figure 7-1 (on the following page) shows the energy production profile that the wind turbine generates and the performance of the battery. The remarkable pattern repeated every day in the case of PV does not apply for wind, as the energy production is not directly linked to the solar radiation. Results show, nevertheless, that the wind allows to produce more electricity than the solar source.

Figure 7-2 represents the number of hours the RO plant is able to operate thanks to the energy supply of the Wind energy; the starting point (in pale blue) was better than the case of PV systems in this region and the results of energy storage systems (in black) prove batteries to be a great option to consider.

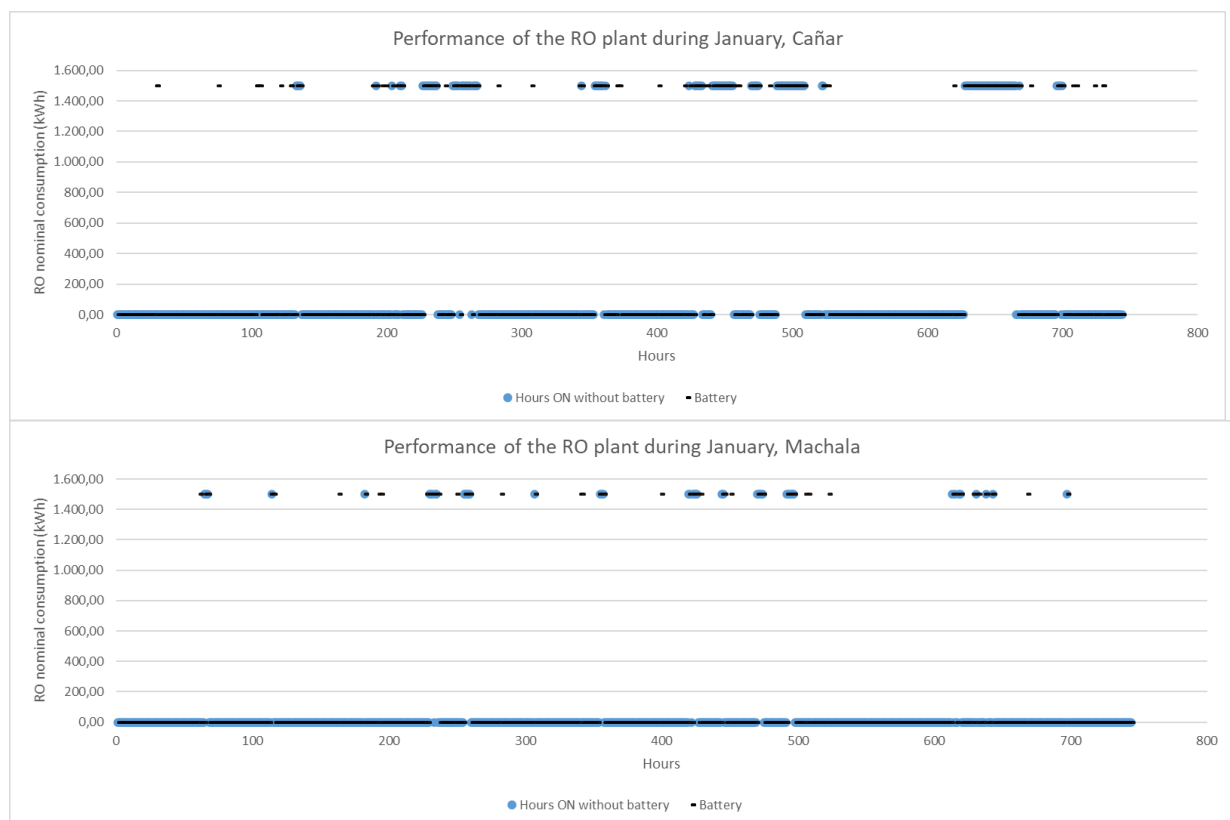


Figure 7-1. Comparison of the number of hours the RO plant is operating without and with batteries in Cañar.

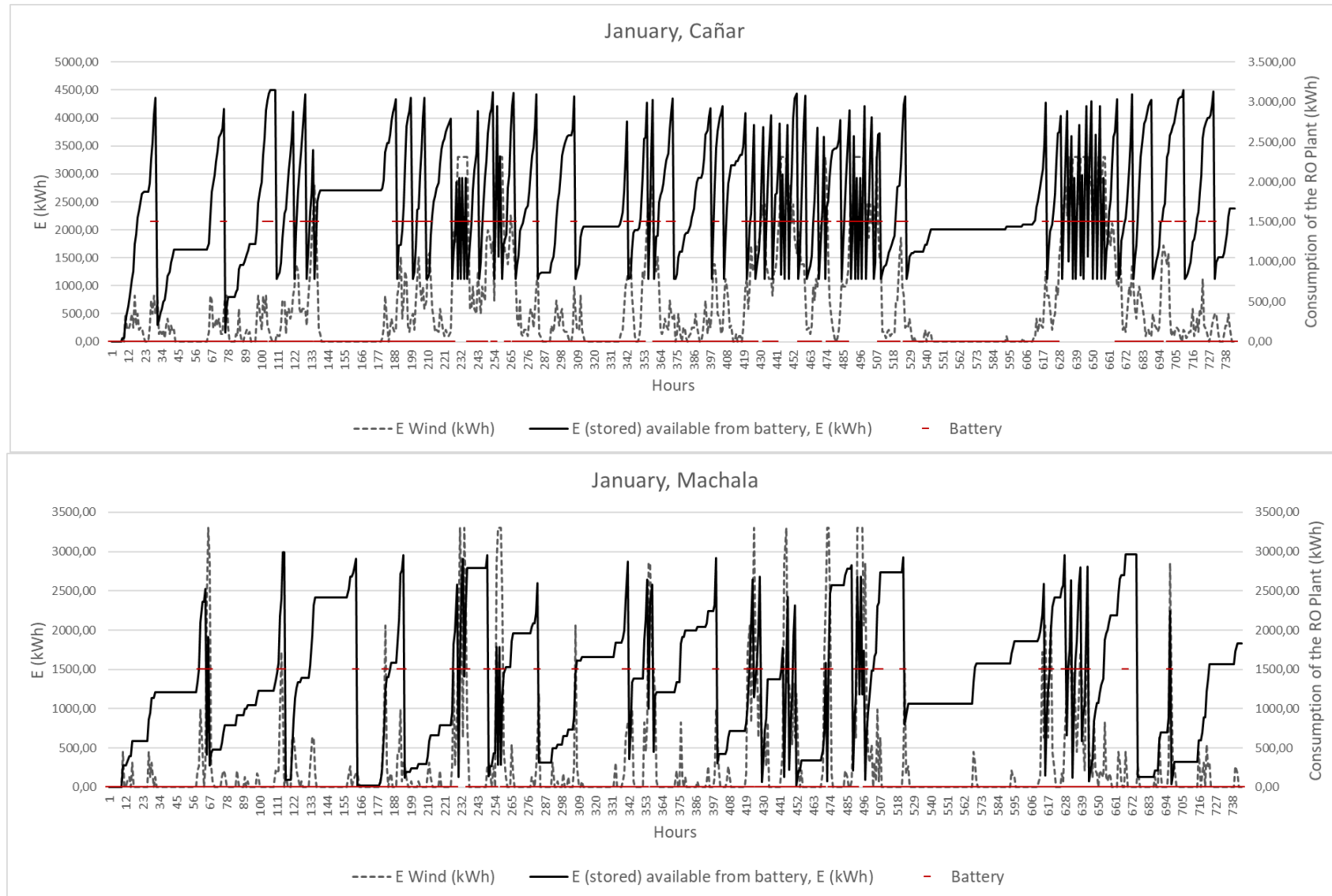


Figure 7-2. Energy collected with wind and energy stored in the battery during January in Cañar and Machala.

Figure 7-3 shows, as its analogous (Figure 6-4 in chapter 6) the effect of the energy storage systems in Cañar and Machala throughout the year. For wind energy batteries still imply a major increase of useful energy, fairly four times the energy production of the system when all the energy surplus is not considered.

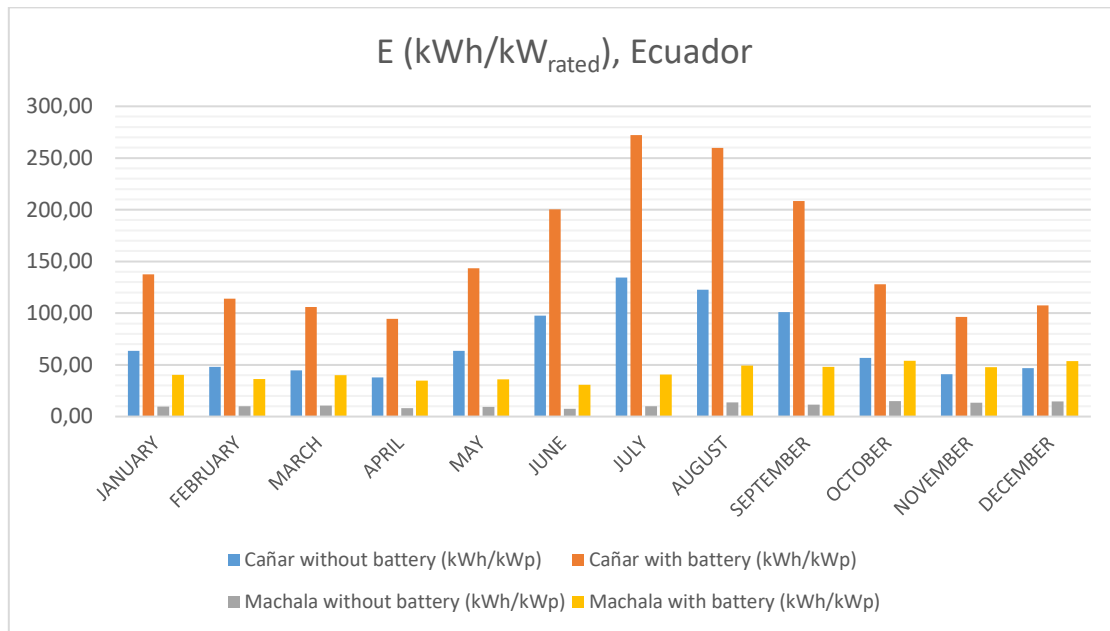


Figure 7-3. Monthly useful energy profile in Ecuador, with two hours of energy storage.

Table 7-1 showcases the exact values of production, from Figure 7-1.

Table 7-1. Energy production in Ecuador, with two hours of energy storage.

MONTH	Energy production in Ecuador (kWh/kW _{rated})			
	CAÑAR		MACHALA	
	Cañar without battery	Cañar with battery	Machala without battery	Machala with battery
JANUARY	63,64	137,41	9,77	40,33
FEBRUARY	48,18	114,10	9,98	36,38
MARCH	44,55	105,82	10,62	39,92
APRIL	37,73	94,52	8,28	34,87
MAY	63,64	143,42	9,35	35,95
JUNE	97,73	200,31	7,43	30,80
JULY	134,55	272,31	9,98	40,66
AUGUST	122,73	259,87	13,81	49,18
SEPTEMBER	100,91	208,33	11,68	48,02
OCTOBER	56,82	127,92	15,08	53,94
NOVEMBER	40,91	96,40	13,38	47,78
DECEMBER	46,82	107,36	14,66	53,68

7.1.1.1 Small scale

Most of the gold mining industry in Latin America is comprised of small facilities in remote, off-grid areas, without supply of electricity or fuels as mentioned which leads to the assessment of smaller RES systems.

Figure 7-4 displays the energy produced along the year in different regions of Ecuador when the wind turbine is 15 kW rated.

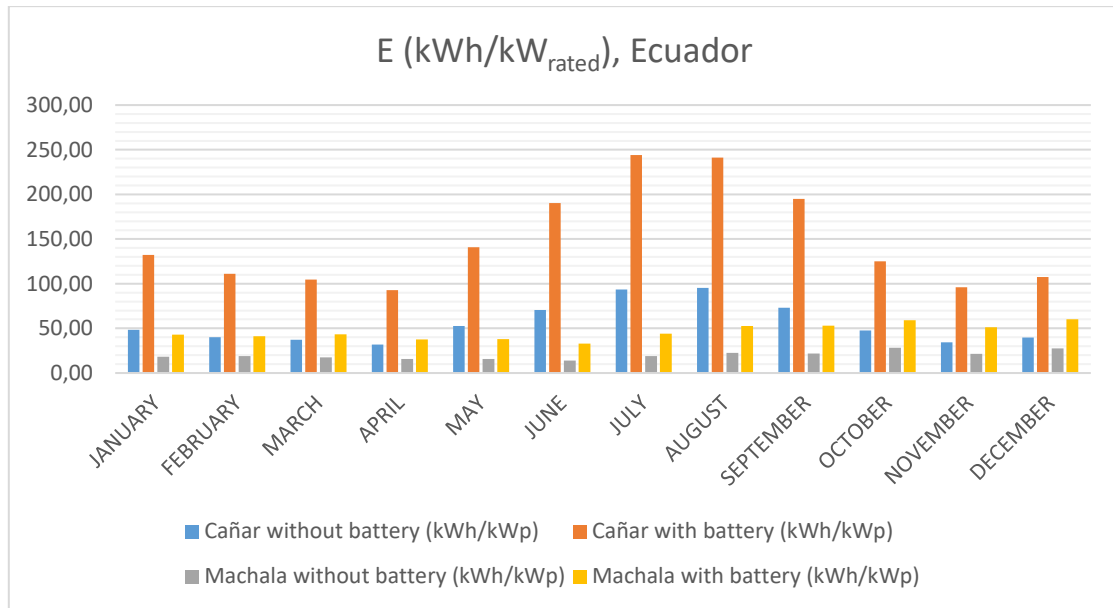


Figure 7-4. Monthly useful energy profile in Ecuador for a 15 kW wind turbine, with two hours of energy storage.

7.1.2 Chile

The same process was followed for the regions located in Chile and the results achieved were very similar, as happened in the case of solar PV. Figure 7-6 (on the following page) shows that the hours the RO plant is able to operate thanks energy storage are visibly more.

Figure 7-6 is analogue to Figure 7-2, representing the number of hours the RO plant can operate thanks to the energy supply of the Wind energy.

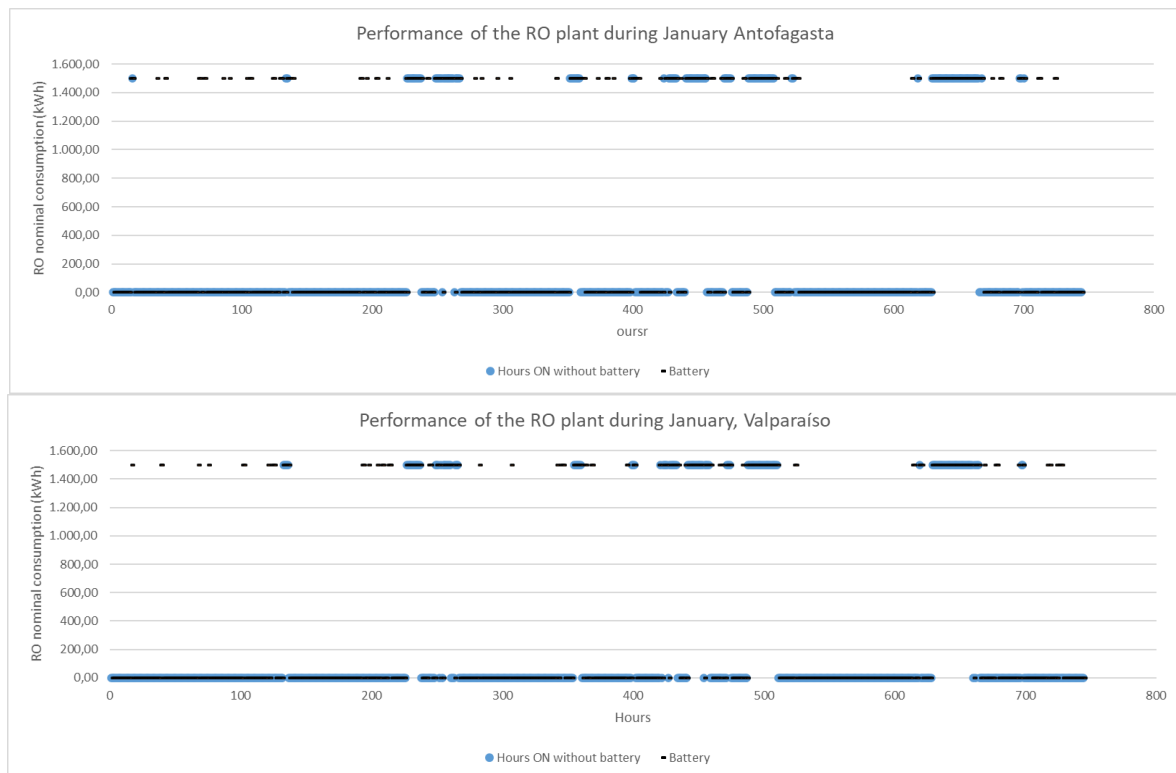


Figure 7-5. Operation of the RO Plant during January in Antofagasta and Valparaíso, Chile.

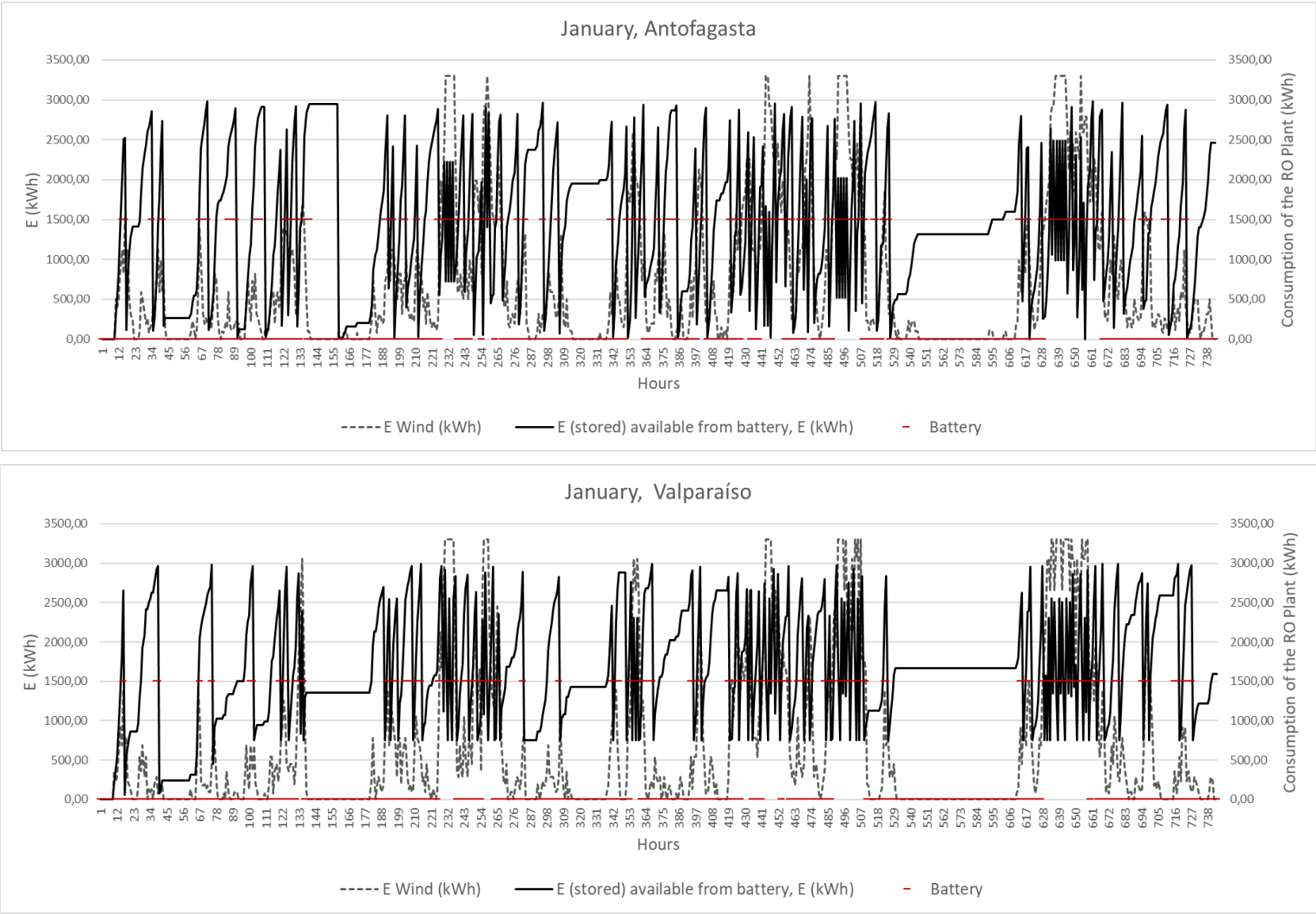


Figure 7-6. Operation of the RO Plant during January in Antofagasta and Valparaíso, Chile.

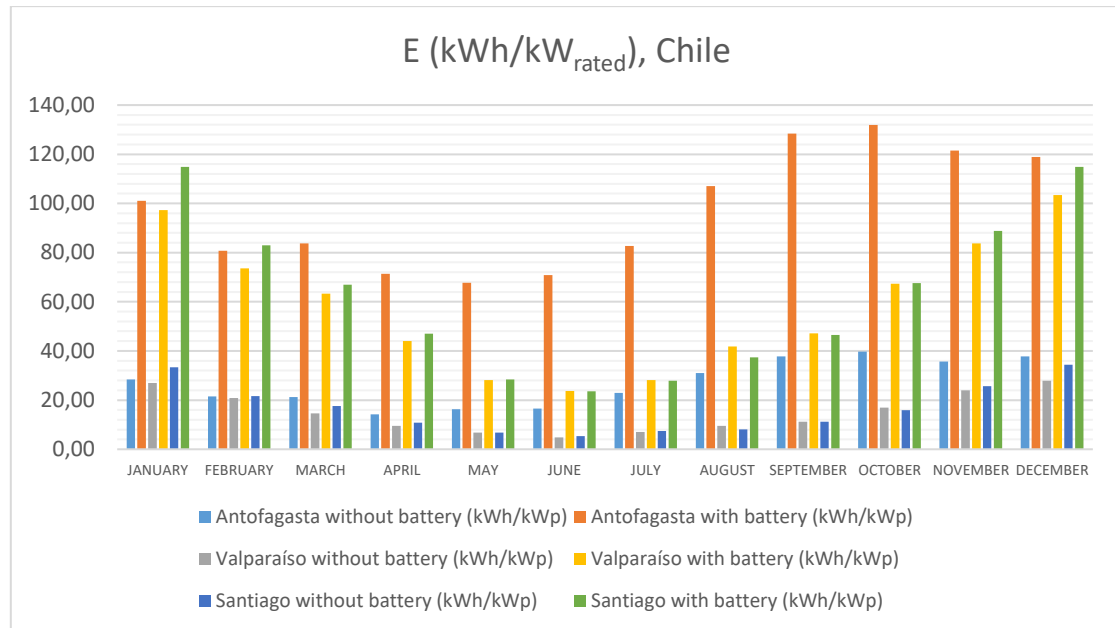


Figure 7-7. Monthly useful energy profile in Chile, with two hours of energy storage.

Table 7–2. Energy production in Chile, with two hours of energy storage.

MONTH	Energy production in Chile (kWh/kW _{rated})					
	SANTIAGO		VALPARAÍSO		ANTOFAGASTA	
	Santiago without battery	Santiago with battery	Valparaíso without battery	Valparaíso with battery	Antofagasta without battery	Antofagasta with battery
JANUARY	33,35	114,84	28,46	101,03	26,98	97,33
FEBRUARY	21,67	83,02	21,45	80,73	20,82	73,56
MARCH	17,63	66,89	21,24	83,79	14,66	63,33
APRIL	10,83	47,01	14,23	71,39	9,56	44,08
MAY	6,80	28,36	16,36	67,70	6,80	28,08
JUNE	5,31	23,57	16,57	70,90	4,89	23,71
JULY	7,43	27,84	22,94	82,70	7,01	28,15
AUGUST	8,07	37,44	31,01	107,04	9,56	41,83
SEPTEMBER	11,26	46,50	37,81	128,34	11,26	47,14
OCTOBER	15,93	67,63	39,72	131,88	16,99	67,37
NOVEMBER	25,70	88,87	35,68	121,51	24,00	83,71
DECEMBER	34,41	114,87	37,81	118,94	27,82	103,43

7.1.2.1 Small scale

Even though most of the mining industry in Chile is comprised of large mining settlements, it is also interesting to study the energy production when the turbine selected has a rated power of 15 kW.

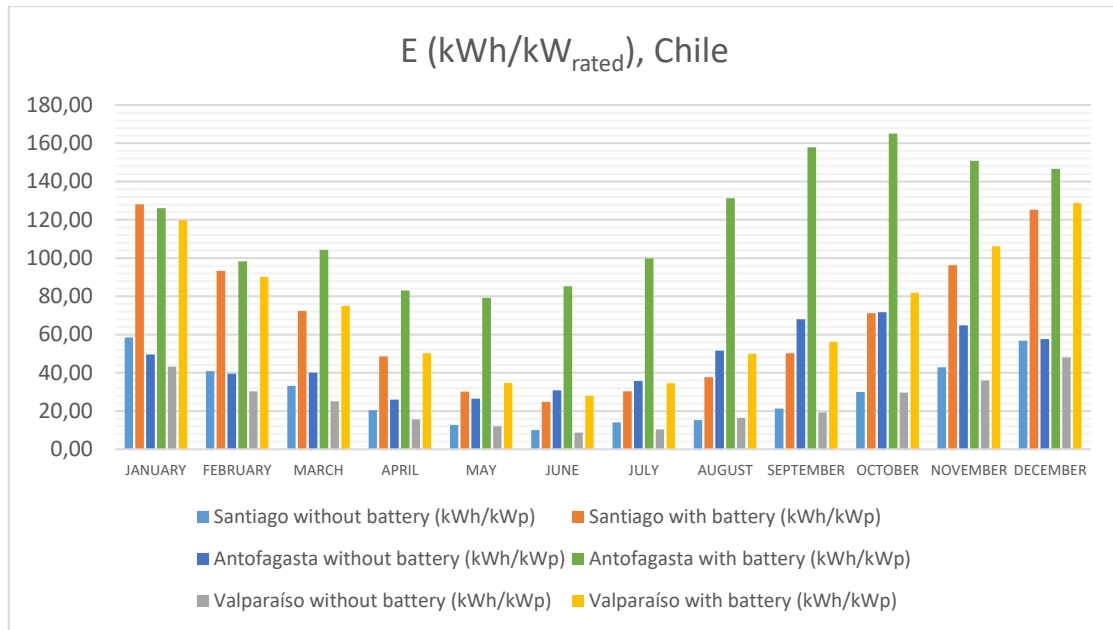


Figure 7-8. Monthly useful energy profile in Chile for a 15 kW wind turbine, with two hours of energy storage.

7.2 Water production

The values of k ratio described in Chapter 4 are the same for wind systems except that for wind systems small plants will also be studied, for which different values of k ratio are analysed.

Table 7–3. Values of k ratio for large scale plants.

Nominal consumption of the RO plant (kW)	Rated energy production of the plant (kW _{rated})	k value
1500	3300	0,4545
1000	3300	0,3030
500	3300	0,1515

Table 7–4. Values of k ratio for small scale capacities.

Nominal consumption of the RO plant (kW)	Rated energy production of the plant (kW _{rated})	k value
6	15	0,4000
4	15	0,2667
2	15	0,1333

7.2.1 Ecuador

Figures 7-9 and 7-10 display the amelioration of water production in Cañar and Machala. This time, for wind system as the RES driving power, results differ from the ones obtained for PV; batteries do represent a clear improvement for all three cases and the investment on energy storage in the case of k ratio equal to 0.152 does have good results, however, the best enhancement in water production is obtained for $k=0,303$, being the case of Machala more visible.

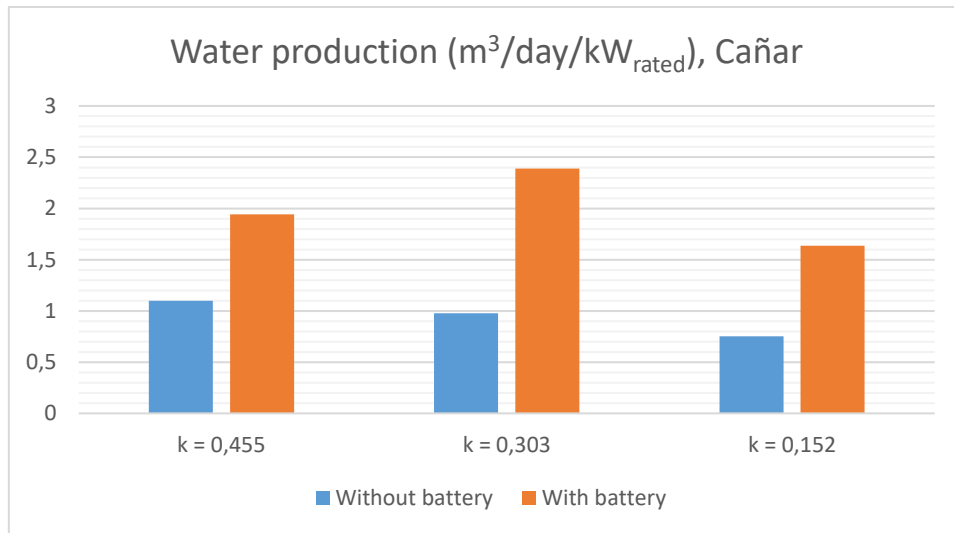


Figure 7-9. Desalinated water production with batteries in Cañar, SEC=2.14 kWh/m³.

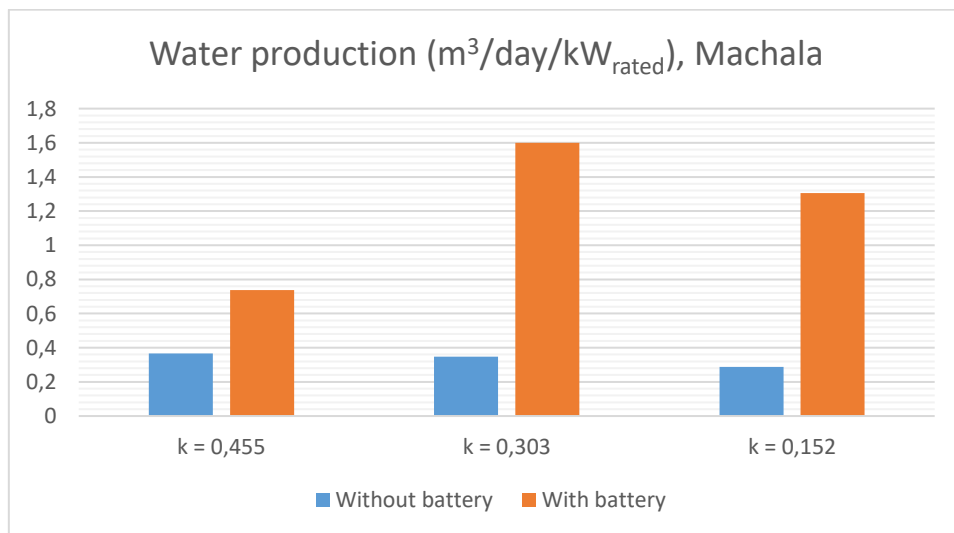


Figure 7-10. Desalinated water production with batteries in Machala, SEC=2.14 kWh/m³.

7.2.2 Chile

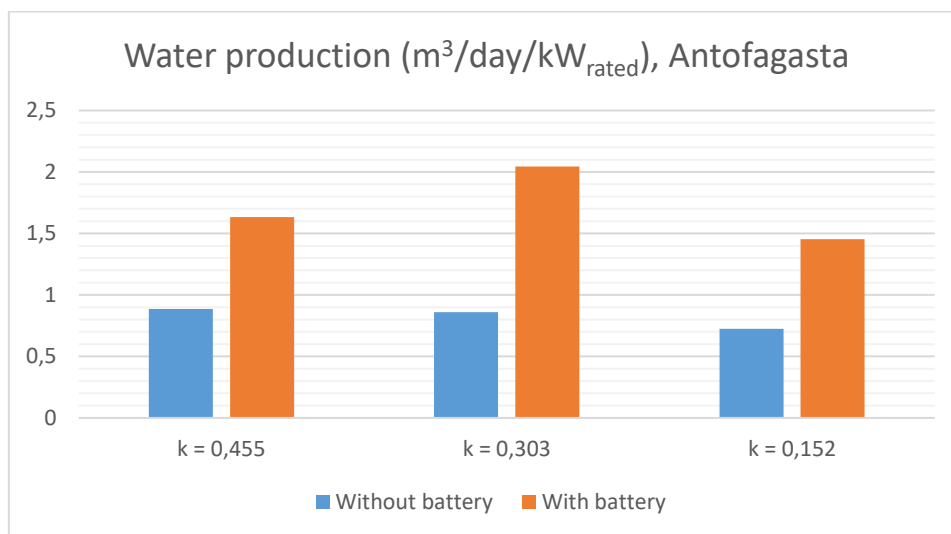


Figure 7-11. Desalinated water production with batteries in Antofagasta, SEC=2.14 kWh/m³.

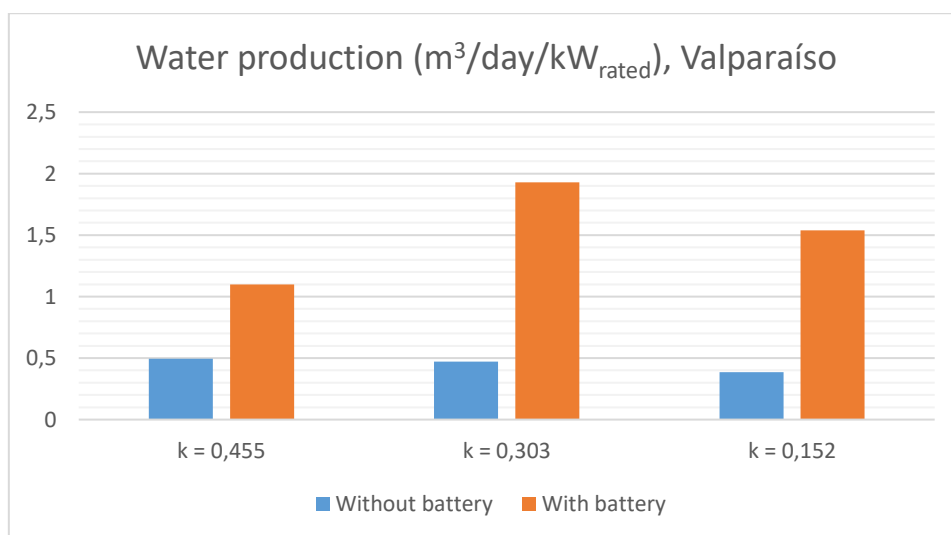


Figure 7-12. Desalinated water production with batteries in Valparaíso, SEC=2.14 kWh/m³.

Table 7-5 and Figure 7-13 summarize what has been exposed throughout the chapter, estimated values of water production capacity per kW rated of the energy source in a day.

Table 7-5. Water production with Wind, SEC=2.14 kWh/m³.

		Water production (m ³ /day/kW _{rated})					
		k = 0,455		k = 0,303		k = 0,152	
		k = 0,455 w/o battery	k = 0,455 w battery	k = 0,303 w/o battery	k = 0,303 w battery	k = 0,152 w/o battery	k = 0,152 w battery
Chile	Cañar	1,10	1,94	0,98	2,39	0,75	1,64
	Machala	0,37	0,74	0,35	1,60	0,29	1,31
Ecuador	Antofagasta	0,89	1,63	0,86	2,04	0,72	1,45
	Valparaíso	0,49	1,10	0,47	1,54	0,38	1,54

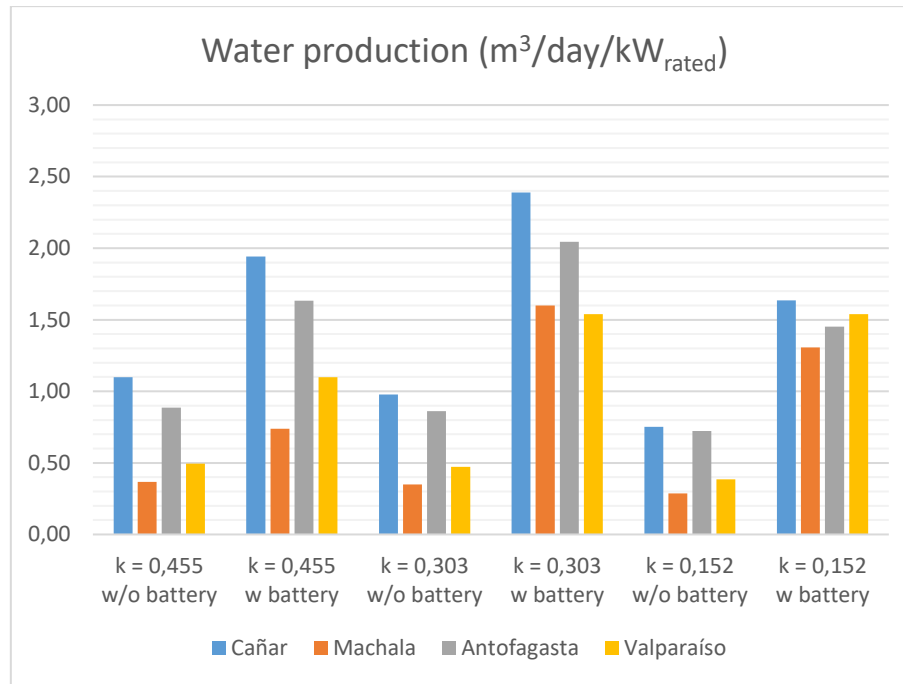


Figure 7-13. Desalinated water production with two hours of energy storage and without batteries, SEC=2.14 kWh/m³.

7.3 Water production for different Specific Energy Consumptions

In the following sections, as well as was carried out on the previous chapter, the results for water production when the SEC has the values of 1 kWh/m³ and 0.5 kWh/m³ will be presented.

7.3.1 SEC=1 kWh/m³

Table 7-6. Water production with Wind, SEC=1 kWh/m³.

		Water production (m ³ /day/kW _{rated})					
		k = 0,455		k = 0,303		k = 0,152	
		k = 0,455 w/o battery	k = 0,455 w battery	k = 0,303 w/o battery	k = 0,303 w battery	k = 0,152 w/o battery	k = 0,152 w battery
Chile	Cañar	2,35	4,16	2,09	5,11	1,61	3,50
	Machala	0,79	1,58	0,75	3,43	0,62	2,79
Ecuador	Antofagasta	1,90	3,50	1,84	4,38	1,55	3,11
	Valparaíso	1,06	2,35	1,01	3,29	0,82	3,29

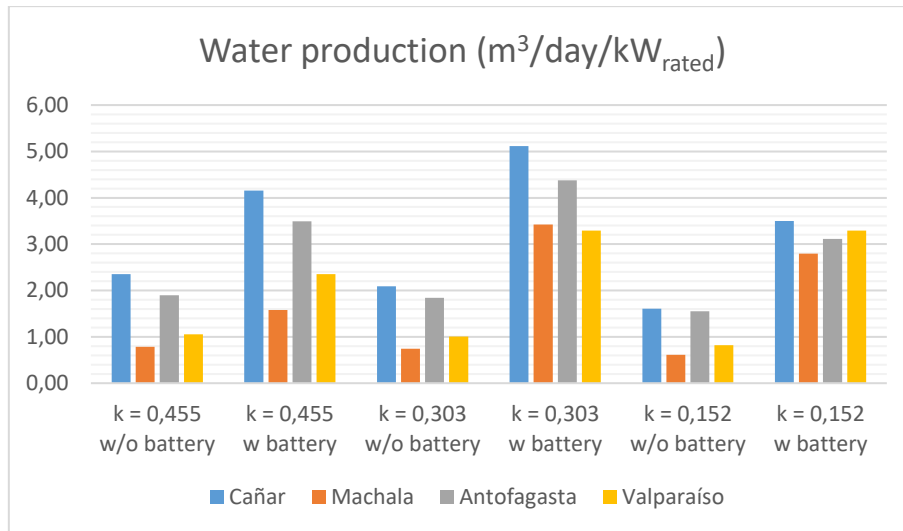


Figure 7-14. Desalinated water production with two hours of energy storage and without batteries, SEC=1 kWh/m³.

7.3.1.1 Small scale, SEC=1 kWh/m³

Table 7-7. Water production for a 15 kW wind turbine, SEC=1 kWh/m³.

		Water production (m ³ /day/kW _{rated})					
		k = 0,455		k = 0,303		k = 0,152	
		k = 0,455 w/o battery	k = 0,455 w battery	k = 0,303 w/o battery	k = 0,303 w battery	k = 0,152 w/o battery	k = 0,152 w battery
Chile	Cañar	2,28	4,63	2,22	5,45	1,70	3,81
	Machala	0,73	1,98	0,74	4,45	0,65	3,52
Ecuador	Antofagasta	1,92	4,41	2,05	5,73	1,68	3,73
	Valparaíso	1,01	2,60	1,09	4,58	0,87	3,57

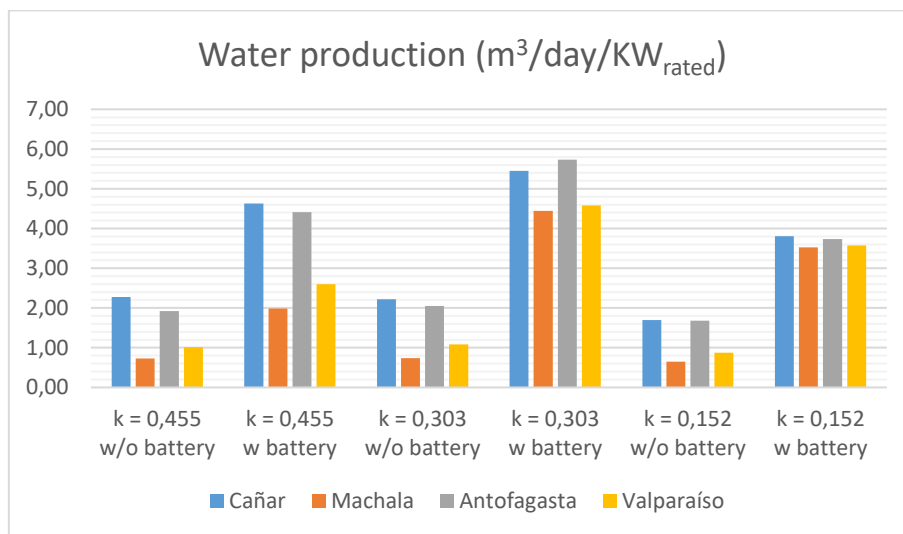
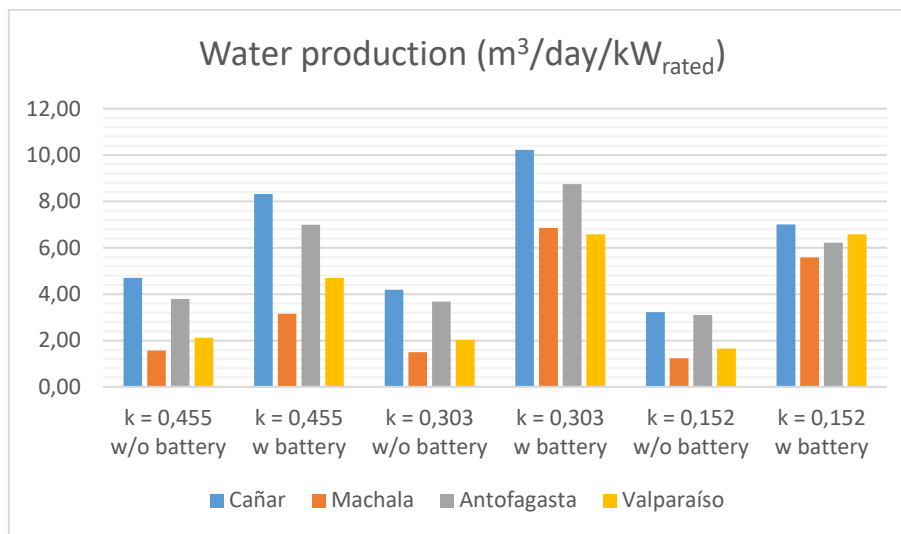


Figure 7-15. Desalinated water production with two hours of energy storage and without batteries for a 15 kW wind turbine, SEC=1 kWh/m³.

7.3.2 SEC=0.5 kWh/m³

Table 7–8. Water production with Wind, SEC=0.5 kWh/m³.

		Water production (m ³ /day/kW _{rated})					
		k = 0,455		k = 0,303		k = 0,152	
		k = 0,455 w/o battery	k = 0,455 w battery	k = 0,303 w/o battery	k = 0,303 w battery	k = 0,152 w/o battery	k = 0,152 w battery
Chile	Cañar	4,70	8,31	4,19	10,22	3,22	7,00
	Machala	1,57	3,16	1,49	6,85	1,23	5,59
Ecuador	Antofagasta	3,79	6,99	3,68	8,75	3,10	6,22
	Valparaíso	2,11	4,70	2,02	6,58	1,64	6,58

Figure 7-16. Desalinated water production with two hours of energy storage and without batteries, SEC=0.5 kWh/m³.

7.3.2.1 Small scale, SEC=0.5 kWh/m³

Table 7–9. Water production for a 15 kW wind turbine, SEC=0.5 kWh/m³.

		Water production (m ³ /day/kW _{rated})					
		k = 0,455		k = 0,303		k = 0,152	
		k = 0,455 w/o battery	k = 0,455 w battery	k = 0,303 w/o battery	k = 0,303 w battery	k = 0,152 w/o battery	k = 0,152 w battery
Chile	Cañar	4,55	9,26	4,44	10,90	3,40	7,62
	Machala	1,46	3,97	1,47	8,89	1,29	7,05
Ecuador	Antofagasta	3,85	8,82	4,09	11,47	3,37	7,47
	Valparaíso	2,02	5,21	2,17	9,15	1,75	7,14

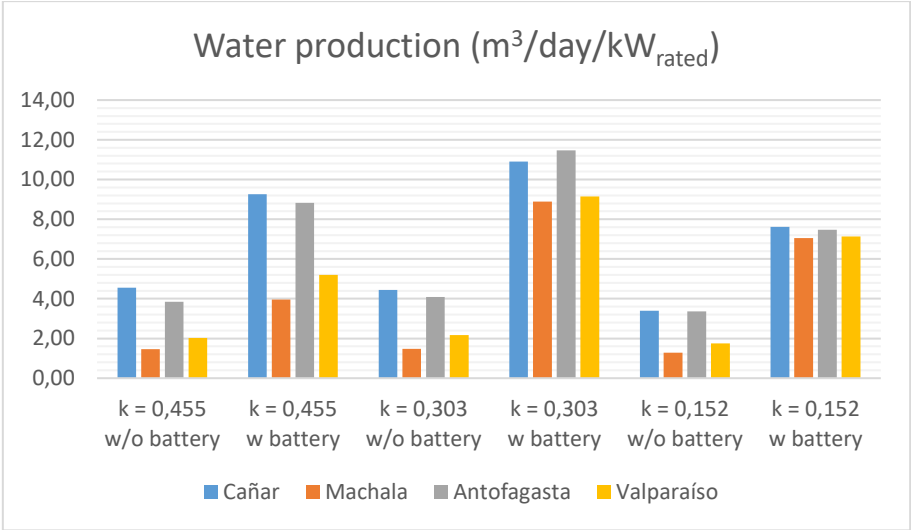


Figure 7-17. Desalinated water production with two hours of energy storage and without batteries for a 15 kW wind turbine, SEC=0.5 kWh/m³.

8 GENERALISATION TO OTHER APPLICATIONS AND EMPLACEMENTS

The methodology described throughout previous chapters was only applied to mining facilities in Ecuador and Chile, but it can be an effective method of calculating water production for any kind of Renewable Energy Source driven water treatment. Chapter 8 pretends to offer a comparative example of different emplacements to show the usefulness of the tool implemented.

The “tool” implemented is practical for different water treatments and technologies, allowing the calculation of water production approximations for any type of plant and region, since the calculations only depend on the typical meteorological year, the SEC of the RO and k ratio:

- Water pumping and delivery can be defined as $SEC=0,5 \text{ kWh/m}^3$ or $SEC=1 \text{ kWh/m}^3$ depending on the distance between the source of water and the consumer.
- In the case of urban wastewater treatment plant, it could also be defined by the SEC, depending on the pumping needed for the processes and the adequate discharge of water or reuse according to regulation. The SEC would consist of $0,5 \text{ kWh/m}^3$ plus the energy consumption related to oxygen supply and the RO tertiary treatment.
- Brackish water applications would only proceed in Spain and Portugal, typically with $SEC=0,5 \text{ kWh/m}^3$, plus water capturing pumping and distribution pumping.
- Seawater desalination, with $SEC=2,14 \text{ kWh/m}^3$ for Pacific Ocean and $SEC=2,03 \text{ kWh/m}^3$ for Atlantic Ocean, considering exclusively main consumption (generic process with SEC due to desalination).

It has also been tested to calculate water production in locations belonging to the Atlantic area. The emplacements have been chosen for the study because of their wide range within the same regions, these are:



Figure 8-1. Map of the regions selected for the study.

Table 8–1. Localisations selected for the study

Wales	Ireland	Brittany France	Alentejo	Canary Islands
Tywyn	Dublin Airport	Saint Malo	Melides	Corralejo
Aberporth	Youghal	Saint-Breiuç Armor	Sines	Gran Canaria
Kidwelly	Valentia	Brest	Vila Nova de Milfontes	Santa Cruz de la Palma
Cardiff	Bellmulet	Concarneau	Cavaleiro	Puerto de la Estaca

Using the Software Q+ (LGChem), realistic specific energy consumption for a Reverse Osmosis plant located in Atlantic area can be defined, as was described in Chapter 4. To define water composition Wilf 2007 [24] was taken as reference:

Constituent	Mediterranean	Persian Gulf	Red Sea	Caribbean	Pacific	Atlantic	Canary Islands
Temperature	14°C, 28°C	16°C, 34°C	16°C, 26°C	26°C	20°C	20°C	22°C
pH	8.1	7.0	7.8	8.2	8.0	8.0	7.8
Ca ⁺ , ppm	483	478	500	477	440	410	464
Mg ⁺ , ppm	1557	1672	1540	1160	1300	1302	1526
Na ⁺ , ppm	12200	14099	13300	11322	10200	10812	11700
K ⁺ , ppm	481	530	490	386	380	389	429
CO ₃ ⁻ , ppm	5	4.2	2.3	2.3	2.0	2.0	3.2
HCO ₃ ⁻ , ppm	162	154	126.8	137	170	143	204
SO ₄ ²⁻ , ppm	3186	3314	3240	2600	3000	2713	3059
Cl ⁻ , ppm	22599	24927	23180	20034	18500	19441	21344
F ⁻ , ppm	1.4	-	-	-	-	-	-
NO ₃ ⁻ , ppm	-	-	-	-	-	-	-
B ⁺ , ppm	5	5	5.3	5.3	4.5	4.5	4.5
SiO ₂ , ppm	1.6	-	-	-	-	-	-
TDS, ppm	40686	45199	42389	36149	34000	35240	38739

Figure 8-2. Exemplary cases of water composition in several plant locations.¹⁸

Once the specific energy consumption for a RO plant located in Atlantic Ocean is known, water production can be obtained regarding hourly energy production profile.

The simulations performed with Q+ prove specific energy consumption in Atlantic are to be 2.03 kWh/m³:

$$SEC = \frac{\sum P_{W,HPP}}{q_{VP}} = 2.03 \frac{kWh}{m^3} \quad (8-1)$$

The study analyses the impact energy storage systems have in production for photovoltaic and wind driven RO plants, the results are presented as a function of the k ratio, presented on Chapter 4.

¹⁸ Wilf, M., & Awerbuch, L. (n.d.). The Guidebook to membrane desalination technology : reverse osmosis, nanofiltration and hybrid systems, process, design, applications and economics / . Balaban Desalination Publications.

8.1 Photovoltaic Systems

8.1.1 Ireland

Table 8–2. Water production with PV in Ireland, SEC=2.03 kWh/m³.

	Water production (m ³ /day/kW _p)					
	k = 0,455		k = 0,303		k = 0,152	
	k = 0,455 w/o battery	k = 0,455 w battery	k = 0,303 w/o battery	k = 0,303 w battery	k = 0,152 w/o battery	k = 0,152 w battery
Belmullet	0,46	1,06	0,53	0,87	0,43	0,79
Dublin	0,47	1,05	0,54	1,25	0,45	0,80
Valentia	0,44	1,06	0,52	1,24	0,44	0,80
Youghal	0,49	1,09	0,56	1,25	0,46	0,79

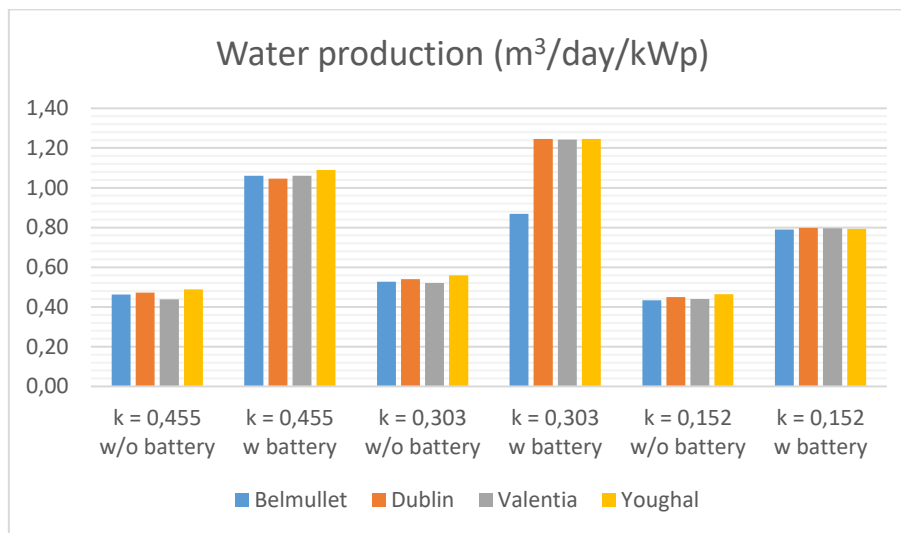


Figure 8-3. Desalinated water production with PV plant in Ireland with two hours of energy storage and without energy storage given a k ratio, SEC=2.03 kWh/m³.

8.1.2 Wales, United Kingdom

Table 8–3. Water production with PV in Wales, SEC=2.03 kWh/m³.

	Water production (m ³ /day/kW _p)					
	k = 0,455		k = 0,303		k = 0,152	
	k = 0,455 w/o battery	k = 0,455 w battery	k = 0,303 w/o battery	k = 0,303 w battery	k = 0,152 w/o battery	k = 0,152 w battery
Aberporth	0,54	1,10	0,58	0,91	0,48	0,80
Cardiff	0,66	1,20	0,68	1,29	0,52	0,79
Kidwelly	0,57	1,14	0,60	1,24	0,48	0,80
Tywyn	0,51	1,04	0,56	1,21	0,45	0,79

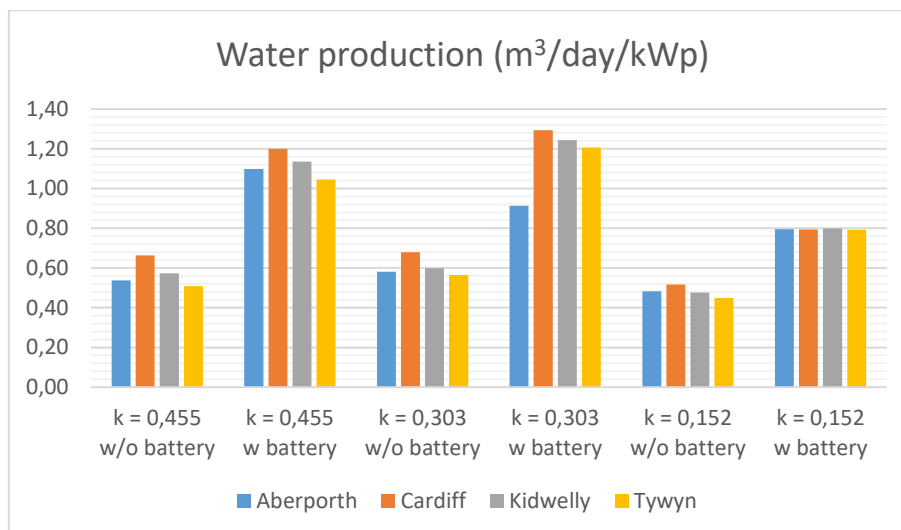


Figure 8-4. Desalinated water production with PV plant in Wales with two hours of energy storage and without energy storage given a k ratio, SEC=2.03 kWh/m³.

8.1.3 Brittany France, France

Table 8-4. Water production with PV in Brittany France, SEC=2.03 kWh/m³.

	Water production (m³/day/kWp)					
	k = 0,455		k = 0,303		k = 0,152	
	k = 0,455 w/o battery	k = 0,455 w battery	k = 0,303 w/o battery	k = 0,303 w battery	k = 0,152 w/o battery	k = 0,152 w battery
Brest	0,53	1,15	0,60	1,33	0,49	0,80
Concarneau	0,60	1,19	0,64	1,44	0,50	0,79
Saint Malo	0,60	1,17	0,62	1,31	0,49	0,80
Saint Brieuc Armor	0,57	1,21	0,62	1,29	0,50	0,80

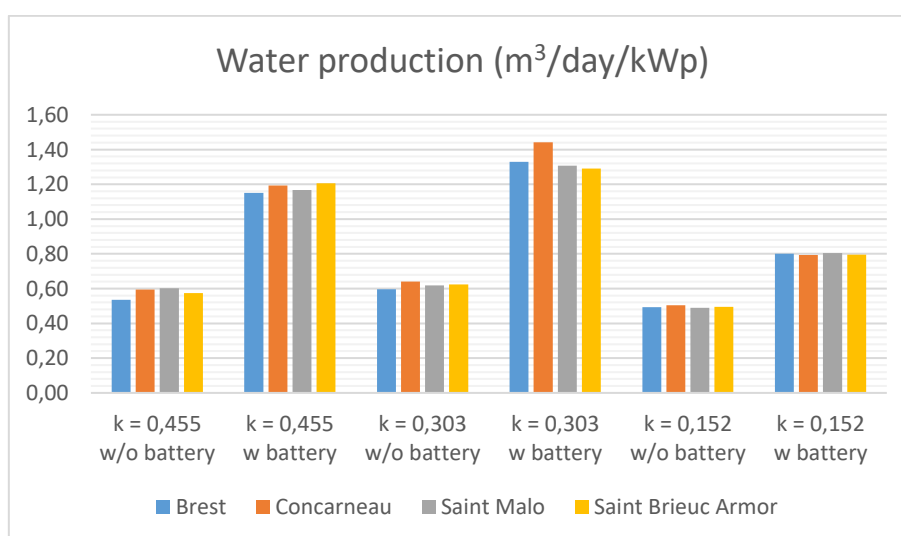


Figure 8-5. Desalinated water production with PV plant in Brittany France with two hours of energy storage and without energy storage given a k ratio, SEC=2.03 kWh/m³.

8.1.4 Alentejo, Portugal

Table 8–5. Water production with PV in Alentejo region, SEC=2.03 kWh/m³.

	Water production (m ³ /day/kW _p)					
	k = 0,455		k = 0,303		k = 0,152	
	k = 0,455 w/o battery	k = 0,455 w battery	k = 0,303 w/o battery	k = 0,303 w battery	k = 0,152 w/o battery	k = 0,152 w battery
Cavaleiro	1,33	1,80	1,15	1,37	0,72	0,81
Melides	1,30	1,78	1,13	1,50	0,71	0,81
Sines	1,32	1,81	1,13	1,50	0,72	0,81
Vila Nova	1,34	1,82	1,14	1,51	0,72	0,82

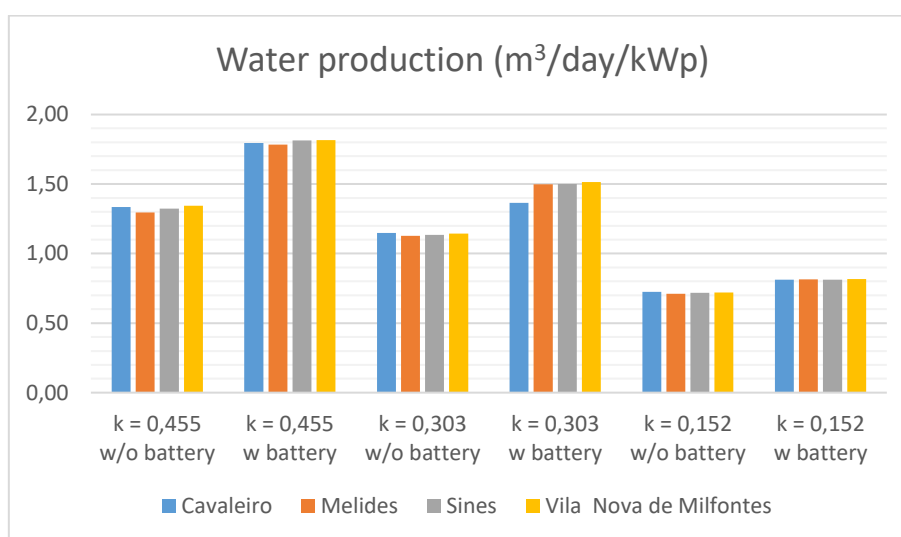


Figure 8-6. Desalinated water production with PV plant in Alentejo regions with two hours of energy storage and without energy storage given a k ratio, SEC=2.03 kWh/m³.

8.1.5 Canary Islands, Spain

Table 8–6. Water production with PV in Canary Islands region, SEC=2.03 kWh/m³.

	Water production (m ³ /day/kW _p)					
	k = 0,455		k = 0,303		k = 0,152	
	k = 0,455 w/o battery	k = 0,455 w battery	k = 0,303 w/o battery	k = 0,303 w battery	k = 0,152 w/o battery	k = 0,152 w battery
Puerto de la Estaca	1,30	1,76	1,13	1,31	0,70	0,81
Corralejo	1,30	1,81	1,11	1,52	0,69	0,82
Gran Canaria	1,07	1,62	1,01	1,45	0,67	0,81
Santa Cruz	0,90	1,48	0,91	1,42	0,62	0,81

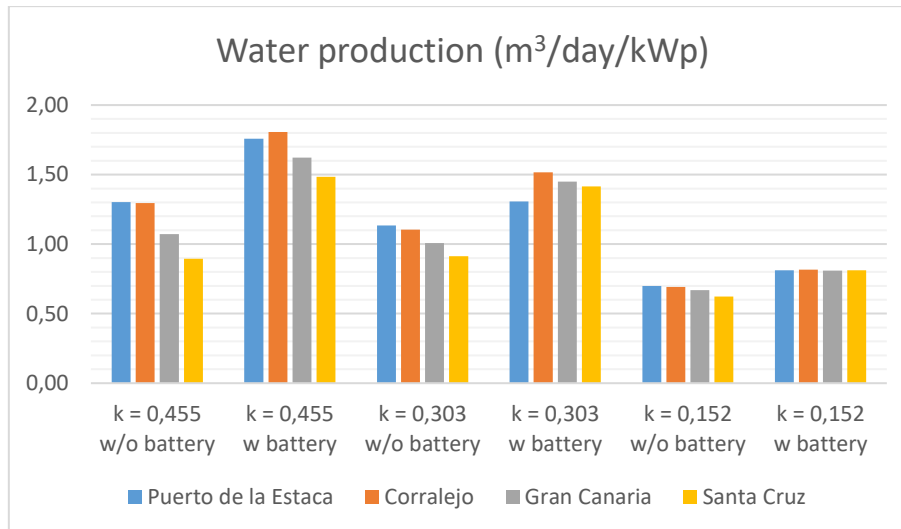


Figure 8-7. Desalinated water production with PV plant in Canary Islands with two hours of energy storage and without energy storage given a k ratio, SEC=2.03 kWh/m³.

8.2 Wind Systems

8.2.1 Ireland

Table 8-7. Water production with wind in Ireland, SEC=2.03 kWh/m³.

	Water production (m³/day/kW _{rated})					
	k = 0,455		k = 0,303		k = 0,152	
	k = 0,455 w/o battery	k = 0,455 w battery	k = 0,303 w/o battery	k = 0,303 w battery	k = 0,152 w/o battery	k = 0,152 w battery
Belmullet	2,99	3,70	2,26	3,13	1,36	1,77
Dublin	2,46	3,10	1,97	2,79	1,24	1,63
Valentia	1,98	2,89	1,63	2,92	1,09	1,76
Youghal	1,98	2,70	1,67	2,66	1,11	1,61

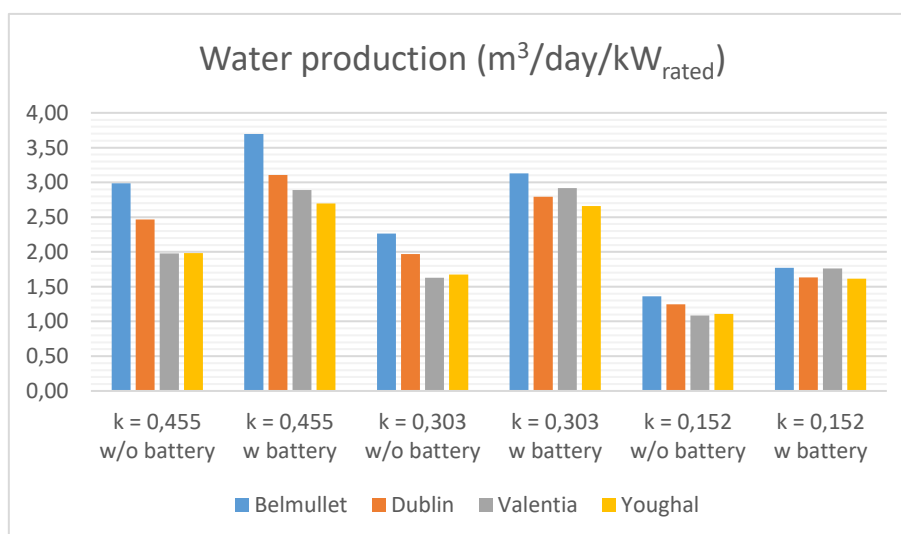


Figure 8-8. Desalinated water production with Wind plant in Ireland with two hours of energy storage and without energy storage given a k ratio, SEC=2.03 kWh/m³.

8.2.2 Wales, United Kingdom

Table 8–8. Water production with wind in Wales, SEC=2.03 kWh/m³.

	Water production (m ³ /day/kW _{rated})					
	k = 0,455		k = 0,303		k = 0,152	
	k = 0,455 w/o battery	k = 0,455 w battery	k = 0,303 w/o battery	k = 0,303 w battery	k = 0,152 w/o battery	k = 0,152 w battery
Aberporth	3,13	3,82	2,37	3,18	1,39	1,78
Cardiff	1,80	2,50	1,52	2,54	1,04	1,63
Kidwelly	2,22	3,15	1,80	2,94	1,17	1,77
Tywyn	1,39	2,07	1,21	2,42	0,90	1,52

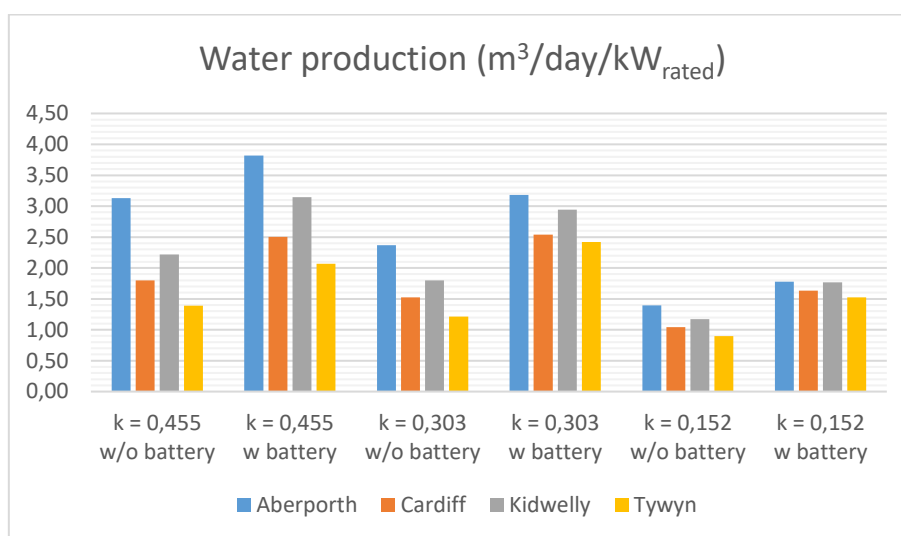


Figure 8-9. Desalinated water production with Wind plant in Wales with two hours of energy storage and without energy storage given a k ratio, SEC=2.03 kWh/m³.

8.2.3 Brittany France, France

Table 8–9. Water production with wind in Brittany France, SEC=2.03 kWh/m³.

	Water production (m ³ /day/kW _{rated})					
	k = 0,455		k = 0,303		k = 0,152	
	k = 0,455 w/o battery	k = 0,455 w battery	k = 0,303 w/o battery	k = 0,303 w battery	k = 0,152 w/o battery	k = 0,152 w battery
Brest	1,43	2,41	1,26	2,73	0,92	1,73
Concarneau	2,30	2,99	1,86	2,75	1,20	1,62
Saint Malo	1,64	2,56	1,40	2,75	0,98	1,74
Saint Brieuc Armor	1,61	2,33	1,36	2,46	0,97	1,59

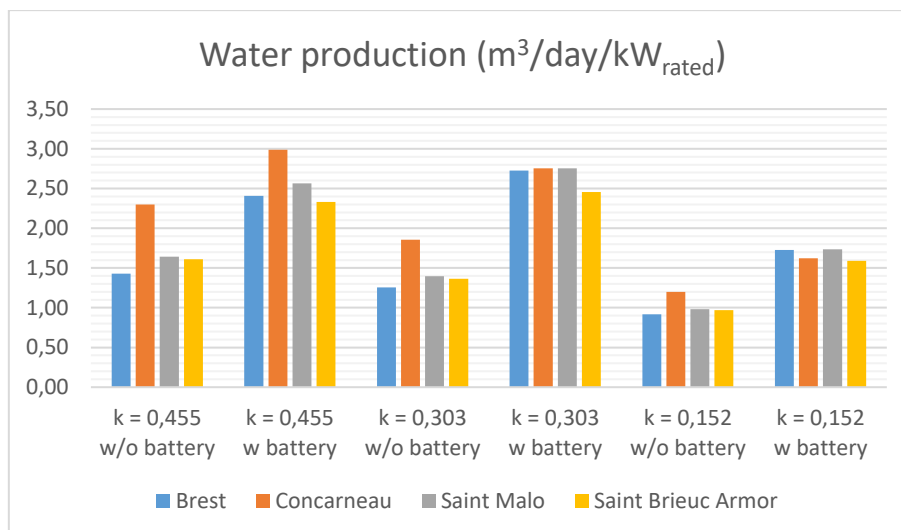


Figure 8-10. Desalinated water production with Wind plant in Brittany France with two hours of energy storage and without energy storage given a k ratio, SEC=2.03 kWh/m³.

8.2.4 Alentejo, Portugal

Table 8–10. Water production with wind in Alentejo region, SEC=2.03 kWh/m³.

	Water production (m ³ /day/kW _{rated})					
	k = 0,455		k = 0,303		k = 0,152	
	k = 0,455 w/o battery	k = 0,455 w battery	k = 0,303 w/o battery	k = 0,303 w battery	k = 0,152 w/o battery	k = 0,152 w battery
Cavaleiro	1,37	2,22	1,17	2,53	0,83	1,72
Melides	1,38	2,07	1,19	2,27	0,83	1,56
Sines	1,45	2,30	1,21	2,63	0,86	1,73
Vila Nova	1,44	2,10	1,22	2,33	0,86	1,55

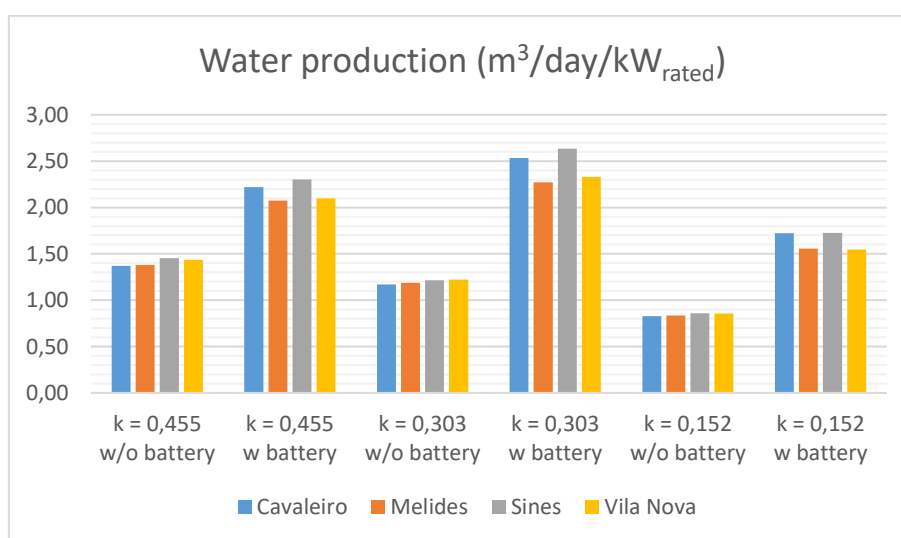


Figure 8-11. Desalinated water production with Wind plant in Alentejo regions with two hours of energy storage and without energy storage given a k ratio, SEC=2.03 kWh/m³.

8.2.5 Canary Islands, Spain

Table 8–11. Water production with wind in Canary Islands, SEC=2.03 kWh/m³.

	Water production (m ³ /day/kW _{rated})					
	k = 0,455		k = 0,303		k = 0,152	
	k = 0,455 w/o battery	k = 0,455 w battery	k = 0,303 w/o battery	k = 0,303 w battery	k = 0,152 w/o battery	k = 0,152 w battery
Puerto de la Estaca	2,81	3,64	2,20	3,15	1,37	1,79
Corralejo	2,84	3,41	2,23	2,97	1,37	1,75
Gran Canaria	3,12	3,85	2,37	3,19	1,41	1,79
Santa Cruz	1,87	2,61	1,60	2,65	1,12	1,71

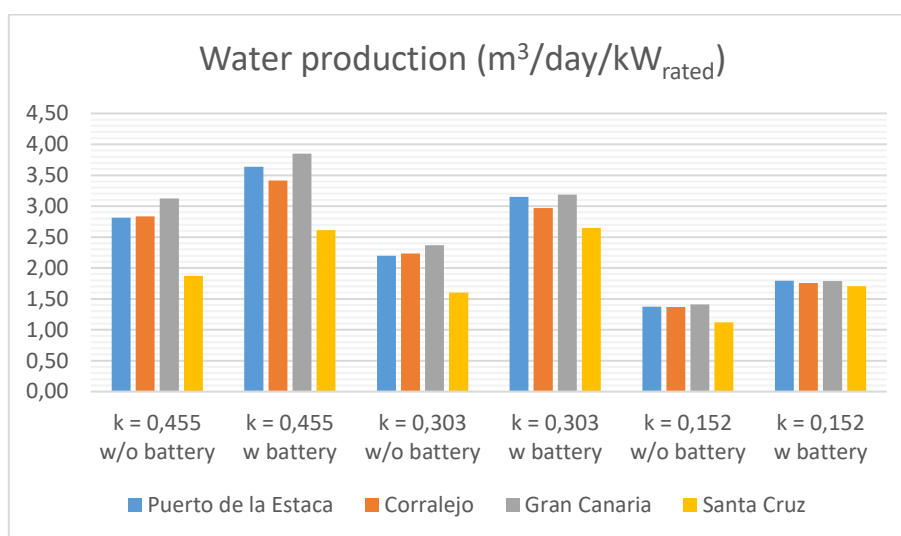


Figure 8-12. Desalinated water production with Wind plant in Canary Islands with two hours of energy storage and without energy storage given a k ratio, SEC=2.03 kWh/m³.

8.3 Discussion of the results

As brief summary of the results obtained, water production in terms of m³/kW_p per year, appears to be much lower in the case of photovoltaic systems for the localisations emplaced in the northern region of Europe (Ireland, Wales and Brittany France) in comparison with the ones in the south (Portugal and Canary Islands) as might be expected. However, in the case of wind powered RO water production in terms of m³/kW_{rated} per year, not surprisingly Wales presents the highest production, followed by Canary Islands -world leader in wind energy driven desalination-, Ireland and Brittany France.

This is definitely due to the weather, whereas the regions in the North undergo less hours of sun, they tend to present maximal wind resource, with the exception of Canary Islands, an enclave.

Results do show a substantial dependency on k ratio and energy storage implementation, therefore, for each application, once known the cost of the technology and batteries, the cost of the product must be analysed case-by-case.

9 ECONOMIC ASSESSMENT

Thus far, costs were never considered in the assessment, being cost analysis particularly relevant in the case of renewable energies, into the spotlight because of their increasing importance on the energy current picture. The objective of this chapter is not to present realistic costs of the implementation, but to evaluate the economic feasibility of the systems presented on the previous chapters by comparing the technologies with IRENA (International Renewable Energy Agency) methodology.

The cost of the final product in desalination, is a crucial criterion that defines the feasibility and success of the technology. The total costs of the water produced include the cost of investment, as well as the operating and maintenance costs, furthermore, costs such as those associated to energy storage have to be included as they have, in fact, a major impact on overall costs.

Generally, a SWRO unit has low capital cost and significant maintenance cost due to the high cost of the membrane replacement. The cost of the energy used to drive the plant is also significant. The major energy requirement for RO desalination is for pressurizing the feedwater, the main reason why energy recovery devices are used, as mentioned beforehand. [26] The implementation of IRENA methodology has limitations since it is contemplated from the point of view of the investor.

9.1 Levelised Cost of Energy

The LCOE is the price of electricity required for a project where revenues would equal costs, including making a return on the capital invested equal to the discount rate. An electricity price above this would yield a greater return on capital, while a price below it would yield a lower return on capital, or even a loss.

The LCOE of renewable energy technologies varies by technology, country and project based on the renewable energy resource, capital and operating costs, and the efficiency / performance of the technology. The approach used in the analysis presented here is based on a discounted cash flow (DCF) analysis. This method of calculating the cost of renewable energy technologies is based on discounting financial flows (annual, quarterly or monthly) to a common basis, taking into consideration the time value of money. Given the capital intensive nature of most renewable power generation technologies and the fact that fuel costs are low, or often zero, the weighted average cost of capital (WACC), often also referred to as the discount rate, used to evaluate the project has a critical impact on the LCOE.

The formula used for calculating the LCOE of renewable energy technologies is [27]:

$$LCOE = \frac{\sum_{n=1}^N \left[\frac{I_n + M_n + F_n}{(1+d)^n} \right]}{\sum_{n=1}^N \left[\frac{E_n}{(1+d)^n} \right]} \quad (9-1)$$

Where:

- I_n is the investment expenditures in the year n .
- M_n is the operations and maintenance expenditures in the year n .
- F_n is the fuel expenditures in the year n .
- E_n is the electricity generation in the year n .
- d is the discount rate.
- N is the life of the system.

The specific investment costs will be presented on the following section.

A discount rate is the rate of return used to discount future cash flows back to their present value, it depends on the country:

Table 9–1. Discount rate values.¹⁹

Country	Value
Ecuador	8.17 (December 2011)
Chile	3.35 (December 2015)
Ireland	0.05 (December 2015)
United Kingdom	0.25 (December 2016)
France	0 (December 2016)
Portugal	0 (December 2017)
Spain	0.05 (December 2017)

The economical assessment performed in this Chapter includes the emplacements studied in Ecuador, Chile and the Atlantic coast of Europe, for PV and onshore wind utility scale and small scale installations. Table 9-3 summarises the main parameters selected for the economical assessment

Table 9–2. Parameters used for the economical assessment.

Region	SEC (kWh/m ³)	k ratio (utility scale)	k ratio (small scale)	RO plant
Pacific	2,14	k = 0,4545	k = 0,4	Conventional
Atlantic	2,03	k = 0,4545	k = 0,4	Conventional

9.1.1 Solar photovoltaics

PV systems are capital intensive, but do not have fuel costs. The three key drivers of the LCOE of these systems are:

- The capital and the installation costs of PV modules (the interconnected array of PV cells) and balance of system, which includes the structural system (e.g. structural installation, racks, site preparation and other attachments), the electrical system costs (e.g. the inverter, transformer, wiring and other electrical installation costs) and the battery or other storage system cost in the case of off grid applications.
- Discount rate.
- The average annual electricity yield (kWh/kW), a function of the local solar radiation and the solar technical performance.
- The cost of finance for the PV system.

¹⁹ <https://www.cia.gov/library/publications/the-world-factbook/fields/230rank.html>

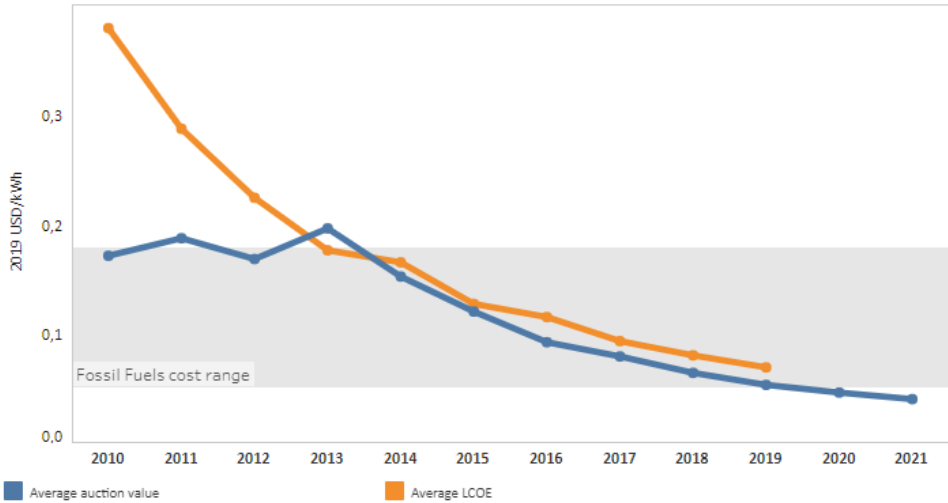


Figure 9-1. Global weighted average LCOE and auction values 2010-2020.²⁰

9.1.2 Onshore wind

The key parameters that define the LCOE for wind power systems are:

- Capital costs.
- Wind resource quality which affects expected annual energy production.
- Technical characteristics of the wind turbines.
- Discount rate.
- Operation and maintenance costs.

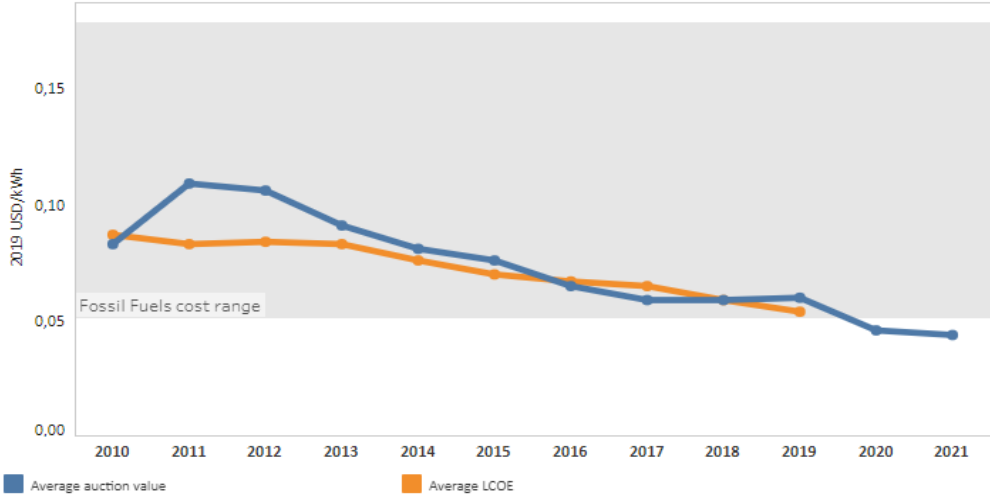


Figure 9-2. Global weighted average LCOE and auction values 2010-2020.²¹

²⁰ IRENA, available on: <https://www.irena.org/Statistics/View-Data-by-Topic/Costs/Global-LCOE-and-Auction-values>

²¹ IRENA, available on: <https://www.irena.org/Statistics/View-Data-by-Topic/Costs/Global-LCOE-and-Auction-values>

9.1.3 Capital Expenditure (CAPEX)

One of the most significant drawbacks of RES-driven RO is the high associated costs, including CAPEX (Cost Expenditure). Table 9-2 shows the summary of specific investment costs used for the calculations. Along the last years, both PV and Wind components have reduced their capital expenditure costs largely in benefit of the off-grid systems implementation.

Table 9–3. Capital costs of components.

Subsystem	Specific Cost	References
Total installed cost of PV	995 USD/ kWp	[27]
O&M for PV	6,5 USD/ kWp	[27]
Wind turbine	828 €/ kW _{rated}	[23]
Small wind turbine	3000 USD/ kW _{rated}	[27]
O&M for PV	33 USD/ kW _{rated}	[27]
Maintenance-less gel batteries	4.53 €/Ah	[28]
	1.72 €/Ah	[29]
SWRO plant	1000 €/m ³ day	[23]
SWRO plant (small scale)	850 €/m ³ day	[23]
BWRO plant	750 €/m ³ day	[23]

Life of the RES system: 25 years

Life of the RO system: 15 years

9.1.4 Ecuador and Chile regions

This section includes the results in Ecuador and Chile emplacements; Table 9-3 and Figure 9-1 represent a summary of LCOE. Energy storage systems do not imply a rise in the LCOE in all cases and the values are in the range of 0,012 and 0,533 €/kWh.

Batteries do not make a big difference in the LCOE since the rise in energy production compensates with the increase of investment in the case of PV but do represent a big enhancement in the case of wind in some locations such as Machala, Santiago and Valparaíso.

Table 9-4. LCOE (€/kWh) values in Ecuador and Chile.

	PV				WIND			
	Utility scale		Small scale		Utility scale		Small scale	
	w/o batteries	w batteries						
Cañar	0,023	0,012	0,025	0,013	0,045	0,023	0,193	0,042
Machala	0,024	0,016	0,026	0,014	0,287	0,083	0,533	0,140
Santiago	0,022	0,014	0,024	0,012	0,194	0,057	0,361	0,097
Valparaíso	0,031	0,018	0,033	0,016	0,213	0,060	0,435	0,086
Antofagasta	0,018	0,012	0,020	0,011	0,119	0,036	0,228	0,053

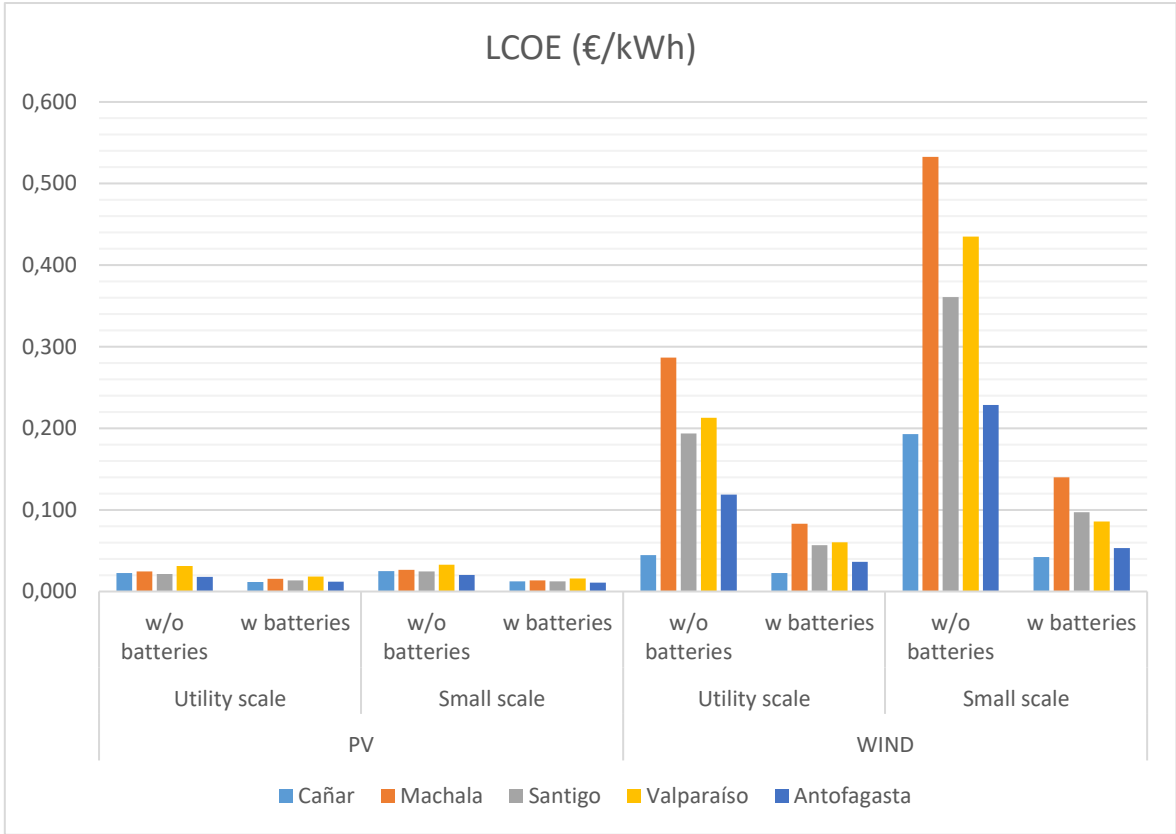


Figure 9-3. LCOE (€/kWh) for every location in Ecuador and Chile.

9.1.5 Atlantic region

This section includes the results in Atlantic Ocean emplacements; Table 9-4 and Figure 9-2 represent a summary of LCOE. The results are very different from the ones obtained in Ecuador and Chile and energy storage systems imply indeed a drop in the LCOE in all cases, except on wind utility scale, where batteries do not outcome in lower LCOE. The values are in the range of 0,009 and 0,081 €/kWh.

In Atlantic region, the addition of energy storage systems results in better LCOE than the case of Ecuador and Chile, although the underlying data (the LCOE without batteries) was good to begin with.

Table 9–5. LCOE (€/kWh) values in Atlantic region.

	PV				WIND			
	Utility scale		Small scale		Utility scale		Small scale	
	w/o batteries	w batteries						
Portugal	0,016	0,009	0,019	0,010	0,038	0,019	0,081	0,031
Spain	0,017	0,009	0,019	0,010	0,039	0,015	0,034	0,017
Ireland	0,044	0,020	0,047	0,022	0,056	0,019	0,055	0,025
UK	0,033	0,016	0,037	0,018	0,062	0,022	0,060	0,023
France	0,037	0,017	0,040	0,019	0,048	0,016	0,049	0,020

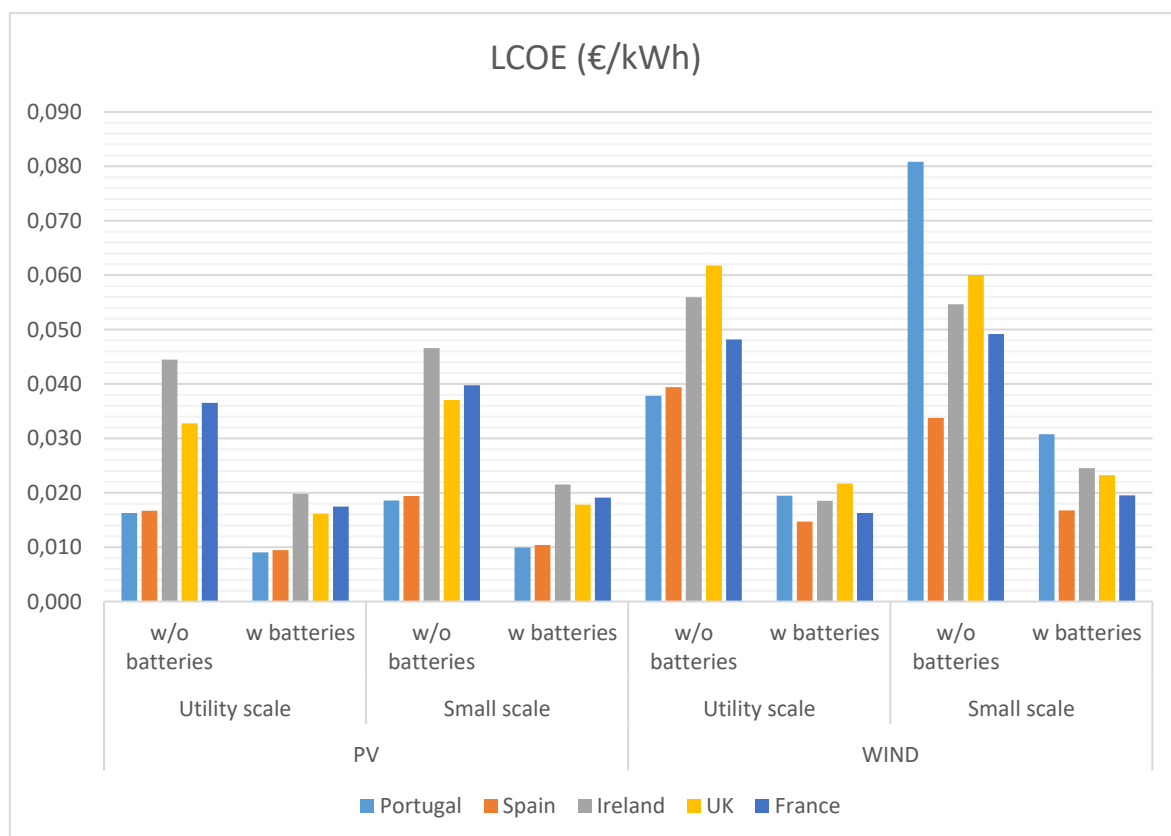


Figure 9-4. LCOE (€/kWh) for every location in Europe.

Figures 9-5 and 9-6 display the values of LCOE of newly commissioned installations of solar PV and onshore wind for France, Spain and United Kingdom, and prove that the range of results obtained for the locations in Europe are coherent with the ones calculated during last decades by the International Renewable Energy Agency (IRENA) and therefore, validate the results.

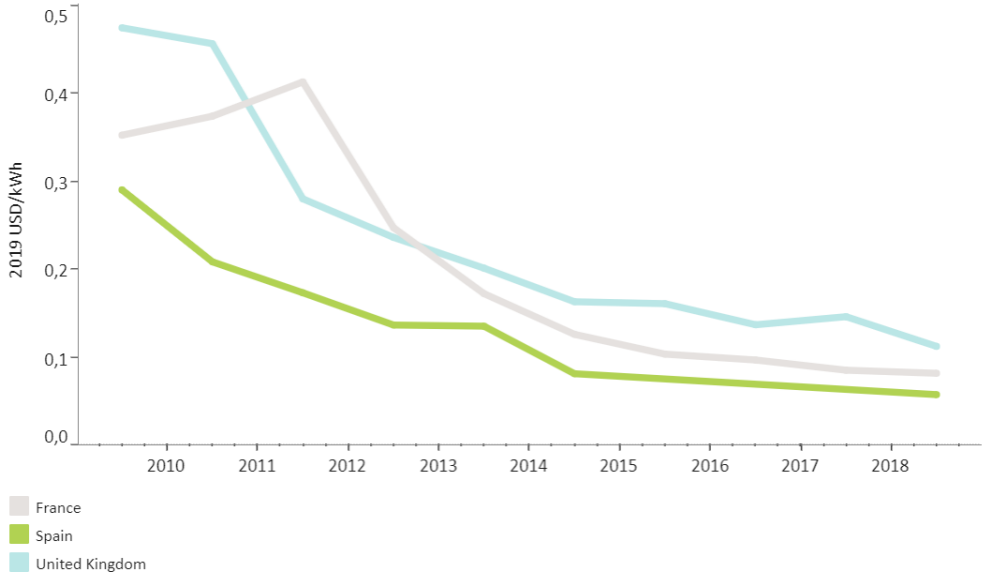


Figure 9-5. Weighted average LCOE of newly commissioned utility-scale solar PV projects 2010-2020.²²

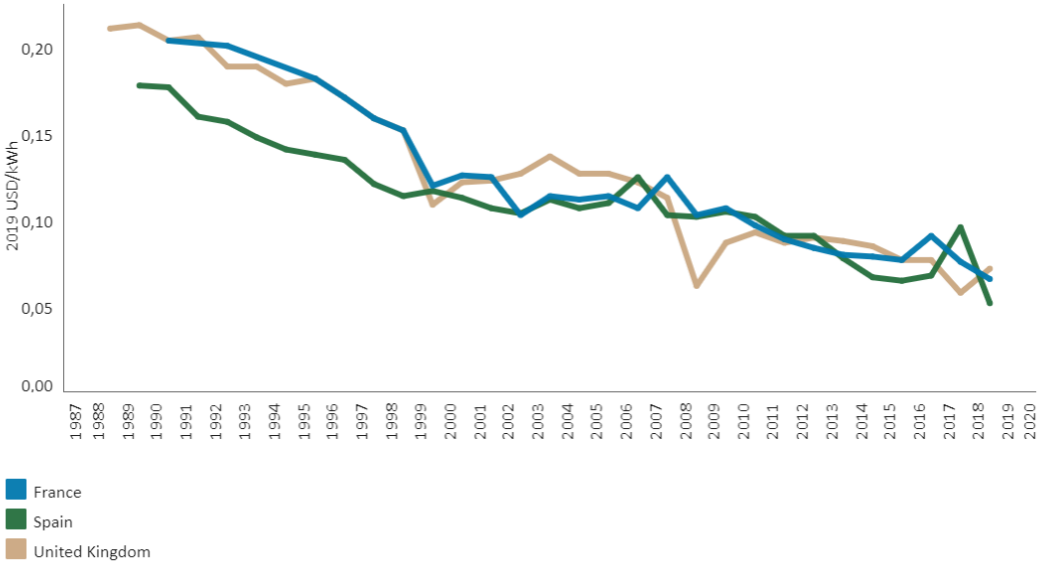


Figure 9-6. Weighted average LCOE of newly commissioned onshore wind projects 1984-2019.²³

²² IRENA, available on: <https://www.irena.org/Statistics/View-Data-by-Topic/Costs/Solar-Costs>
²³ IRENA, available on: <https://www.irena.org/Statistics/View-Data-by-Topic/Costs/Wind-Costs>

9.2 Levelised Cost of Water

Levelised cost of water (LCOW) is a useful indicator to compare and analyse the economic feasibility of a desalination technology. With the estimation of capital cost and annual operational and maintenance costs, the LCOW can be computed to evaluate the overall economic viability of the process and benchmark with the other desalination technologies. As the variable cost components such as chemical cost, utility cost, operators wage etc. are expected to vary over time due to the effect of inflation, the effect of cost escalation is considered in this study during the evaluation of LCOW. [30]

The formula used for calculating the LCOW of renewable energy technologies is [27]:

$$LCOW = \frac{\sum_{n=1}^N \left[\frac{I_n + M_n + LCOE \cdot E_n}{(1+d)^n} \right]}{\sum_{n=1}^N \left[\frac{W_n}{(1+d)^n} \right]} \quad (9-2)$$

Where:

- I_n is the investment expenditures in the year n.
- M_n is the operations and maintenance expenditures in the year n.
- F_n is the fuel expenditures in the year n.
- E_n is the electricity generation in the year n.
- d is the discount rate.
- N is the life of the system.

9.2.1 Ecuador and Chile regions

In LCOW case, in the case of PV batteries cause the LCOW to rise in all cases and in the case of Wind systems, to lower. Batteries, as well as happened with LCOE, do not make a big difference in the LCOW since the rise in water production compensates with the increase of investment.

Table 9–6. LCOW (€/m³) values in Ecuador and Chile.

	PV				WIND			
	Utility scale		Small scale		Utility scale		Small scale	
	w/o batteries	w batteries						
Cañar	0,487	0,367	0,451	0,434	0,534	0,397	0,591	0,493
Machala	0,491	0,375	0,454	0,435	0,725	0,495	0,999	0,619
Santiago	0,485	0,476	0,450	0,434	0,632	0,554	0,797	0,560
Valparaíso	0,505	0,481	0,468	0,439	0,651	0,544	0,833	0,567
Antofagasta	0,476	0,466	0,441	0,430	0,557	0,510	0,626	0,497

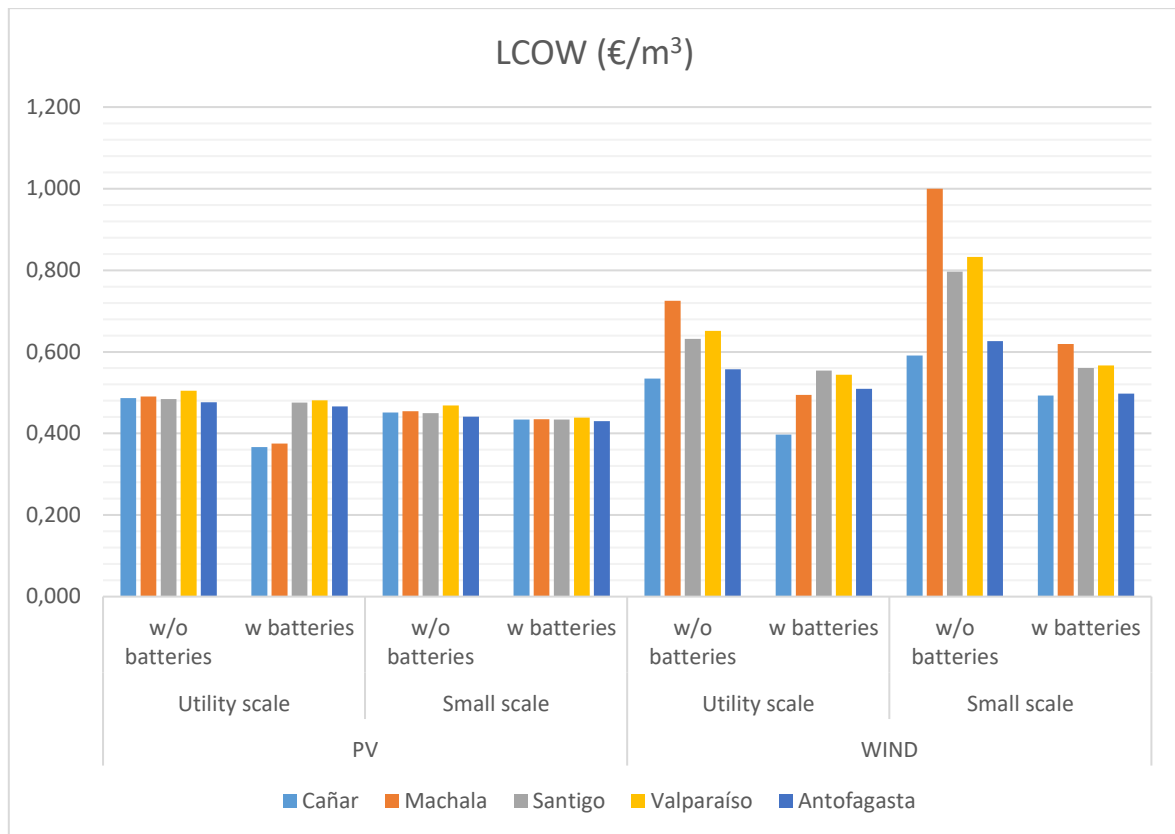


Figure 9-7. LCOW (€/m³) for every location in Ecuador and Chile.

9.2.2 Atlantic region

Table 9-7. LCOW (€/m³) values in Atlantic region.

	PV				WIND			
	Utility scale		Small scale		Utility scale		Small scale	
	w/o batteries	w batteries						
Portugal	0,471	0,362	0,436	0,428	0,515	0,390	0,571	0,488
Spain	0,472	0,363	0,437	0,429	0,476	0,369	0,484	0,456
Ireland	0,529	0,378	0,492	0,447	0,491	0,380	0,515	0,468
UK	0,505	0,374	0,473	0,411	0,497	0,384	0,526	0,472
France	0,513	0,375	0,478	0,441	0,484	0,376	0,503	0,464

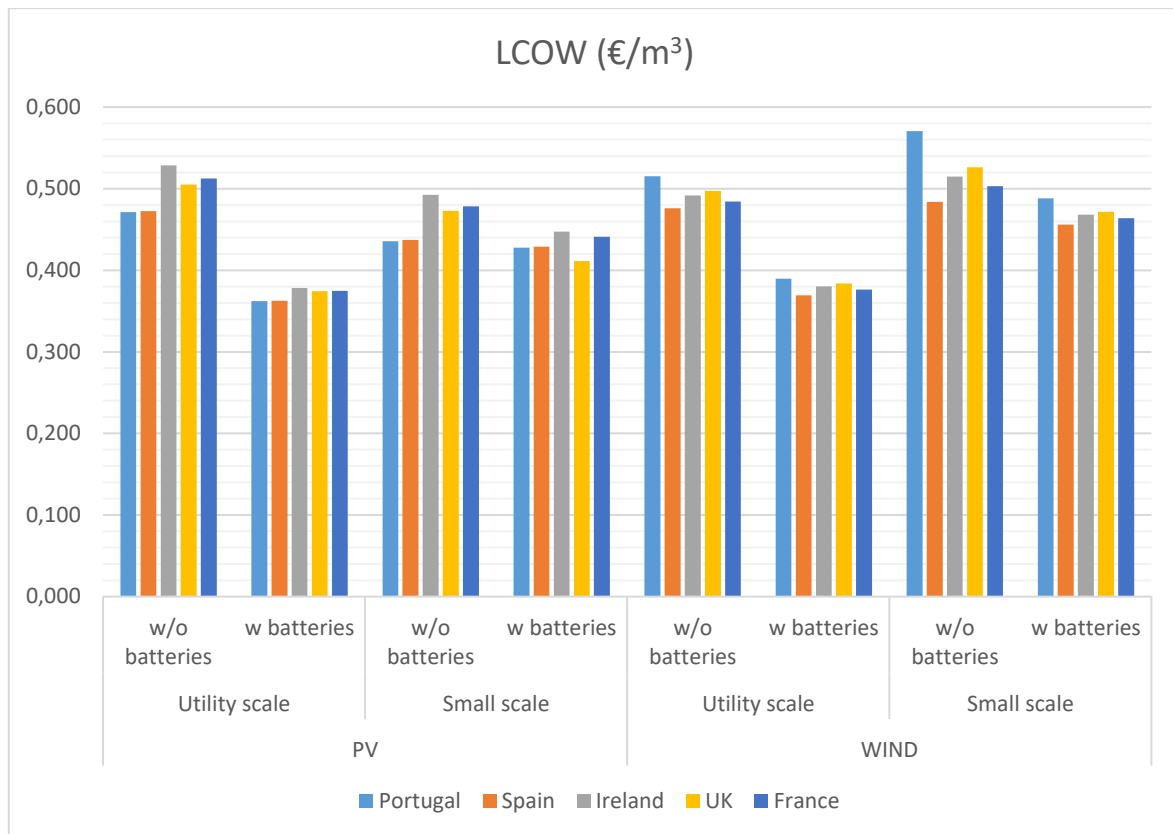


Figure 9-8. LCOW (€/m³) for every location in Europe.

9.3 Optimisation of water cost

In the case of photovoltaics technologies, both utility and small scale, it is clear that the addition of energy storage systems increases LCOW in all cases and regions.

For wind systems, the results must be examined more closely since results are cannot be generalised; energy storage systems seem to raise LCOW for Atlantic emplacements but considerably lower it in Ecuador and Chile.

Since the methodology can be applied to different water treatments and technologies, water pumping and delivery, can be defined as $SEC=0,5 \text{ kWh/m}^3$ or $SEC=1 \text{ kWh/m}^3$ depending on the distance between the source of water and the consumer. For these cases, for LOCW calculation, the investment cost of desalination plant would be replaced by the investment cost of the water pumping station.

10 CONCLUSIONS

This final Chapter addresses all the objectives stated at the beginning of the Master Thesis and their degree of achievement, as well as summarising the conclusions drawn from all the previous Chapters.

The “tool” implemented is useful to give good approximation of water production given meteorological data and the type of water of the facility for installations with power ranging from small scale 12 kW to utility scale 3.3 MW. To prove its effectiveness, experimental testing would be needed.

Although this master thesis focuses on applications to mining industry mainly (water desalination, industrial wastewater treatments), the “tool” implemented is practical for different water treatments and technologies, allowing the calculation of water production approximations for any type of plant and region, since the calculations only depend on the typical meteorological year, the SEC (Specific Energy Consumption) of the water treatment and the ratio of nominal power consumption to rated power production. Therefore, different technologies of the water cycle could be analysed as follows:

- Water pumping and delivery.
- Urban and industrial wastewater treatments.
- Brackish water desalination.
- Seawater desalination.

Water production is a direct function of the Specific Energy Consumption, the lower the Specific Consumption of the process, the higher the water production the RO plant may offer as the energy required to operate is lower, the tool implemented allows the quantification of these influences for any emplacement.

The results make clear that the selection of whether to implement energy storage in the RES system or gradual capacity in the RO plant is highly influenced by their capital costs and an economical assessment must be carried out in order to conclude their feasibility, in other words; the costs will be the decisive parameter when selecting the best design.

Gradual capacity must undertake an in-depth study, since it is necessary to count with a technical expert to estimate the costs associated to it. A remarkably interesting option to also study in more depth is using gradual capacity plants with energy storage systems to upgrade water production. Both are the following steps to be taken in the assessment.

On the subject of including energy storage systems, a viability assessment must be carried out for each emplacement, since results show that the localisation has a strong influence on the outcomes and that a general rule cannot be extracted and a case-by-case examination must be performed.

REFERENCES

- [1] Ma, Q., & Lu, H. (2011). *Wind energy technologies integrated with desalination systems: Review and state-of-the-art*. *Desalination*, 277(1), 274–280.
<https://doi.org/10.1016/j.desal.2011.04.041>
- [2] Source
<https://www.ngwa.org/what-is-groundwater/About-groundwater/information-on-earths-water>
- [3] *Nature-based Solutions for Water*. The United Nations World Water Development Report 2018.
- [4] Caldera, U., Bogdanov, D., & Breyer, C. (2018). *Desalination Costs Using Renewable Energy Technologies*. In *Renewable Energy Powered Desalination Handbook: Application and Thermodynamics* (pp. 287–329). Elsevier Inc.
<https://doi.org/10.1016/B978-0-12-815244-7.00008-8>
- [5] Source
<https://australianmuseum.net.au/get-involved/citizen-science/streamwatch/water-catchment/streamwatch-water-around-the-world/>
- [6] Veza Iglesias, J. (2002). *Introducción a la desalación de aguas*. Las Palmas de Gran Canaria: Consejo Insular de Aguas de Gran Canaria ; Universidad de Las Palmas de Gran Canaria.
- [7] *Proyección de consumo de agua en la minería de cobre 2019-2030*. DEPP 23/2019
Available:
<https://www.cochilco.cl/Listado%20Temtico/proyeccion%20agua%20mineria%20del%20cobre%202019-2030%20VF.pdf>
- [8] Recuperado de <https://cordis.europa.eu/project/rcn/218321/factsheet/en>.
- [9] IEA-ETSAP, IRENA, *Water desalination using renewable energy, technology brief*, 2012.
<https://www.irena.org/publications/2012/Mar/Water-Desalination-Using-Renewable-Energy>
- [10] J. Montes, B. de Weert, B. Petit, G.S. Martínez, L. García-Rodríguez, D. Sánchez. *Micro gas turbines supporting renewable energy systems in off-grid water treatment facilities in the mining industry*. Proceedings of ASME Turbo Expo 2020.
- [11] Ghaffour, N., Bundschuh, J., Mahmoudi, H., & Goosen, M. (2015). *Renewable energy-driven desalination technologies: A comprehensive review on challenges and potential applications of integrated systems*. *Desalination*, 356(C), 94–114.

- <https://doi.org/10.1016/j.desal.2014.10.024>
- [12] Jan Remund, Stefan Müller, Christian Studer, René Cattin, «*METEONORM. Handbook part I: Software*», METEOTEST.
Available on: <https://meteonorm.com/en/meteonorm-documents>
- [13] Jan Remund, Stefan Müller, Christian Studer, René Cattin, «*METEONORM. Handbook part II: Theory*», METEOTEST
Available on: <https://meteonorm.com/en/meteonorm-documents>
- [14] Al-Karaghoul, A., Renne, D., & Kazmerski, L. (2010). *Technical and economic assessment of photovoltaic-driven desalination systems*. *Renewable Energy*, 35(2), 323–328.
<https://doi.org/10.1016/j.renene.2009.05.018>
- [15] Gude, V., Nirmalakhandan, N., & Deng, S. (2010). *Renewable and sustainable approaches for desalination*. *Renewable and Sustainable Energy Reviews*, 14(9), 2641–2654.
<https://doi.org/10.1016/j.rser.2010.06.008>
- [16] “PVSyst Photovoltaic Software,” PVSyst,
Available on: <https://www.pvsyst.com/support/>
- [17] Al-Karaghoul, A., & Kazmerski, L. (2013). *Energy consumption and water production cost of conventional and renewable-energy-powered desalination processes*. *Renewable and Sustainable Energy Reviews*, 24(August 2013), 343–356.
<https://doi.org/10.1016/j.rser.2012.12.064>
- [18] Vicente, R. (2008). *Influence of the fitted probability distribution type on the annual mean power generated by wind turbines: A case study at the Canary Islands*. *Energy Conversion and Management*, 49(8), 2047–2054.
<https://doi.org/10.1016/j.enconman.2008.02.022>
- [19] Kucera, J. (n.d.). *Reverse Osmosis: industrial processes and applications* (2nd ed.). Scrivener Publishing.
- [20] Peñate, B., & García-Rodríguez, L. (2012). *Current trends and future prospects in the design of seawater reverse osmosis desalination technology*. *Desalination*, 284, 1–8.
<https://doi.org/10.1016/j.desal.2011.09.010>
- [21] Mahmoudi, H. (Ed.), Ghaffour, N. (Ed.), Goosen, M. F. (Ed.), Bundschuh, J. (Ed.). (2017). *Renewable Energy Technologies for Water Desalination*. London: CRC Press, Chapter 15.
<https://doi.org/10.1201/9781315643915>
- [22] Peñate, B., Castellano, F., Bello, A., & García-Rodríguez, L. (2011). *Assessment of a stand-alone gradual capacity reverse osmosis desalination plant to adapt to wind power availability: A case study*. *Energy*, 36(7), 4372–4384.
<https://doi.org/10.1016/j.energy.2011.04.005>

- [23] Subiela Ortín, V., García Rodríguez, L., & Peñate Suárez, B. (2018). *Techno-economic optimization of reverse osmosis desalination plants powered by off-grid generation systems based on wind and photovoltaic energy*.
- [24] Wilf, M., & Awerbuch, L. (n.d.). *The Guidebook to membrane desalination technology: reverse osmosis, nanofiltration and hybrid systems, process, design, applications and economics* / . Balaban Desalination Publications.
- [25] Ghaffour, N., Lattemann, S., Missimer, T., Ng, K., Sinha, S., & Amy, G. (2014). *Renewable energy-driven innovative energy-efficient desalination technologies*. *Applied Energy*, 136(C), 1155–1165.
<https://doi.org/10.1016/j.apenergy.2014.03.033>
- [26] Caldera, U., Bogdanov, D., & Breyer, C. (2016). *Local cost of seawater RO desalination based on solar PV and wind energy: A global estimate*. *Desalination*, 385(C), 207–216.
<https://doi.org/10.1016/j.desal.2016.02.004>
- [27] IRENA *Renewable Power Generation Costs in 2019*, 2019.
- [28] <https://solarmat.es/es/baterias/Baterias-estacionarias-GEL/>
- [29] <https://atersa.shop/baterias-solares-de-gel/>
- [30] Duffy, A., Rogers, M., & Ayompe, L. (2015). *Renewable energy and energy efficiency: Assessment of projects and policies*. West Sussex, England: Wiley Blackwell. John Wiley & Sons, Incorporated, 2015. ProQuest Ebook Central
<https://ebookcentral.proquest.com/lib/uses/detail.action?docID=1895514>.

